**Minor comments from editor**

*The first digit of line numbers >100 have been cut off in the PDF. So Comments >line 100 are page + 2nd 2 digits of the line number*

L7: Add space in zip code (AB24 3UF)

Corrected.

L15: minimal. Response to editor comments states this has been changed to 'some'. Change has not been made.

Corrected from minimal to some.

L20: 'Evaluate past glaciation on Mars' is vague. Say something like 'to better understand the potential contribution of glaciation to landscape evolution in Deuteronilus Mensae, Mars'.

Corrected.

L21: Here and throughout: avoid the term 'icy geomorphic' as this is ambiguous. Implies the feature itself is icy, but this isn't always the case – some are inferred as having formed by ice that is no longer there. Better 'geomorphic evidence for past glacial occupation of these cirque-like alcoves'

Corrected.

L24-25: These don't really work as alternatives to one-another as currently written - one is posed as a mechanism, and one as a requirement.

Additionally…

If tying to obliquity, then the high-insolation scenario is a different obliquity state to the low-insolation/high-accumulation state. Or it arises from a climate regime that has not yet been well constrained. Can you make this clearer?

We agree that this was previously phrased in a confusing way. We have modified it to read as follows: "One possibility to explain this trend is that southward facing cirque-like alcoves in the northern mid-latitudes formed when conditions were more favorable for ice accumulation during periods of high obliquity."

It is true that originally the intent of the sentence was to propose two possibilities for obliquity states (and periods for when cirque-like alcoves formed), but for the sake of simplicity, we only focus on one (which is also more consistent with the southern aspect observed for gullies).

L26: 'both glacier-like forms' – 'both the estimated ages of glacier-like forms'

Corrected.

L30: Add 'and the timing of the formation of cirque-like alcoves' to this statement

We edited the statement to read as follows: "Future work is needed to specify the timing of the formation of cirque-like alcoves and whether their formation requires warm-based erosion."

L42: these aren't 'ice flow regimes' they are thermal regimes.

Corrected to thermal regime.

L43: Could add Gallagher et al. 2021 – they found grooves

Corrected to include Gallagher et al., 2021.

L64: space after lag

Corrected.

L65: estimates ranging from > thickness estimates ranging from

Corrected.

L73: As stated in a previous review, the caption first needs to introduce the general purpose of the figure. E.g. 'Examples of viscous flow features and alcoves mapped in this study'. Ensure all figure captions have such a statement at the start.
This sentence was added for Fig. 1: "Examples of alcoves mapped in this study and viscous flow features mapped in prior studies."
The following sentences were added for other figures:
Fig. 2: "Example of a cirque-like alcove on Mars alongside cirques from different regions on Earth."
Fig. 12: "Examples of geomorphic features corresponding to past glacial occupation of cirque-like alcoves."
Fig. 13: "Examples of mesa slopes with shallow alcoves, larger alcoves, and adjacent ice."
Fig. 14: "Scatterplot of mean elevation versus latitude."
L75: aprons plural x 2
Corrected.
L81-82: Given the new addition of Figure 7 , and the sample sizes discussed, this isn't correct as 'all alcoves mapped in this study'. It is an example of alcoves mapped in a sub-region of the study area.
Corrected to "A zoomed out view of all alcoves (not just cirque-like alcoves) mapped in a sub-region of the study area."
L88: These processes don't result in basal slip. Basal slop drives (some of) these processes (quarrying and abrasion, not frost weathering).
Corrected to read as follows: "This occurs via a combination of basal slip, quarrying, abrasion (e.g., White, 1970), and frost weathering (e.g., Sanders et al., 2012), which all contribute toward a tendency for rotational flow (Evans, 2020)."
L88-89: Delete the detail about meltwater through the bergschrund and randkluft. Too much detail, and inaccurate – meltwater can reach the bed from elsewhere too, e.g. crevasses.
Deleted so that it now reads as follows: "This occurs via a combination of basal slip, quarrying, abrasion (e.g., White, 1970), and frost weathering (e.g., Sanders et al., 2012), which all contribute toward a tendency for rotational flow (Evans, 2020)."
L95: Since we've changed planet, re-state glacier-like forms *on Mars.*
Corrected.
L98: Avoid the term putative. This means generally accepted, which isn't always true particularly for recent papers. Instead use hypothesised, or equivalent.
Corrected and changed to hypothesized.
P4,L00: Should this just be 'alcoves' here? Referring in general to alcoves, not your cirque like ones specifically.
Yes, good catch. Corrected to just alcoves.
P4,L02: If above change implemented, this can then become 'dedicated to identifying cirque-like alcoves'.
Corrected.
P4,L02: Here and elsewhere in the manuscript this should be regional population scale. Population without qualification implies global.
Corrected.

Figure 2: contour labels need to be larger in ii, and caption to state where panels are  oblique views e.g. at least bii, and possibly also cii, as this distorts the shape significantly. It is also not made clear that aii and bii are the same cirque.
The caption now specifies that aii and bii are the same cirque as the caption for b) now states: “(b) Uinta Mountains, Utah, USA (40.74°N, 110.05°W), same location as (a)(ii).”
aii was adjusted so that the image is no longer an oblique view, and contour labels were increased in size:

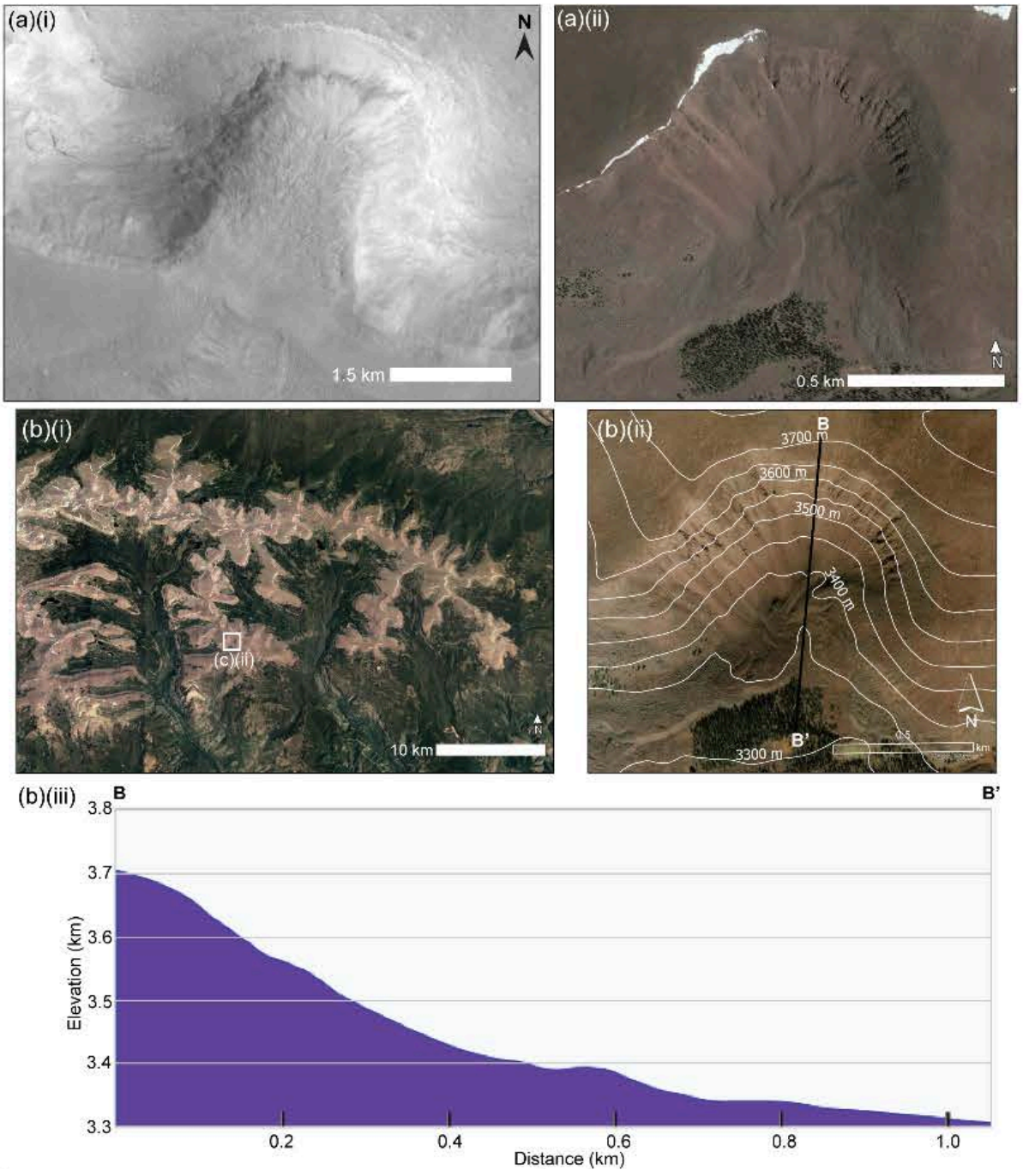
(a)(i)
N
1.5 km
(a)(ii)
N
0.5 km
(b)(i)
(c)(ii)
N
10 km
(b)(ii)
B
3700 m
3600 m
3500 m
3400 m
B'
3300 m
N
0.5
km
(b)(iii)
B
B'
3.8
3.7
3.6
3.5
3.4
3.3
Elevation (km)
0.2
0.4
0.6
0.8
1.0
Distance (km)

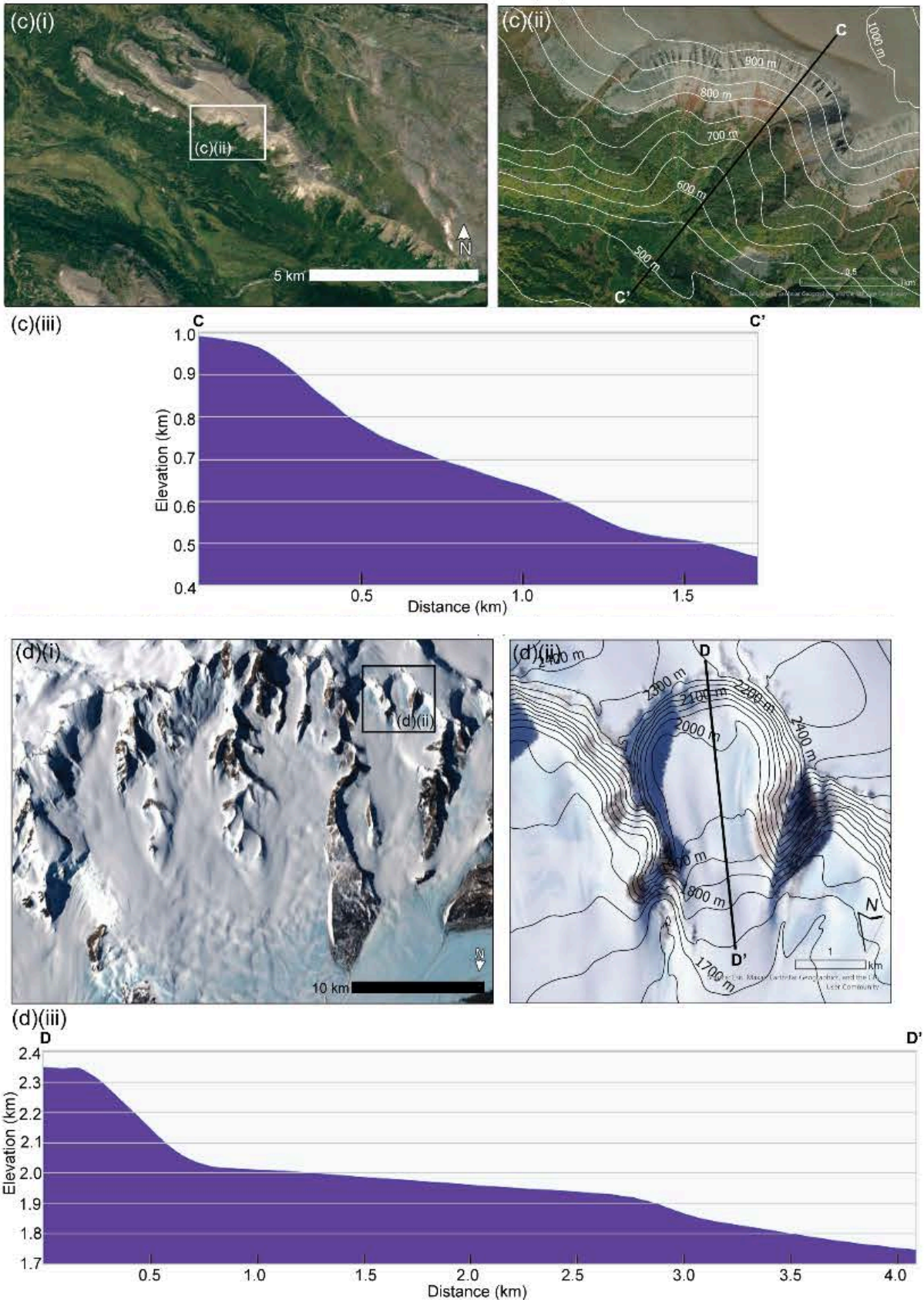


P8,L27: not clear what is meant by candidates here. One of the regions on Mars

where available data is most highly consistent with...
Corrected to read “one of the regions on Mars…”
P8,L30: avoid fretted - this is jargon and not particularly important. the key thing is that the terrain hosts valleys, plateaus and mesas.
Changed to “terrain hosting valleys and mesas.”
Also, I don’t think you need to say ‘of disputed origin’. It just adds unnecessary confusion. What is important is that it is just the antecedent topography for glaciation.
Corrected and deleted “of disputed origin.”
P8, L31-32: Wouldn’t this be better in the intro before you talk about the climate of the last 3Gyr? This also allows you to define Amazonian once only.
Moved to the Intro.
P8,L34: Mention glaciers specifically here.
We added the following sentences: “Much of the mantling unit also overlies the viscous flow features in the region (Baker and Head, 2015; Baker and Carter, 2019). These viscous flow features likely formed in the Middle to Late Amazonian (Head et al., 2010).”
P8,L38: sections on > sections towards
Corrected.
P8, L39: ‘including’. These are the only features labelled. Delete
Corrected to read as follows: “The major surface features Lyot Crater, Sinton Crater, and Mamers Valles are noted.”
P9,L9: For this extent of study area, this projection will induce distortions towards the longitudinal extremes. The reviewer requested an explanation of the magnitude of these distortions, but this has not been provided in the revisions. For future reference (assuming the calculated uncertainties in sinusoidal are tolerable), a lambert projection, as in Fig 3 would have reduced these distortions.
Good to know for future reference, thanks!
P9, L65-71: This works well – thanks for sticking with us!
Great to hear, thanks for the comments!
P10,L77: the stated equation doesn’t match the words. Need to add ‘taking the cube root of the product of’
This was edited to include volume as well. The corrected text now reads: We also calculate the total cavity volume of the alcove by multiplying the length, width, and height (LWH) and find the size by then taking the cube root of volume: $\sqrt[3]{LWH}$, following previous work (e.g., Barr and Spagnolo, 2015)
P10, L94: delete ‘to fit a table format’
Deleted.
P11, Altitudinal range row, column 4: delete minus – already say subtract
Corrected to read as follows: “Range of elevations found by subtracting minimum ax elevation from maximum elevation.”
P11, Elevation row, column 4: Mean elevation of what? All pixels within the polygon?
Corrected to “Mean elevation of all pixels within the polygon.”
P11, Aspect row, column 2: delete north (or degrees relative to north, but that isn’t typically stated).
Deleted.

Figure 4: Contour labels need to be larger
Corrected in the figure below:

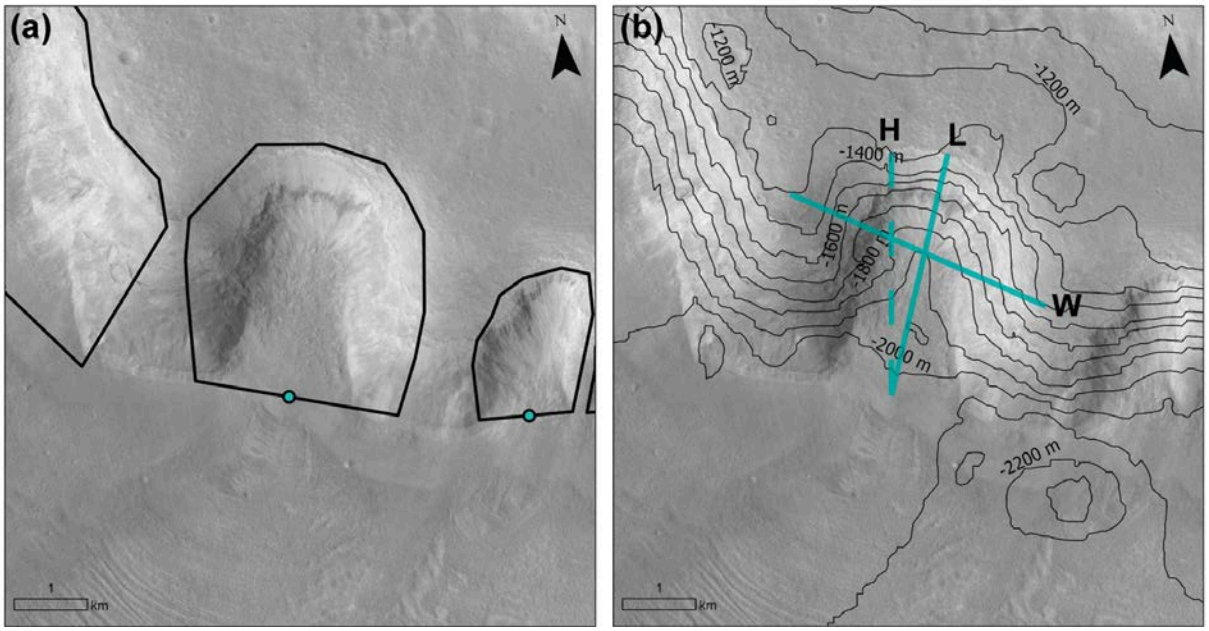


Also Figure 4: the revisions to panel B have introduced an error - the H line should end at the end of the L line. currently the H line measures outside the alcove boundary.
Corrected, see figure above.
P13, L08: alcove > alcoves
Corrected.
P13,L09: This isn't 'alignment', it is projection.
The word "aligned" was changed to "projected."
P13, L10: is 100m this the typical magnitude of misalignment? Are there any which exceed this?
Following the reviewer's comments, we have deleted that sentence and rephrased for clarification to the following: To evaluate any potential error introduced by misalignment between the CTX imagery and mosaicked HRSC DEM, we compared a CTX DEM to the mosaicked HRSC DEM for nine cirque-like alcoves. The CTX DEM that included coverage of nine cirque-like alcoves had the ID j02_045640_2209_xn_40n339w_j16_050901_2209_xn_40n339w. We found the average percent changes for these nine cirque-like alcoves between the two DEMs to be 2.55% for height, 6.44% for aspect, and 2.35% for slope. Since these percent changes were minimal, all less than 7%, we determine that the mosaicked HRSC DEM is an accurate method to evaluate the cirque-like alcoves.
P15,L26: The lip in this profile appears to correspond to where the transect intersects mantling materials, so I suspect it is not a true lip but the mantling deposit.
This figure was deleted based on the reviewer's comments.
P15, L35: see earlier comment re icy geomorphic features. Better would be 'geomorphic features related to ice' - this could then include features *containing* ice and features formed by ice.
Corrected.

P15, L38: Better would be ‘mantling deposit’ – remember the mantle is a thing!
Corrected to mantling deposit—though not that as in Table 3 and throughout, we were referring to the latitude-dependent mantle.
P16, linear terrain row, column 5: accelerating flow is inherently extensional. Not clear therefore what is meant by compressed accelerating flow.
Good catch, we deleted that part.
P16, mantle row, column 3: This isn't the main descriptor of mantling deposits. There should be a preceding statement which is a primary description, then this can supplement it.
Edited to include the following description: “A deposit of layers of ice and dust from meters to tens of meters thick; Characterized by a ‘raised curvilinear edge for the upslope boundary’ (Khuller et al. 2021).”
P16, mound and tail row, column 3: core of ice? not really possible to tell this at this scale. More likely to be sedimentary. Definitely not a core of ice if equivalent to drumlins.
This was a typo, deleted “core of ice.”
P16, mound and tail row, column 4: I'd rephrase this as 'Drumlins, but with some morphometric differences'
Corrected.
P18, L53: alcoves *which* no
Corrected.
P18, L53: ‘and raised moraine like ridge’ this comes after 'no longer appear to', yet I can see arcuate features beyond the alcoves. Should this say that they *have* raised moraine-like ridges at their termini? If not, mention the arcuate features but state that they don't have significant relief - this is evidence that they once did contain glacial ice.
This was rephrased as follows: “(b) and (c) represent previously unmapped cirque-like alcoves which no longer appear to contain a volume of ice. While the unmapped cirque-like alcoves have arcuate features similar to moraine-like ridges that indicate past glacial ice, these arcuate features no longer have significant vertical relief.”
Figure 7: This is a really useful figure - thanks for adding. However, it needlessly repeats elements of Figure 3, and comes too late. Replace Figure 3 with this. You could also then use this figure to point to the locations of the examples shown in other figures.
We were initially hesitant to do this because it brings the results early into the work prior to when cirque-like alcoves are introduced in the Methods section, but we have made the suggested change.
P22, L83: Is it mean size? Or just size? Individual points are plotted. Please clarify and make clear in text.
Corrected, it should just be size and area.
P22, Table 4, column 4: Define somewhere how alcove volume was calculated. this isn't in the acme2 output table.
The following sentence was added in 3.2.2: We also calculate the total cavity volume of the alcove by multiplying the length, width, and height ($LWH$) and find the size by then taking the cube root of volume: $\sqrt[3]{LWH}$, following previous work (e.g., Barr and Spagnolo, 2015).
Fig 11: Could simplify this by only showing iii column – it repeats I and ii but is more useful because they are scaled.

Simplified to only show iii column:

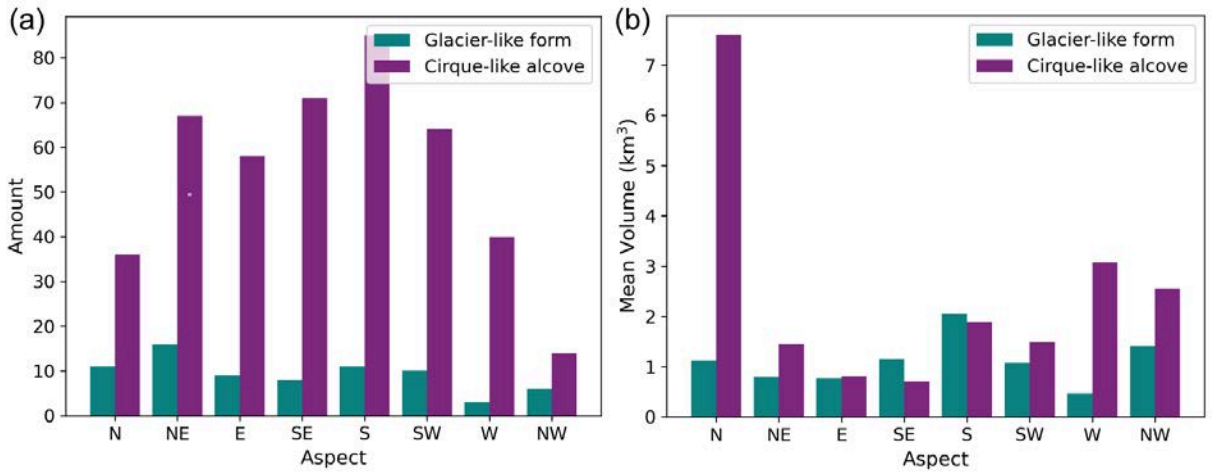


Figure 9: a) Bar plots of the aspect compared to the quantity of both cirque-like alcoves and glacier-like forms. b) Bar plots of the aspect compared to the average volume in each aspect direction for both cirque-like alcoves and glacier-like forms.

P23,L11. 'Average area'. Axis label says volume not area

Corrected to average volume.

P23, L16: I would argue that a feature such as a moraine or streamlined bedform does not necessarily mean that there is still ice (be that active or relict). It just means there was once ice there.

We agree and have edited the sentence to read as follows: "In addition to morphometric observations, we identified geomorphic features in association with the cirque-like alcoves as consistent with either past, remnant, or active ice in order to evaluate aspects of the glacial history in the cirque-like alcoves."

P24, Table 5. Change imagery to images. This is a metric of occurrence (yes/no) per image, not according to the area of image in which it occurs. Imagery could be interpreted as the latter. You could make it even clearer by 'Percent of HiRISE images containing feature' (same with CTX column).

Corrected.

P24,L28: presence *or past presence* of ice, or processes of ice loss.

Corrected.

P26,L53: by being called cirque-like, they are inherently *candidate* cirques. Rephrase to 'whether cirque-like alcoves are *indeed* cirques

Corrected.

P27, L63: 'more episodes + lasted a longer amount of time': these are listed as part of the same hypothesis, but should be separated. Then at the end, you can say it could have been a combination of these factors.

Corrected as follows: "This suggests that compared to Earth, the cirque-like alcoves in Deuteronilus Mensae on Mars may have formed due to more frequent glaciation events, longer-lasting glaciation, larger initial hollows for snow accumulation, faster glacial erosion rates (though this is considered unlikely; see Table 7), or a combination of these factors."

P27, L64 'erosion rates on Mars were much more rapid'. I don't think anyone is realistically suggesting this. It is ok to explain which are the least likely explanations. So I recommend counteracting this hypothesis before the future modelling statement.

This component was rephrased to state: “faster glacial erosion rates (though this is considered unlikely; see Table 7).”

P27,L69: winds don't have a lee side, slopes do. So more likely to grow on the lee side of slopes crossed by westerly winds?

Good point, corrected.

P27, L72: ‘northern winter’: under higher obliquity?

Yes, corrected to include “under higher obliquity.”

P27,L72-73: a bit repetitive given cirque bias is already stated. Simply state here that the observed bias is similar to glacier-like forms.

The earlier sentence was moved down an combined with this sentence to read as follows: “Similar to cirque-like alcoves in Deuteronilus Mensae, the glacier-like form population in the northern hemisphere also has an eastward bias (Souness et al., 2012).”

P27, L74: get rid of northerly, confusing when direction is opposite sense to a northerly wind. Just say poleward facing

Corrected to just say poleward facing.

P27,L77: what pattern? this reads as if they have an easterly bias (the main topic of the preceding paragraph). But I think you mean to compare to cirques on Earth.

We rephrased to “This poleward bias is typically seen…”

P27,L77 ‘found glacier-like forms to have a poleward bias’ – at global scales

Corrected to the following sentence and moved to 5.1.4 per a later comment: “Even though most glacier-like forms face the pole, the glacier-like forms with the largest volume face southwards in Deuteronilus Mensae (Souness et al., 2012; Fig. 9).”

P27,L78-79: grammar here is messy. Cut the sentence after 'glacier-like forms face southwards'. Then: in contrast, cirque-like alcoves in Deuteronilus.

These sentences were edited to as follows and moved to section 5.1.4 as per the later comment: “Even though most glacier-like forms face the pole, the glacier-like forms with the largest volume face southwards in Deuteronilus Mensae (Souness et al., 2012; Fig. 9). This may be due to a localized topographic effect for glacier-like forms in Deuteronilus Mensae. Glacier-like forms flowing northward are larger than those flowing southward by about 20%, in the northern hemisphere (Brough et al., 2019). The largest cirque-like alcoves by volume face north and west, which may be due to topographic effects as well, since most alcoves face south. For both glacier-like forms and cirque-like alcoves, the aspect with the highest amount of the regional population does not correspond to the aspect with the largest mean volume (Fig. 9).”

P27,L78: Grammatically, 'this' is referring to the cirques, but you mean to refer to the GLF trend. Revisit the grammar of this entire paragraph - it could be a lot tighter.

We reordered these two sentences as follows and moved them to 5.1.4 as per the later comment: “This may be due to a localized topographic effect for glacier-like forms in Deuteronilus Mensae because overall for the northern hemisphere, glacier-like forms flowing northward are larger than those flowing southward by about 20% (Brough et al., 2019). The largest cirque-like alcoves by volume face north and southwest, which may be due to topographic effects as well, since most alcoves face south.”

P27, L81-82: Move ‘for both…’ statement before the statement where you talk about the largest cirque-like acloves by volume.

We instead moved the following sentences to section 5.1.4 as per a later comment: “In contrast, the largest cirque-like alcoves by volume face north and southwest. For both glacier-like forms and cirque-like alcoves, the aspect with the highest percentage of the regional population does not correspond to the aspect with the largest mean volume.”

P27,L83-84: again, this is not written very clearly. Revisit this entire paragraph and tighten it up.

This sentence was deleted for clarity.

P27,L86: should the equator-facing statement be covered by the citations too?

This isn’t really explicitly stated, but we edited it to say “relatively less insolation” and moved the citation to the end of the sentence: “To explain the southward bias of cirque-like alcoves, we propose that this is consistent with periods of higher obliquity >45° on Mars, when poleward facing slopes received higher insolation and summer day temperatures, and equator-facing slopes received relatively less insolation (Costard et al., 2002; Kreslavsky et al., 2008).”

P27, L87-87:. Statement starting ‘as a result’. This sentence lacks a citation. I would also qualify southward-facing with (equator-facing), as you do in the conclusions - that is clearer

Corrected to the following sentence, note that a citation was not included because this was a statement from this work: “As a result, during periods of high obliquity, equator-facing cirque-like alcoves in the northern mid-latitudes would have been more favorable for ice accumulation.”

P28,L90: ‘remains unclear’… ...and alternative mechnisms which do not require liquid water have been demonstrated as possible mechansims for gully formation on Mars (citation).

The following sentences were added instead: “Meltwater generation is more commonly invoked for the formation of older, inactive gullies during periods of higher obliquity (e.g., Dickson et al., 2023; Noblet et al., 2024), while gullies that have been observed to be recently active invoke $CO_2$ frost, well as dry mass wasting during frost-free seasons (e.g., Dundas et al., 2022), though melting within dusty $H_2O$ ice is also a possibility (e.g., Khuller et al., 2021).”

P28, L91-92: ‘water ice precipitation’…otherwise known as snow ����

Simplified to “snow.”

P28, L96: ‘would allow for increased insolation’ need to explain under what climate/obliquity regime, since the earlier passage says that equator-facing slopes received less insolation. Separate these hypotheses out (there are currently contradictary statements in the same paragraph), and make clear when things are alternatives.

This was referring to present-day conditions (instead of high obliquity), but we have removed this sentence for clarity.

P28, L97-98: we explored this potential association in Section 5.1.2 – this is 5.1.2, delete.

Deleted.

P28, L98-99, sentence beginning ‘on the other hand’. move this up amongst the explanation of DM GLF distributions at the start of this paragraph. You say the largest ones face southward, but it is an important point that most are pole-facing.

This paragraph was split into four paragraphs, and the section beginning with “on the other hand” was moved up as the second paragraph before the last two paragraphs on gullies in section 5.1.2.

Figure 14: Captions need to have an introductory statement about what the figure shows overall.

The caption (for what is now figure 13) first reads: “Scatterplot of elevation versus latitude.”

P29, L21: It would make more sense for the GLF comparisons in the aspect section to move here.

Corrected so that the earlier two paragraphs are now in this section 5.1.4.

P30,L56: space in may lack

Corrected.

P30, L56-57: Not sure what you mean by elongation out of the alcove

This was rephrased as follows: “At a potentially earlier stage of evolution of the glacier-like forms, moraine-like ridges may reside within the alcove (Fig. 11a) rather than outside of the alcove (e.g., Fig. 11b, Fig. 5), potentially similar to a terrestrial cirque glacier sitting within the cirque basin instead of extending into the valley below and depositing a moraine there.”

Section 5.2.2: I still agree with the reviewer that this section is too speculative. I suggest deleting, to focus on the actual results of the data collection.

This section was deleted. Following the reviewer’s suggestion, the figure was modified and a portion of the text retained, though altered. This remaining text was moved to the end of section 5.1.2:

“Regardless of how gullies are initiated, they may act as a local depression in a location where snow could later accumulate for cirque-like alcove formation, such as if the gullies acted as a cold trap for snow (e.g., Dickson et al., 2023). For example, gullies could provide the initial concavity for a later cirque-like alcove to develop when glaciation occurs (Fig. 12), which is consistent with gully heads that have been proposed as initiation points for cirques on Earth (Derbyshire and Evans; 1976). In turn, deglaciation may also prime the landscape by exposing unconsolidated sediment for later gullying (e.g., Jawin and Head, 2021). Black arrows in Fig. 12a provides examples of shallow alcoves incised along the mesa slope. Fig. 12b includes similar shallow, elongate alcoves alongside larger alcoves with multiple channels. The shallow alcoves in Fig. 12a may indicate initial erosion of the mesa sidewall, while the larger alcoves in Fig. 12b may represent later stages of alcove development. While outside the scope of this study, additional analyses are necessary to evaluate this potential cycle as shallow alcoves or even gullies could create initiation points for cirque-like alcove formation and then deglaciation acts to prime the landscape for later gullying. Future work is necessary to elucidate this potential cyclical relationship of repeated ice accumulation and melt on the landscape.”

P31,L75-76: I don’t understand the need to invoke this alternative interpretation. Seems very unlikely.

This section was deleted.

P34,L42: millions of years > million years.

Corrected.

P35, L76-78: this should explain how the temperature at Beacon valley differs from the current mean annual temperature on Mars. The mention of the Butcher et al. velocities right at the end of this section - which are under Mars' current mean annual temperature comes too late, and contradicts the preceding statement that

mars glacier surface velocities are unknown.

The text was edited to include the mention earlier, including differences in temperatures: "Both the past temperatures and surface velocities of glacier-like forms on Mars are not well constrained and may have included short, warm periods that allowed for melting (Hubbard et al., 2014). Recent modeling using a mean annual present-day surface temperature of 210 K found a maximum surface velocity of $20 \times 10^{-6}$ m/yr for a thin (<100 m) viscous flow feature on a steep slope (Butcher et al., 2024), which would yield an unrealistic age for the cirque-like alcoves that is older than the age of Mars. For our estimates, for the wet-based case, we use a surface velocity of 2 m/yr (Cook et al., 2020) and for the cold-based case we use a surface velocity of $1 \times 10^{-3}$ m/yr corresponding to a mean annual ground temperature of 250 K, which was measured for a rock glacier in the Beacon Valley sector of the McMurdo Dry Valleys of Antarctica (Rignot et al., 2002). This cold-based case represents a low glacier flow speed on Earth."

P36, L96-97: but this should be qualified by the fact that this is based on surface velocities for terrestrial glaciers, which (as the butcher et al study shows) may not be realistic for the typical temperatures at Mars' mid latitudes. Can note that the temperature history is not well understood and could have been warmer at times, but the temperature assumption in the calculations needs to be addressed.

As mentioned above, the sentence now reads: "Both the past temperatures and surface velocities of glacier-like forms on Mars are not well constrained and may have included short, warm periods that allowed for melting (Hubbard et al., 2014)."

P37, L27: This should move up to qualify the statement that surface velocities of glaciers are unknown. You should also note that this was for a thin VFF (<100m thick), *but* on a steep slope (these two effects will somewhat counter eachother, but perhaps thicker ice flowed faster, though perhaps also a thin vff is an ok analogue for a cirque glacier).

As mentioned above, the sentence now reads: "Recent modeling using a mean annual present-day surface temperature of 210 K found a maximum surface velocity of $20 \times 10^{-6}$ m/yr for a thin (<100 m) viscous flow feature on a steep slope (Butcher et al., 2024), which would yield an unrealistic age for the cirque-like alcoves that is older than the age of Mars."

P38, L48: 'Kilometer-scale glaciation' odd phrasing. I don't think you really need to suggest you've extended the knowledge of glacial extent. The identification of cirque like alcoves is enough - e.g., extended knowledge about the landscape imprints of formerly more extensive glaciation in Dueteronius Mensae in the past, and potential landscape evolution processes.

Following this suggestion, we edited the sentence to now read as follows: "Thus, these cirque-like alcoves expand our knowledge about the landscape imprints of formerly more extensive glaciation in Dueteronius Mensae in the past and potential landscape evolution processes in this region."

P38,L54: Make the first conclusion: 435 alcoves in Deuteronilus Mensae are morphometrically consistent with origins as glacially-eroded cirques.

We accept this change and made it the first concluding point.

P38,L57-58: does this explicitly explain the latitudinal gradient *within* the mid latitudes (as opposed to favourable ice accumulation in the mid-lats relative to the poles?)

We agree that the phrasing here was confusing. We have reworded the last sentence here: “The largest cirques are in the lower latitudes of the study region at 40-42.9°N (Fig. 7a). This is likely the result of local topography because the local mesa height at different latitudes may limit local cirque-like alcove height and size (Section 5.1.3).”
We also moved the previous sentence to a different bullet point: “There is a dominant southward bias in the aspect of the cirque-like alcoves (Fig. 6), which becomes more pronounced above 46.5°N. This likely suggests cirque-like alcove formation during a period of high obliquity when conditions were more favorable for glacier growth at these latitudes because poleward-facing slopes received higher insolation and warmer summer daytime temperatures than equator-facing slopes.”

P39, L80 ‘glacial conditions’. arguably using terrestrial velocities is not 'using Mars glacial conditions'.

We changed “glacial conditions” to “temperatures.”

P39,L83-84: Qualify this with 'however, these estimates are highly dependent upon the past flow velocity chosen, which is poorly constrained for past climate regimes on Mars.

We added in the statement “These estimates are highly dependent upon the past flow velocity chosen, which is poorly constrained for past climate regimes on Mars.”

Data availability statement: Previous versions of the manuscript stated that the alcove data would be released. Now it reads that it will be available by email. Following ESurf policy, if data will not be released, a robust justification must be given in the statement. I recommend releasing the data as previously stated.

We will release the data as previously stated.

**egusphere-2023-2568 Review by S. Conway**

The manuscript has greatly improved in readability, clarity and robustness since the last review and I congratulate the authors on this. Notably they have sufficiently toned down the message on wet based glaciation, and made a good effort to shorten the manuscript. However, there are two aspects outstanding from my previous review that must be addressed before publication, together with a few other remaining loose ends detailed at the end and in the annotated PDF.

We thank the reviewer for taking the time to provide detailed comments on the manuscript. Below we include responses to the reviewer's main comments, and responses for shorter comments are in the attached annotated PDF.

1) the authors have to acknowledge and assess the impact of the uncertainties and errors in the elevation data they use for their analysis (see below for further details).

We have addressed the impact of uncertainties and errors below using three methods to demonstrate that any error introduced by mosaicking the HRSC DEM data is negligible. To summarize, this included negligible differences between CTX and HRSC DEM values, negligible differences in HRSC profiles across seamlines, and consistency in point locations in overlaps between HRSC DEM frames.

2) the authors should remove the highly speculative section 5.2.2 in the discussion, which detracts from the solid data they present in the results by making highly speculative interpretations based on image data and analysis techniques that are not reported in their methods/results. The discussion in section 5.2.2 is not needed as a basis of the main conclusions because the authors already make the point that former-gullies could be the initiation points for cirque growth when discussing the aspect trends. The existence of notches that resemble gully alcoves, if retained, needs to be demonstrated by showing some gully alcoves for comparison.

We have removed section 5.2.2. Figure 12 is a modified version of a prior figure from that section, and the associated text are now in section 5.1.2.

Associated text and figure (also provided below):

"In turn, deglaciation may also prime the landscape by exposing unconsolidated sediment for later gullying (e.g., Jawin and Head, 2021). Fig. 12a provides examples of shallow alcoves incised along the mesa slope. Fig. 12b includes similar shallow, elongate alcoves alongside larger alcoves with multiple channels. The shallow alcoves in Fig. 12a may indicate initial erosion of the mesa sidewall, while the larger alcoves in Fig. 12b may represent later stages of alcove development. Flow features indicate downslope flow of ice away from the mesa sidewalls. While outside the scope of this study, additional analyses are necessary to evaluate this potential cycle as shallow alcoves or even gullies could create initiation points for cirque-like alcove formation and then deglaciation acts to prime the landscape for later gullying. Future work is necessary to elucidate this potential cyclical relationship of repeated ice accumulation and melt on the landscape."

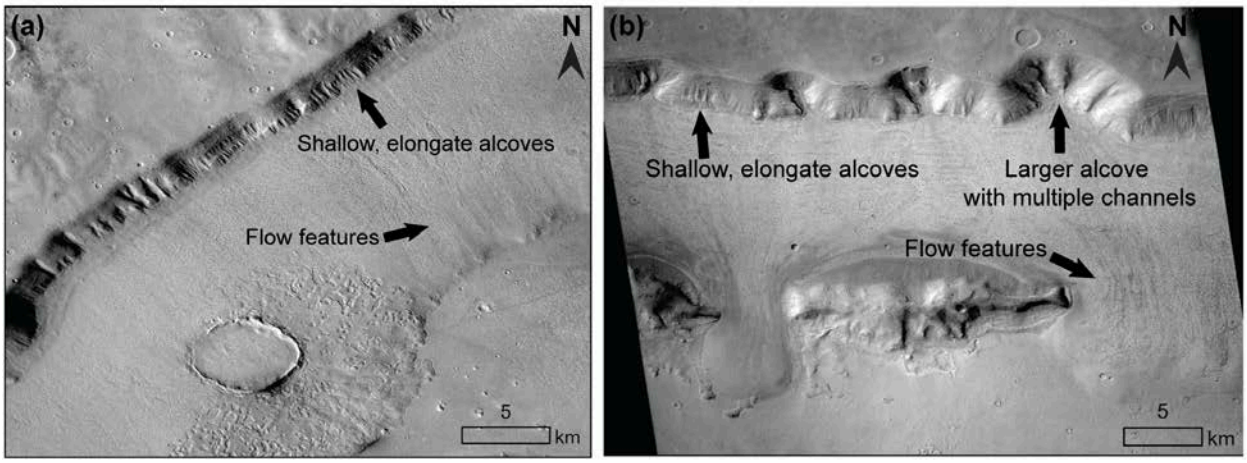


**Figure 12: Examples of mesa slopes with shallow alcoves, larger alcoves, and adjacent ice. (a) Shallow alcoves may indicate ice-associated erosion all along the mesa sidewall. Flow features indicate the downslope direction of ice flow. Centered at 41.06°N, 17.88°E in CTX image D04_0288880_2193_XI_39N342W. (b) Shallow alcoves may indicate ice-associated erosion while larger alcoves with multiple channels may represent a later stage of development. Flow features indicate the downslope direction of ice flow. Centered at 40.02°N, 23.20°E in CTX image D21_035499_2203_XN_40N336W. HiRISE data credit: NASA/JPL/University of Arizona. CTX data credit: Caltech/NASA/JPL/MSSS.**

**General comments from previous review**

Original comment (c) when considering the uncertainties in the elevation data in section 3.2.3 please address how these may also affect the ACME data collection, specifically consider the noise in the HRSC product (clearly visible as step-artefacts on Figs 4 and 6), and how well the CTX and HRSC data were co-registered. Noise is accentuated in topographic derivatives such as slope, which is amongst the parameters extracted. Presumably the position of the long profile was determined based on the CTX image data (if this or is not the case then it should be described in the methods as mentioned in point b), hence co-registration is critical to have reliable and representative elevation data. Please state what projection system was used for the morphometric analyses and consider whether this introduced any uncertainties/distortion (including the slope calculation from the HRSC DTM). RESPONSE: We added the following text to what is now section 3.2.3 "Uncertainties in elevation and alcove longitudinal profile": We mapped the cirque-like alcove and identified the mid-threshold point using the CTX imagery. As mentioned in Section 3.1, both the CTX imagery and HRSC DEM were aligned to a Sinusoidal projection centered on longitude 25.5 degrees East, and were based on the IAU Mars 2000 Sphere datum. Any misalignment of up to 100 m between the image and the DTM is of little concern when it translates into metrics made by ACME2 since most metrics rely on multiple pixel measurements. This is certainly the case for slope, aspect and average elevation along the cirque length or the entire cirque area. Any misalignment might affect minimum and maximum elevation, but this is not a concern when using a

large sample size to evaluate population-scale metrics."

I don't think this is sufficient and I have included annotations in the PDF, but the main points are coped here:

- Line 53 "Mosaic to Raster" - describe what this tool does for those who might want to use another software, for example it is important to know what was done at the seamlines as this can cause big jumps in topography. Also what was the pixel size of the resulting DEM? Presumably the data were all reprojected to the sinusoidal projection of the measurements -

this should also be specified because reprojection can introduce artefacts when resampling the raster data.

We added the following lines: "The HRSC DEMs were mosaicked together using the Mosaic to New Raster tool in ArcGIS Pro using the method of "Last", which is where the output cell value of the overlapping areas will be the value from the last raster dataset mosaicked into that location. The pixel size of the resulting DEM was 100 m." The last sentence of the paragraph was also edited to be stated earlier in the paragraph and mention the projection: "Measurements from all of the imagery and DEMs were projected to use a Sinusoidal projection centered on longitude 25.5 degrees East, and were based on the IAU Mars 2000 Sphere datum."

To evaluate consistency across DEM frames, we found the elevation values of 20 random points that were at overlap locations and found the average percent change to be negligible at only 0.86%. The values for each point are provided in the table below. Note that DEM A and DEM B are different DEMs in each row in the table.

| Point | DEM A (meters) | DEM B (meters) | Percent Change |
|---|---|---|---|
| 1 | -3447 | -3403 | 1.293 |
| 2 | -3355 | -3330 | 0.751 |
| 3 | -3214 | -3233 | 0.588 |
| 4 | -3558 | -3525 | 0.936 |
| 5 | -3877 | -3882 | 0.129 |
| 6 | -1294 | -1276 | 1.411 |
| 7 | -1452 | -1439 | 0.903 |
| 8 | -767 | -783 | 2.043 |
| 9 | -2620 | -2548 | 2.826 |
| 10 | -2843 | -2809 | 1.210 |
| 11 | -1024 | -1023 | 0.098 |
| 12 | -3048 | -3065 | 0.555 |
| 13 | -3214 | -3233 | 0.588 |
| 14 | -1043 | -1027 | 1.558 |
| 15 | -2989 | -3004 | 0.499 |

| | | | |
|---|---|---|---|
| 16 | -2956 | -2957 | 0.034 |
| 17 | -3214 | -3233 | 0.588 |
| 18 | -1785 | -1791 | 0.335 |
| 19 | -2227 | -2230 | 0.135 |
| Average | | | 0.867 |

In addition, we evaluated the profiles across five random seamline locations of HRSC DEMs. Screenshots are provided below with points at the seams. Four of the profiles definitively demonstrate that there are no jumps between seams (pictured above the profile) in the mosaicked HRSC profile (used for the DEM profile). In one of the profiles, it is unclear if there is a jump or if it is the nature of the terrain. Either way, the difference is ~40 m, which is within the 100 m pixel resolution of the HRSC mosaic.

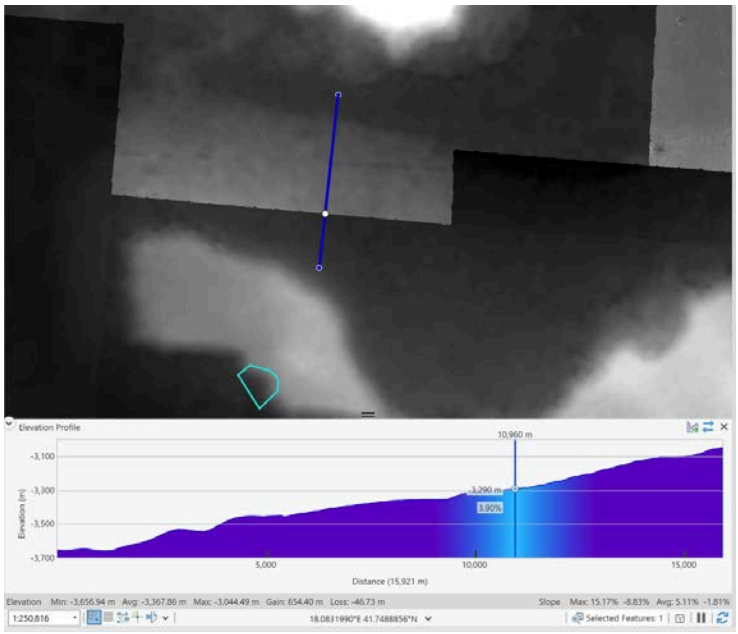

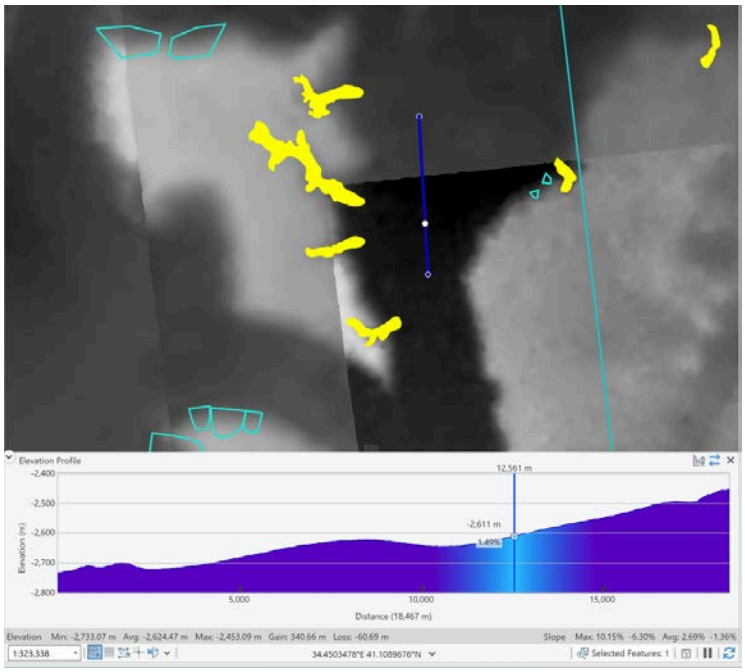


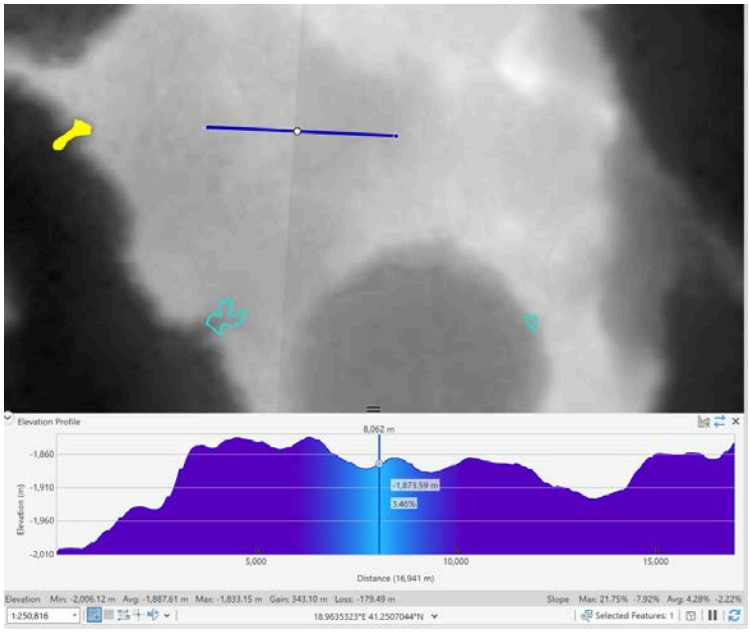


In the example below, there is a dip in elevation by ~40 m where the seamline is. This seems to be indicative of the actual terrain rather than a seamline jump. However, even if this is caused by the seamline between the two DEMs, this difference is within the 100 m pixel size for the DEM mosaic.

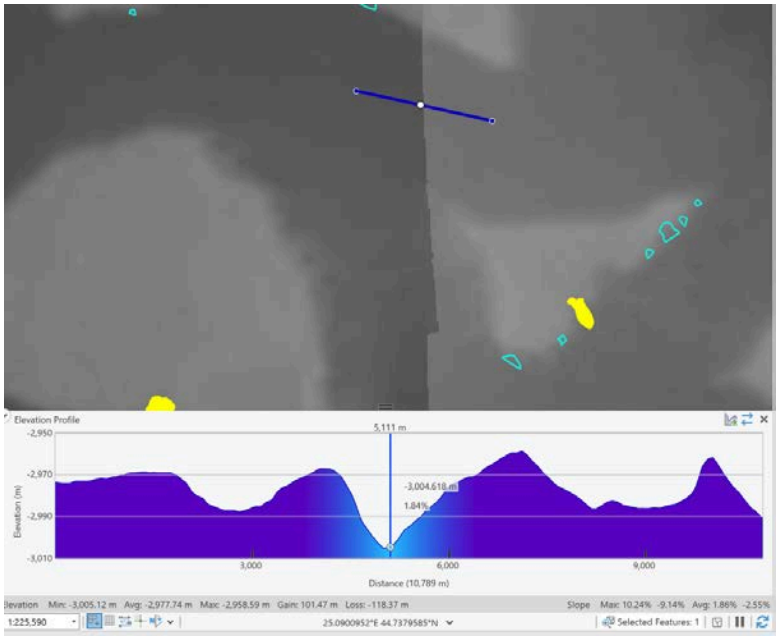


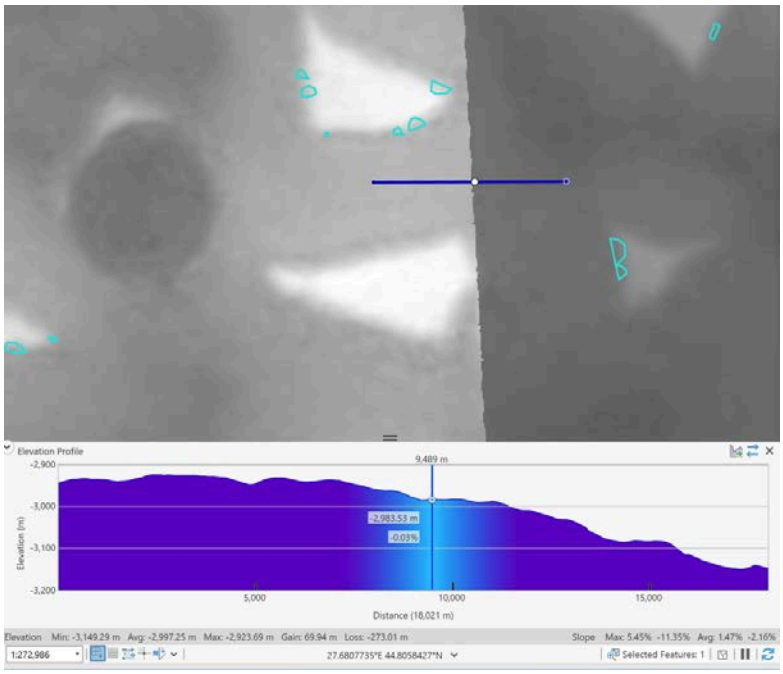


- Line 107 onwards: This section should evaluate the influence of the poor resolution and noisy quality of the HRSC data for making measurements with the ACME2. As the authors have compared to CTX an obvious way of doing this is to apply the software to alcoves and CTX
and HRSC DEMs and then compare the results. But at the VERY LEAST the fact that noise exists in the HRSC data and seams from the mosaicking process should be acknowledged and some attempt to evaluate how this noise/artefacts influence the results. Notably the noise can bias the results for aspect and slope, e.g. lots of noise means lots of steep pixels that don't really exist so the slopes will be

systematically too high. For aspect there may be over or under representation of certain orientations due to the shadows in the original images that make up the HRSC stereopair.

We have investigated the potential error introduced by using HRSC as follows:

1) There is limited CTX DEM coverage, however, we found one CTX DEM j02_045640_2209_xn_40n339w_j16_050901_2209_xn_40n339w publicly available that includes nine cirque-like alcoves. We reran ACME2 for the nine cirque-like alcoves using the CTX DEM to compare with the results from the HRSC DEM using percent change, calculated by using the following equation: |HRSC value - CTX value| / CTX value * 100%. As expected, length, width, and 2D area were exactly the same. The average percent changes for these nine alcoves were 2.55% for height, 6.44% for aspect, and 2.35% for slope. Since these percent changes were minimal, all less than 7%, we determine that the HRSC DEM is an accurate method to evaluate the cirque-like alcoves. We added the following text to section 3.2.3: "To evaluate any potential error introduced by misalignment between the CTX imagery and mosaicked HRSC DEM, we compared a CTX DEM to the HRSC DEM mosaic for nine cirque-like alcoves. The CTX DEM that included coverage of nine cirque-like alcoves had the ID j02_045640_2209_xn_40n339w_j16_050901_2209_xn_40n339w. We found the average percent changes for these nine cirque-like alcoves between the two DEMs to be 2.55% for height, 6.44% for aspect, and 2.35% for slope. Since these percent changes were minimal, all less than 7%, we determine that the mosaicked HRSC DEM is an accurate method to evaluate the cirque-like alcoves."
2) To evaluate any issues in mosaicking between HRSC frames, we evaluated 20 random points that are located on overlapping frames and compared their elevation values. We found the percent change to be negligible, at only 0.86%. The exact elevation values at each point are provided in the table above.
3) We also provide five examples of profiles from the mosaicked HRSC DEM across where there were seamlines. Four of these demonstrate that there are no obvious jumps. In one case, it is unclear if there is a potential jump of ~40 m, but regardless, it is within the 100 m pixel size of the DEM.

- Line 109: in Section 3.1 there was no mention of "alignment" just "Measurements from all of the imagery and DEMs used a Sinusoidal projection centered on longitude 25.5 degrees East", so please detail the alignment performed in section 3.1 (or say if no alignment was performed)

We added the following sentence in section 3.1: "No alignment was performed, however, we assessed the alignment by examining 20 random points across boundaries of various HRSC frames and found the difference to be negligible because the average percent change was only 0.86%."

- Line 111 "of little concern" - this is a subjective statement, please instead elucidate why it is of little concern and the quantitative data to support this statement

We have deleted this statement and added the following: "To evaluate any potential error introduced by misalignment between the CTX imagery and mosaicked HRSC DEM, we compared a CTX DEM to the HRSC DEM mosaic for nine cirque-like alcoves. The CTX DEM that included coverage of nine cirque-like alcoves had the ID j02_045640_2209_xn_40n339w_j16_050901_2209_xn_40n339w. We found the average percent changes for these nine cirque-like alcoves between the two DEMs to be 2.55% for

height, 6.44% for aspect, and 2.35% for slope. Since these percent changes were minimal, all less than 7%, we determine that the mosaicked HRSC DEM is an accurate method to evaluate the cirque-like alcoves."

- Line 111: in what ways do multiple pixels help? If for example the offset CTX-HRSC was always 100m to the west, aspect would be systematically wrong.

We apologize for poor phrasing. What we meant to say here was not that there is a misalignment of 100 m between the image and the DTM, but rather that there is a 100 m native resolution in the mosaicked DEM. This means that any time a mapped polygon touches a DEM pixel, it will be included in the analysis. This can result in up to a 100 m difference. However, over a 100 m length scale, the topography doesn't change much for these cirque-like alcoves. We have rewritten this section as follows: "To evaluate any potential error introduced by misalignment between the CTX imagery and mosaicked HRSC DEM, we compared a CTX DEM to the HRSC DEM mosaic for nine cirque-like alcoves. The CTX DEM that included coverage of nine cirque-like alcoves had the ID j02_045640_2209_xn_40n339w_j16_050901_2209_xn_40n339w. We found the average percent changes for these nine cirque-like alcoves between the two DEMs to be 2.55% for height, 6.44% for aspect, and 2.35% for slope. Since these percent changes were minimal, all less than 7%, we determine that the mosaicked HRSC DEM is an accurate method to evaluate the cirque-like alcoves."

To illustrate this issue of noise in the HRSC DEM data (here at its native 75 m/pix), I show below CTX beta01 compared to a portion of hillshaded HRSC ND4 h5213_0000 and its slope map. Clearly the red pixels which appear in bands across the smooth hillslope and exceed 30° are erroneous – such bands would have a strong influence on a mean value of slope across these hillslopes. The black box is an object approximately the size of the alcoves studied here. Seams between the HRSC DEMs would create significant E-W steps, rather than across slope steps, depending on the mosaic method utilised.

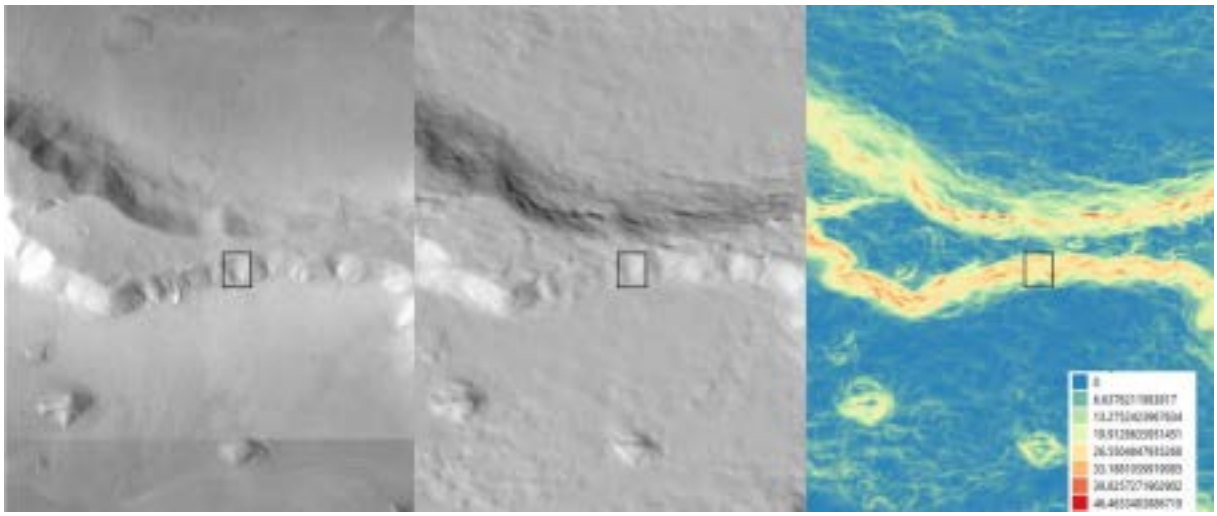

As mentioned above, we use three methods to demonstrate that any error introduced by mosaicking the HRSC DEM data is negligible. To summarize, this included negligible differences between CTX and HRSC DEM values, negligible differences in HRSC profiles across seamlines, and consistency in point locations

in overlaps between HRSC DEM frames.

Original Comment on Page 30 *** it is impossible to know if what you interpret as "less developed" landforms is how the "more developed ones" looked without a time machine or at least a good knowledge of the process(es) and their rates. I suggest complete removal of this section, it is complete speculation.

RESPONSE: We find it plausible that in the order of increasing amount of erosion, the mesa edge would go from straight to having shallow depressions then deeper depressions. As such, we kept this section and added the following sentences at the beginning of the second paragraph:

"Here, we assume that the side of the mesa evolves from a straight edge to an increasing number and depth of depressions. An alternative interpretation might be that the deeper depressions were subsequently filled up to create a straight edge, however, we do not see evidence for this amount of infilling." If the reviewer thinks that further analyses might be beneficial, we are open to any suggestions for additional analyses here.

Following the sentence "We suggest that the observed notches are gullies and would be able to act as necessary initiation points for ice accumulation that would later support glaciation and erosion that could form cirque-like alcoves," we also added this reference since this idea of gullying tied to alcove formation has been previously proposed in a paraglacial by Jawin et al. 2018 as well: "This is consistent with the mechanism proposed by Jawin et al. (2018)."

This response does not address my main concern that this section is too speculative – notably the figure includes interpretations that are not sufficiently substantiated with insufficient evidence to support them. For example, to demonstrate convincingly that the scarps mid-hillslope are "detached slabs" rather than just tectonic features would require detailed topographic and image analysis beyond the scope of this work (and even how relevant these observations are to the point that is being made is potentially debatable). I suggest the authors could briefly show small alcoves ("notches") that didn't reach their cirque threshold in a figure, compare them to gully alcoves and briefly suggest that there may be a continuum of features, but a whole section should not be devoted to this point. The connection to gullies extends way beyond what results can actually support in the current presentation.

We agree that this section was previously a bit speculative. As suggested, we have removed the section and retained a portion of it that was added to the last paragraph of 5.1.2: "In turn, deglaciation may also prime the landscape by exposing unconsolidated sediment for later gullying (e.g., Jawin and Head, 2021). Fig. 12a provides examples of shallow alcoves incised along the mesa slope. Fig. 12b includes similar shallow, elongate alcoves alongside larger alcoves with multiple channels. The shallow alcoves in Fig. 12a may indicate initial erosion of the mesa sidewall, while the larger alcoves in Fig. 12b may represent later stages of alcove development. Flow features indicate downslope flow of ice away from the mesa sidewalls. While outside the scope of this study, additional analyses are necessary to evaluate this potential cycle as shallow alcoves or even gullies could create initiation points for cirque-like alcove formation and then deglaciation acts to prime the landscape for later gullying. Future work is necessary to elucidate this potential cyclical relationship of repeated ice accumulation and melt on the landscape."

Figure 12 (previously Fig. 14) has been updated as well:

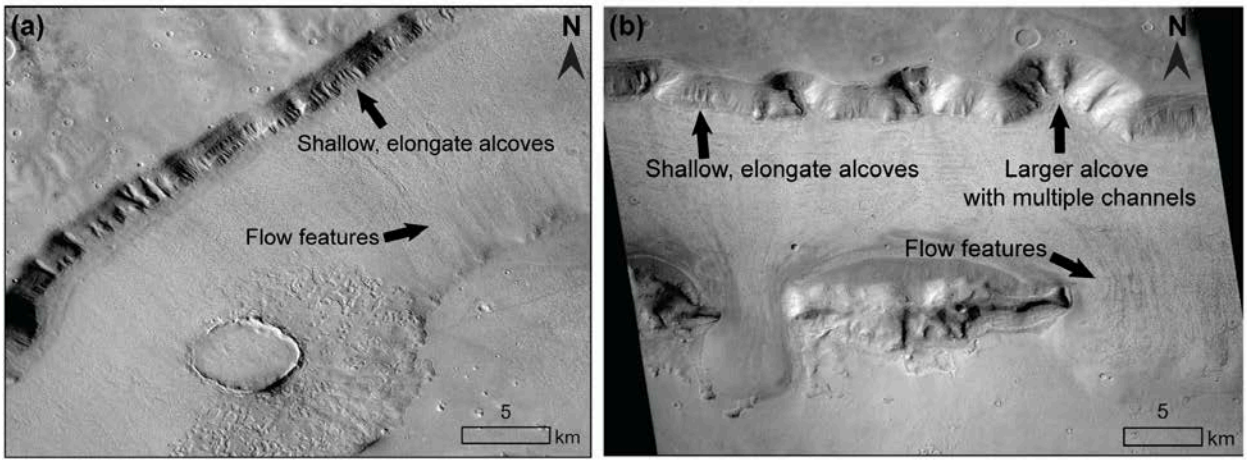


**Figure 12: Examples of mesa slopes with shallow alcoves, larger alcoves, and adjacent ice. (a) Centered at 41.06°N, 17.88°E in CTX image D04_0288880_2193_XI_39N342W. Shallow alcoves may indicate ice-associated erosion all along the mesa sidewall. Flow features indicate the downslope direction of ice flow. (b) Centered at 40.02°N, 23.20°E in CTX image D21_035499_2203_XN_40N336W. Shallow alcoves may indicate ice-associated erosion while larger alcoves with multiple channels may represent a later stage of development. Flow features indicate the downslope direction of ice flow. HiRISE data credit: NASA/JPL/University of Arizona. CTX data credit: Caltech/NASA/JPL/MSSS.**

Further points

- The supplementary data and/or data availability statement needs to be improved. Notably these is confusion as to which version of the CTX mosaic was used. It would be best-practise to include the datatable and shapefiles with the paper. Further details on the HRSC data are needed.

The shapefiles and spreadsheet of the cirque-like alcoves mapped in this study are provided. The HRSC DEM is also provided and was mosaicked using the following 29 Level 4 HRSC data frames: h5436_0000_da4, h5418_0000_da4, h5400_0000_da4, h5364_0000_da4, h5339_0000_da4, h5328_0000_da4, h5321_0000_da4, h5310_0000_da4, h5303_0000_da4, h5285_0000_da4, h5267_0000_da4, h5249_0000_da4, h5231_0000_da4, h5213_0000_da4, h3304_0000_da4, h3293_0000_da4, h3249_0000_da4, h3183_0000_da4, h2191_0000_da4, h1644_0000_da4, h1622_0000_da4, h1571_0000_da4, h1289_0000_da4, h1395_0000_da4, h1461_0000_da4, h1450_0000_da4, h1428_0000_da4, h1483_0000_da4, and h1201_0000_da4. The Level 4 HRSC data frames can be accessed at the ESA Planetary Science Archive: http://www.rssd.esa.int/index.php?project=PSA, HRSCview by FU Berlin/DLR: http://hrscview.fu-berlin.de/, or the NASA Planetary Data Science (PDS) http://pds-geosciences.wustl.edu/missions/mars_express/. This paper was prepared using the beta01 CTX mosaic: https://murray-lab.caltech.edu/CTX/beta01.html (Dickson et al., 2018).

- The methods to calculate the alcove volumes presented in section 5.1.1 need to be presented and the

results should also be first presented in the results before appearing in the discussion.

We think that based on additional comments on section 4.2 in the results section, the reviewer meant 4.2 not 5.1.1 in the discussion section (which is about size). We updated the following text in section 3.2.2 in methods to include the volume calculation: "We also calculate the alcove volume by multiplying the length, width, and height (LWH) and size by then taking the cube root of volume: $\sqrt[3]{LWH}$." In addition, in the caption in Table 4, we added the following: "Area and volume for glacier-like forms are found by Brough et al. (2019), where glacier-like form volume, including both debris and ice, is calculated using a volume-area scaling approach. Statistics for the cirque-like alcoves come from the topographic cavity of the alcove. We use total cavity volume as an approximation here, though cirque-like alcoves in their present state are not completely full of ice."

# Cirque-like alcoves in the northern mid-latitudes of Mars as evidence of glacial erosion

An Y. Li[1], Michelle R. Koutnik[1], Stephen Brough[2], Matteo Spagnolo[3], Iestyn Barr[4]

[1]Department of Earth and Space Sciences and Astrobiology Program, University of Washington, Seattle, 98195, USA
[2]Department of Geography and Planning, School of Environmental Sciences, University of Liverpool, Liverpool, L69 7ZT, UK
[3]School of Geosciences, University of Aberdeen, Aberdeen, AB243UF, UK
[4]Department of Natural Sciences, Manchester Metropolitan University, Manchester, M15 6BH UK, UK

*Correspondence to*: An Y. Li (anli7@uw.edu)

**Abstract.** Viscous flow features known as glacier-like forms on Mars have been observed emerging from alcoves that resemble cirques on Earth. However, many alcoves exist without associated glacier-like forms, and these features have never been studied or categorized at a population scale. On Earth, cirques form when depressions on mountain slopes accumulate snow, which gradually compacts into glacial ice. As the glacier flows downhill, it deepens the depression through erosion. Most of this erosion is driven by wet-based glaciers, although cold-based glaciers can also contribute to minimal headward and sidewall retreat in some cases. Here, we present evidence that cirque-like alcoves on Mars, similar to terrestrial cirques, are shaped by glacial erosion. To assess which alcoves on Mars are most "cirque-like", we mapped a population of ~2000 alcoves in Deuteronilus Mensae, a region in the mid-latitudes of Mars characterized by mesas surrounded by glacial remnants. Based on visual characteristics and morphometrics, we refined our dataset to 435 "cirque-like alcoves"–nearly six times the amount of glacier-like forms in the region–and used this to evaluate past glaciation on Mars. High-resolution imagery reveals icy geomorphic evidence of glacial occupation within these cirque-like alcoves, including flow features, linear terrain, mantle, moraine-like ridges, mound-and-tail terrain, polygonal terrain, moraine-like ridges, rectilinear-ridge terrain, and washboard terrain. Most cirque-like alcoves face south to southeast, similar to gullies poleward of 40°. Two possibilities to explain this trend are that southward facing cirque-like alcoves in the northern mid-latitudes were more favorable for ice accumulation during periods of high obliquity, or alternatively, increased insolation and meltwater is necessary for cirque-like alcove erosion. Using wet-based glacial erosion rates, the timescales for martian cirque-like alcoves align with both glacier-like forms (millions to tens of millions of years) and other viscous flow features such as lobate debris aprons (hundreds of millions of years). In contrast, cold-based erosion rates are only consistent with the older ages of lobate debris aprons. By mapping cirque-like alcoves at a large scale for the first time, we expand the catalog of features attributed to glacial erosion on Mars. Future work is needed to determine whether their formation requires warm-based erosion.

## 1 Introduction

The surface morphology of the mid-latitudes of Mars (especially between 30 and 60°, north and south) is characterized by glacial remnants in the form of subsurface ice (Fig. 1; e.g., Brough et al., 2019; Levy et al., 2014), and icy mantling deposits (Mustard et al., 2001). Observations and modeling suggest that the climate of the past 3 Gyr was unlikely to have permitted widespread liquid water on the planet's surface, though spatially-limited liquid may have occurred under some conditions (e.g., Kite, 2019). Glacial remnants in the mid-latitudes of Mars, referred to as viscous flow features, are typically considered to have always been frozen to their beds (cold-based) with limited subglacial erosion and ice flow only by internal deformation and gravity-driven viscous creep throughout their evolution (e.g., Mangold and Allemand, 2001; Head and Marchant, 2003; Shean et al., 2005; Mackay et al., 2014). Previous work has estimated cold-based erosion rates of 0.1-10 m/Myr during Amazonian glaciation on Mars (Levy et al., 2016). However, the presence of glacial landforms such as moraines and lineations observed in tandem with at least select viscous flow features suggests subglacial erosion could have occurred and that the ice-flow regime over the evolution of these landforms could have been formerly wet-based or at least a mixed thermal state as polythermal (e.g., Arfstrom and Hartmann, 2005; Morgan et al., 2009; Hubbard et al., 2011; Hubbard et al., 2014). In addition, recent work proposed that some depositional and erosional evidence of wet-based glaciation within the last 1 Gyr (Middle to Late Amazonian) exists, especially in the form of eskers, which would indicate warmer subglacial conditions at these sites (e.g., Gallagher and Balme, 2015; Butcher et al., 2017; Butcher et al., 2021; Gallagher et al., 2021, Woodley et al., 2022). Englacial debris bands have been found in viscous flow features, though it is unclear if the debris is from rockfall at the headwall or eroded and then entrained from the subglacial bed (e.g., Butcher et al., 2024; Levy et al., 2021).

Viscous flow features include the landform classifications of glacier-like forms (Souness et al., 2012), lobate debris aprons, lineated valley fill, and concentric crater fill (e.g., Squyres, 1979; Milliken et al., 2003; Levy et al., 2014). In the cases where subsurface radar sounding data are available, lobate debris aprons consist of up to ~90% ice (Holt et al., 2008; Plaut et al., 2009), and they account for ~63% of the total volume of ice contained within all viscous flow features (Levy et al., 2014). Lobate debris aprons can be a few to tens of kilometers long and up to one kilometer thick (Holt et al., 2008; Plaut et al., 2009). In comparison, glacier-like forms are generally smaller, on average ~4.66 km long, ~1.27 km wide (Souness et al., 2012), and ~130 m thick (Brough et al., 2019). All mid-latitude viscous flow features are believed to have been deposited during orbital excursions of ≥45° in the Amazonian (Madeleine et al., 2009). Lobate debris aprons, lineated valley fills, and concentric crater fills are estimated to range from ~10 Myr to 1.2 Gyr in age (Morgan et al., 2009; Berman et al., 2015), with most age estimations on the order of hundreds of millions of years (e.g., 300-800 Myr from Fassett et al. 2014). Glacier-like forms can superpose lobate debris aprons or lineated valley fills, suggesting polyphase glaciation with age clusters estimated to be around 2-20 Myr and 45-65 Myr (Hepburn et al., 2020). In addition to viscous flow features, there is a separate icy mantling deposit over the mid-latitudes originating from airfall deposits of ice nucleated on dust, known as the latitude-dependent mantle (e.g., Mustard et al., 2001; Kreslavsky and Head, 2002; Schon et al., 2009; Conway et al., 2018). The latitude-dependent mantle consists of different layers rich in water ice and dust (Schon et al., 2009). The ice was deposited during high obliquity excursions and the dust formed during low obliquities when the ice sublimated and left behind a dusty lag(Schon et al., 2009). Although the mantling unit covers >23% of the surface of Mars (Kreslavsky and Head, 2002), with estimates ranging from 1-30 m thick (Mustard et al., 2001; Conway and Balme, 2014), the mantling unit represents a small contribution ($10^3$-$10^4$ $km^3$) to the overall ice volume (Conway and Balme, 2014). In some locations the mantling unit has been mapped as "pasted-on terrain", though

it remains unclear whether the pasted-on terrain is a thicker mantling layer that is separate from an overlying mantle (Conway et al., 2018). The icy mantling unit is estimated to be younger than glacier-like forms at 0.15 to 10 Myr in age (Willmes et al., 2012; Schon et al., 2012).

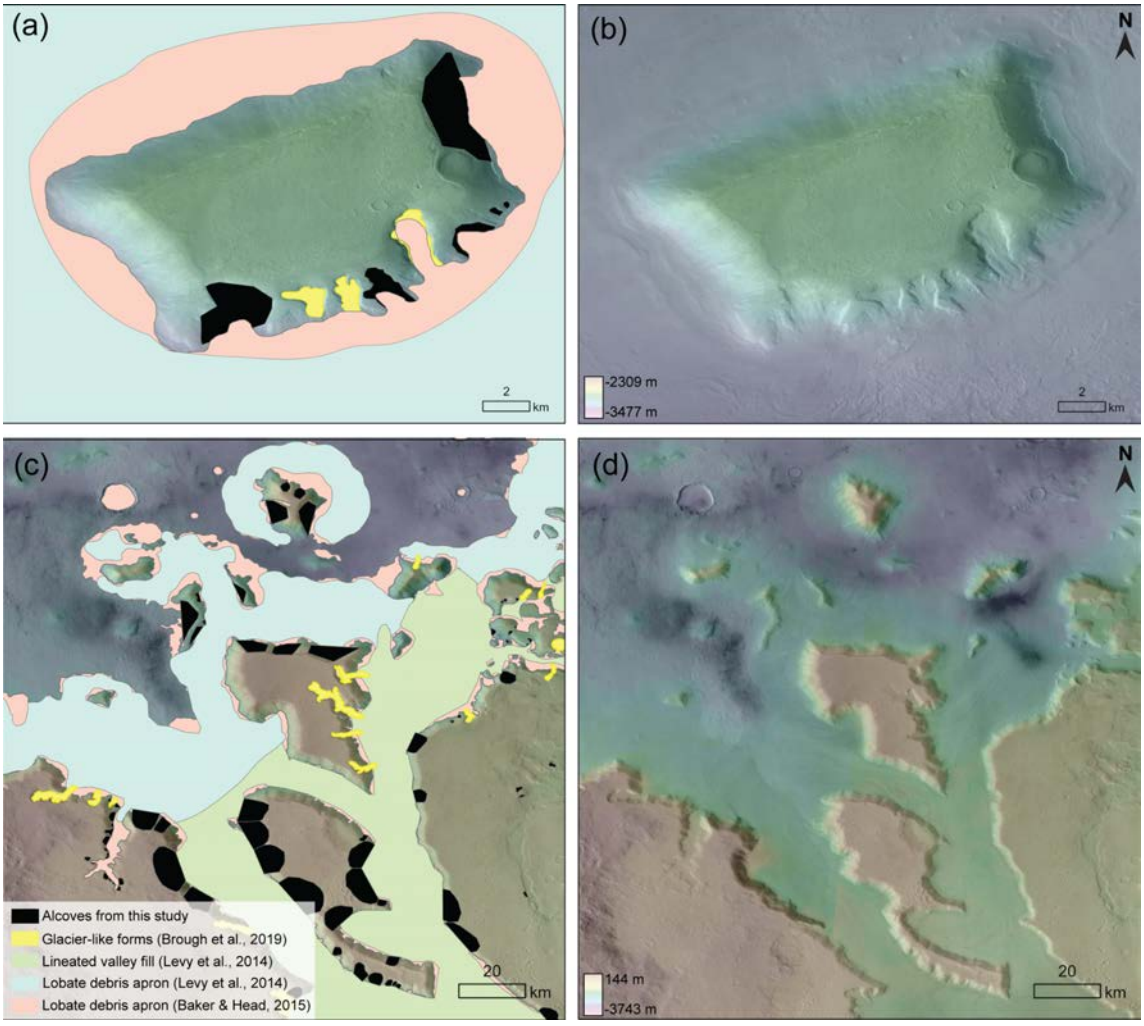


**Figure 1: Legend in the bottom left applies to panels (a) and (c). Black-filled polygons are alcoves mapped as part of this study, yellow-filled polygons are previously mapped glacier-like forms (Brough et al., 2019), blue represents the previously mapped lobate debris apron (Levy et al., 2014), and pink represents an updated map of lobate debris apron (Baker and Head, 2015). Note that there is some overlap between what previous studies generally classified as lobate debris apron and Brough et al. (2019) later specifically defined as glacier-like forms. Green-filled polygons represent lineated valley fill mapped by Levy et al. (2014). (a) Standalone mesa in Deuteronilus Mensae, centered at 45.5°N, 26.3°E. (b) The same mesa as in (a) but without mapped units delineated. The basemap is the CTX mosaic (Dickson et al., 2023a) overlaid on a High Resolution Stereo Camera (HRSC) (Neukum et al., 2004) digital elevation model (DEM)**

**that was mosaicked from 29 frames. (c) A zoomed out view of all alcoves (not just cirque-like alcoves) mapped in this study. The area is centered at 41.5°N, 34.0°E. (d) Same area as in (c) but without mapped units delineated. CTX data credit: Caltech/NASA/JPL/MSSS. HRSC data credit: ESA/DLR/FU Berlin.**

Glacial cirques on Earth are characterized by a concave basin connected to a steep headwall, often with a threshold or lip of higher topography at the lower end of the basin (Fig. 2biii). Cirques develop from incipient depressions in mountain and plateau sides that fill with snow/ice and over time support active glaciers that deepen the depressions by glacial erosion (Evans and Cox, 1974; Glasser and Bennett, 2004). This occurs via a combination of quarrying, abrasion (e.g., White, 1970), and frost weathering (e.g., Sanders et al., 2012) resulting in basal slip that is facilitated by rain and meltwater that goes through the bergschrund and randkluft, which all contribute toward a tendency for rotational flow (Evans, 2020). However, it is debated whether non-glacial processes such as rock-slope failures may have a substantial contribution to erosion as well (e.g., Turnball and Davies, 2006; Coquin et al., 2019; Evans, 2020). Due to their presence at high topographic locations on Earth and due to their concave shape, cirques trap snow and ice and are often the first sites to glaciate and the last sites to deglaciate (Graf, 1976). On Earth, with over 10,000 glacial cirques mapped globally, landform morphometrics are used to reveal regional climatic trends and the extent of glaciation in the past (e.g., Mîndrescu et al., 2010; Evans, 2006; Barr and Spagnolo, 2015).

Previous work described that glacier-like forms are formed in and extend out of "cirque-like alcoves" and that it is unknown whether the glacier-like forms and/or any ice masses that came before them were wet-based (Hubbard et al., 2014). Herein, we use the term "alcove" loosely to describe any hollow with an arcuate headwall and opening downslope, on the scale of hundreds of meters to a few kilometers in width and length. Putative cirques on Mars have been identified in the mid-latitudes (Gallagher et al., 2021) and equatorial regions (Davila et al., 2013; Bouquety, et al., 2019; Williams et al., 2023). While the cirque-like alcoves in areas such as Deuteronilus Mensae have been interpreted as potentially connected to past glaciation (e.g., Head et al., 2006; Morgan et al., 2009, Hubbard et al., 2011; Souness and Hubbard, 2013), there have not been any in-depth studies dedicated to these cirque-like alcoves on a population scale. In this study, we mapped 1991 alcoves in Deuteronilus Mensae in the northern mid-latitudes of Mars and conducted a morphometric analysis to narrow down 435 cirque-like alcoves. We evaluate the presence of icy geomorphic features in these cirque-like alcoves, their aspect as a population, and how they compare to other features such as glacier-like forms and gullies. Through mapping cirque-like alcoves at a large scale for the first time, we expand the extent of features attributed to glacial erosion on Mars.

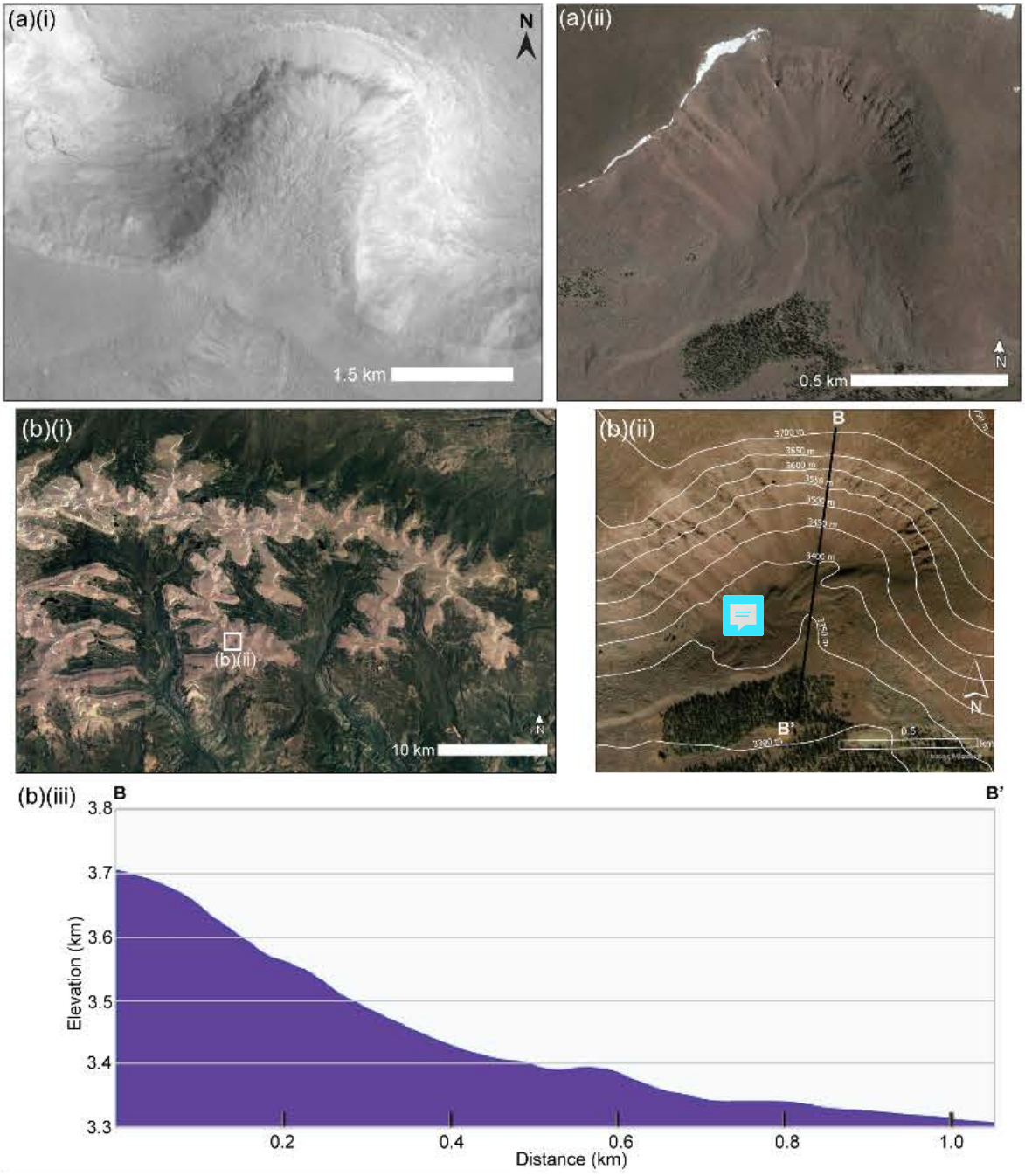
(a)(i)
N
1.5 km
(a)(ii)
N
0.5 km
(b)(i)
(b)(ii)
10 km
N
(b)(ii)
B
B'
N
0.5
(b)(iii)
B
B'
Elevation (km)
3.8
3.7
3.6
3.5
3.4
3.3
0.2
0.4
0.6
0.8
1.0
Distance (km)

07

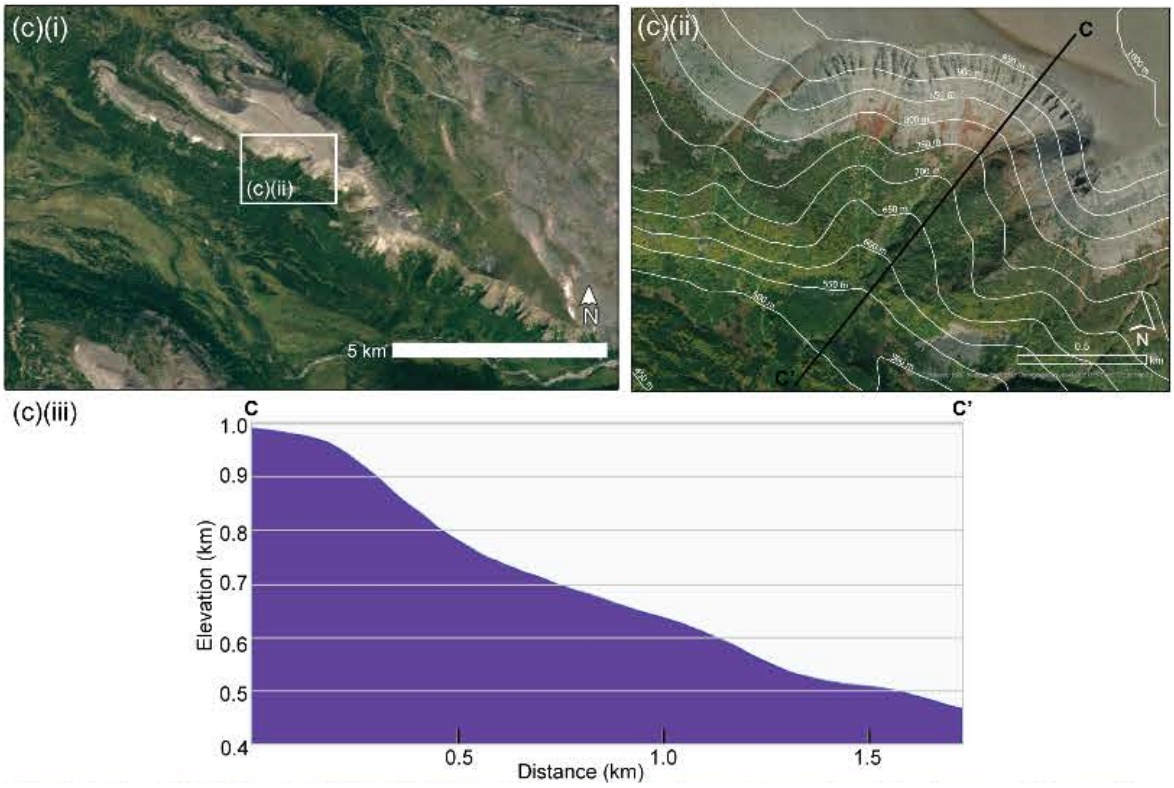
(c)(i)
(c)(ii)
N
5 km
(c)(ii)
C
C'
N
0.5
km
(c)(iii)
C
C'
Elevation (km)
1.0
0.9
0.8
0.7
0.6
0.5
0.4
0.5
1.0
1.5
Distance (km)

08

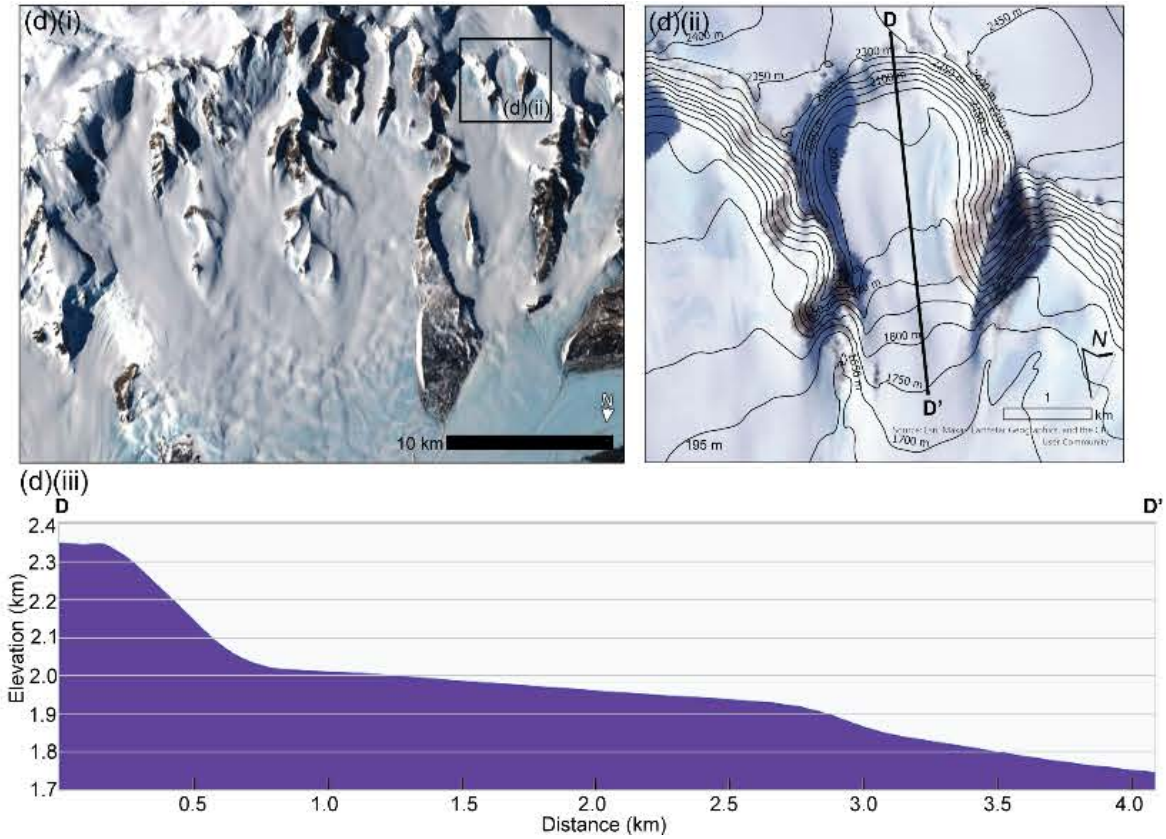


**Figure 2: (a)(i) Example of a cirque-like alcove on Mars (40.24°N, 34.48°E) (CTX mosaic; Dickson et al., 2023a) (a)(ii) a cirque on Earth in the Uinta Mountains (40.712°N, 110.114°W). CTX data credit: Caltech/NASA/JPL/MSSS. Earth imagery is from Google Earth including Landsat/Copernicus/U.S. Geological Survey coverage. (b)-(d) Examples of cirques on Earth incised into mesa topography, along with an example of a cirque profile in each. Part (i) of (b)-(d) provides an overview of the cirques in that location with an inset of the location of part (ii). Part (ii) of (b)-(d) offers a zoomed-in view of an individual cirque. Part (iii) of (b)-(d) shows the profile of the individual cirques in part (ii). (b) Uinta Mountains, Utah, USA (40.74°N, 110.05°W). DEM data: National Elevation Dataset, access via The National Map. (c) Kamchatka Peninsula, Russia (58.48°N, 160.70°E). DEM data: Shuttle Radar Topography Mission, access via EarthExplorer. (d) Transantarctic Mountains, Antarctica (80.01°S, 156.35°E). DEM data: Reference Elevation Model of Antarctica (Howat et al., 2022), access via the Polar Geospatial Center.**

## 2 Study Area: Deuteronilus Mensae

Our study region covers ~600,000 km$^2$ of Deuteronilus Mensae in the northern mid-latitudes of Mars (40-48°N, 16-35°E) (Fig. 3). While we also observe alcoves in other regions in the mid-latitudes of Mars, we focus on Deuteronilus Mensae as a study region for identifying cirque candidates due to its high density of icy viscous flow features (e.g., Levy et al., 2014; Baker and Carter, 2019; Brough et al., 2019). In addition to lobate debris aprons observed by the Mars Reconnaissance Orbiter

(MRO) SHAllow RADar (SHARAD) instrument (e.g., Plaut et al., 2009; Baker and Carter, 2017), recently, the Mars Subsurface Water Ice Mapping (SWIM) project identified Deuteronilus Mensae as one of the candidates where available data is highly consistent with the presence of subsurface ice at the regional scale (Morgan et al., 2021), Thus, Deuteronilus Mensae is a location of interest for future human missions to Mars (e.g., Morgan et al., 2021). Deuteronilus Mensae is characterized by fretted mesa terrain of disputed origin encompassed by remnants from previous glaciations (Sharp, 1973; Squyres, 1978; Carr, 2001; Morgan et al., 2009). The geologic history of Mars is divided into three main epochs: the Noachian around 4.0 to 3.85 Ga, the Hesperian around 3.56 to 3.24 Ga, and the Amazonian around 3.24 Ga to present-day (e.g., Hartmann, 2005; Michael, 2013; Kite, 2019). Previous geomorphic mapping estimated that the mesas date back to the ancient Noachian and the plains to the Hesperian, while younger Amazonian sedimentary deposits and a mantling unit overlay the mesas (e.g., Baker and Carter, 2019).

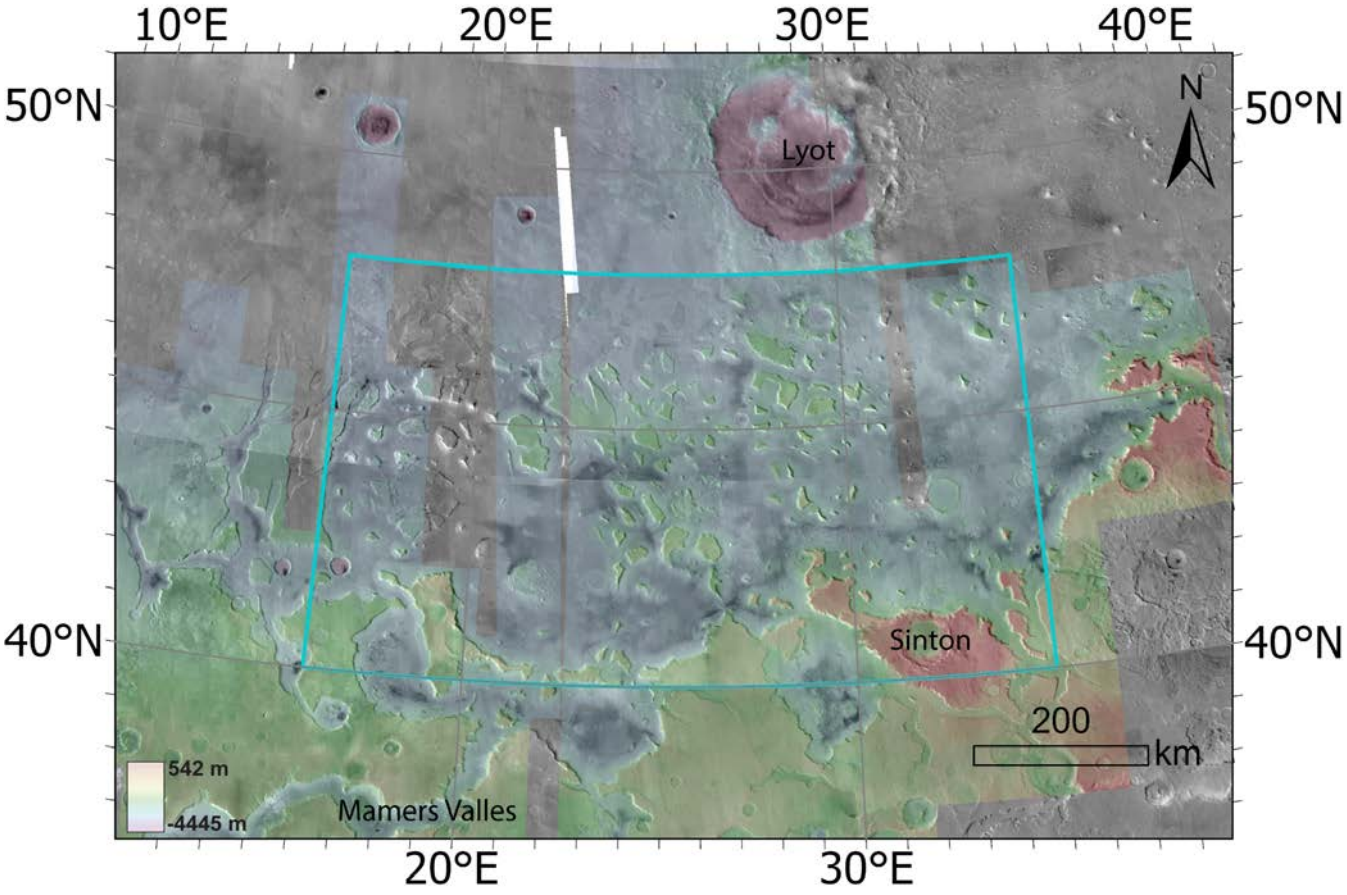


**Figure 3: The study region Deuteronilus Mensae in the northern mid-latitudes of Mars is within the teal box (40-48°N, 16-35°E). Colors represent HRSC DEM data. The white sections on the top left show where the CTX beta01 mosaic does not have coverage and grayscale areas of the map show where the mosaicked HRSC DEM does not have coverage. Major surface features including Lyot Crater, Sinton Crater, and Mamers Valles are noted. CTX data credit: Caltech/NASA/JPL/MSSS. HRSC data credit: ESA/DLR/FU Berlin.**

## 3 Methods and Data

### 3.1 Alcove Mapping

We mapped 1991 alcoves at a 1:30,000 scale using the ~6 m/pixel Context Camera imagery beta01 mosaic (Malin et al., 2007; Dickson et al., 2023a). We only map alcoves that do not contain previously mapped glacier-like forms (Fig. 1). We did allow overlap with previous mapping of lobate debris apron and lineated valley fill because boundaries for these lobate debris aprons and lineated valley fill were different between Baker and Head (2015) and Levy et al. (2014). In addition, it was not always clear how the mapped boundaries for the lobate debris aprons and lineated valley fills were decided on relative to where the alcoves and mesa sidewalls were located, which is why alcoves were mapped regardless of where the boundaries for the lobate debris aprons and lineated valley fills were drawn. We digitized the outlines of the alcoves using ArcGIS software. For morphometric analyses, we used a High Resolution Stereo Camera (HRSC; Neukum et al., 2004) digital elevation model (DEM) of 29 frames mosaicked together that comprises a mix of true resolution between 50-100 m/pixel (see Data Availability section for exact frames). The HRSC DEMs were mosaicked together using the Mosaic to New Raster tool in ArcGIS Pro. Where available, we used ~25 cm/pixel High Resolution Imaging Science Experiment (HiRISE; McEwen et al., 2007) images to examine glacial geomorphic features within and related to features coming out of the alcoves, which are listed in the Data Availability section. Measurements from all of the imagery and DEMs used a Sinusoidal projection centered on longitude 25.5 degrees East, and were based on the IAU Mars 2000 Sphere datum.

### 3.2 Criteria for Identification of Cirque-like Alcoves

#### 3.2.1 Alcove Classes

Cirques on Earth are categorized into five grades ranging from a "classic" cirque that contains "textbook" attributes to a "marginal" cirque, where the cirque status is doubtful (Evans and Cox 1995). In addition, there are also numerous cirque types including simple cirques, compound cirques, cirque complexes, staircase cirques, and cirque troughs (Benn and Evans 2010), which we drew upon to inform our preliminary alcove classes for our Deuteronilus Mensae analyses. Based on their kilometer-scale physical characteristics including shape, size, and associated landforms as seen in CTX imagery, alcoves that show any of the following morphologies: a) joined, b) interiorly ridged, c) staircase, d) channel-related, and e) branching were not included in our database. Descriptions and interpretations of these morphologies are provided in the Supplementary Material section. Although terrestrial glacial cirques may also fall into different categories, for our study of martian alcoves that are considered most analogous to terrestrial cirques, we focus on the alcoves classified as simple alcoves (and that do not have any of the morphologies listed above). Like simple cirques on Earth, simple alcoves on Mars are characterized by an armchair shape with an identifiable headwall, two sidewalls, and an opening downslope.

#### 3.2.2 Alcove Morphometric Calculations

We applied the Automated Cirque Metric Extraction (ACME2; Spagnolo et al., 2017; Li et al., 2024) tool in ArcGIS Pro to calculate alcove morphometrics, specifically, length (L), width (W), elongation (L/W), altitudinal range or height (H; difference between maximum and minimum elevation), area, slope, [illegible]ation, and aspect (Table 1). We also calculate the alcove size by multiplying the length, width, and height as follows: $\sqrt[3]{LWH}$. To use the ACME2 tool, we provided the mapped shape of the alcove, a threshold midpoint, which is defined as the midpoint of the down-valley lip of the cirque, and the HRSC DEM as inputs (Fig. 4). ACME2 outputs the morphometrics into the attribute table of the feature class for alcoves. On Earth, typical L/W ratios are 0.5-4.25 (Derbyshire and Evans, 1976), and based on 10,362 globally distributed cirques, both L/H and W/H ratios typically range between 1.5 to 4.0 (Barr and Spagnolo, 2015).

Note that by only including W/H ratios between 1.5 to 4.0, we expect that craters are excluded since craters typically have depth-to-diameter ratios of 0.1-0.2 (e.g., Robbins and Hynek, 2012), i.e., W/H ratios of 5:1 and 10:1. By using morphometrics, we also exclude other types of mechanisms for alcove formation, including active-layer detachments, deep-seated landslides, and theater-headed valleys (Table 2). This is because the H/L ratio of a terrestrial glacial cirque is expected to be deeper than any of the other alcove landforms with known morphometrics on Earth (Table 2). We focus only on the simple alcoves (based on morphology) that have these morphometric ranges for L/W, L/H, and W/H to constrain the most "cirque-like" alcoves on Mars. By applying these constraints, we were able to identify 435 cirque-like alcoves after downsampling from our initial mapping and classification based on only image analysis of 1991 alcoves. Herein, we use the term "cirque-like alcove" for the martian alcoves that we will evaluate in this study as candidate cirques shaped by glacial erosion.

**Table 1:** Alcove morphometrics as outputted by the Automated Cirque Metric Extraction (ACME2) tool. The content was modified from Spagnolo et al. (2017) to fit a table format.

| **Name** | **Unit** | **ACME2's output name** | **Definition** |
|---|---|---|---|
| Length | Meters | L | Length of the line within the alcove polygon that intersects the alcove threshold midpoint and splits the polygon into two equal halves (Fig. 4) |
| Width | Meters | W | Length of the line perpendicular to the length line and intersecting the length line midpoint (Fig. 4) |
| Elongation | Dimensionless | L/W | Derived from dividing length by width |
| Altitudinal range or height | Meters | Z_range (H in this paper) | Range of elevations found |

| | | | |
|---|---|---|---|
| | | | by subtracting max elevation minus minimum elevation |
| Elevation | Meters | Z_mean | Mean elevation |
| Area | Meters$^2$ | Area_2D | Area of the polygon |
| Slope | Degrees | Slope_mean | Mean value of slope for all DEM pixels included in the alcove polygon. |
| Aspect | Degrees north, within the 0-360° interval | Aspect_mean | Mean of all pixel aspects across the entire surface of alcove by using standard statistical calculation methods for circular features. We also found the relative percentages of cirque-like alcoves in each aspect bin after normalizing by the percent of the total land surface in each aspect bin. We did this by converting the HRSC DEM raster to points, finding the aspect for each point, and calculating the land surface percent that belonged to each aspect bin. We then divided the percent of cirque-like alcoves in each aspect bin by the land surface percent bins and got the normalized percentages. |

**Table 2:** Morphometrics consistent with different alcove-forming erosional mechanisms on Earth and Mars.

| **Formation mechanism/Landform** | **L/W** | **H/L** | **Aspect** | **Related geology** | **Typical scale (m)** |
|---|---|---|---|---|---|
| Glacial cirque on Earth | ~1, generally ranges from 0.5-4.25 (Barr and Spagnolo, 2015) | ~0.67 (Barr and Spagnolo, 2015) | All directions; poleward is favorable (Barr and Spagnolo, 2015) | Overdeepening, moraines | $10^2$-$10^3$ (Barr and Spagnolo, 2015) |

| | | | | | |
|---|---|---|---|---|---|
| Deep-seated landslide on Earth[n.s.] | >2.5 (Fran et al., 2006) | 0.1-0.35 (LaHusen et al., 2016; landslide scars from glacial sediment) | Not available* | Hummocky landslide deposits | $10^1$-$10^2$ (LaHusen et al., 2016) |
| Impact crater on Mars | ~1 | 0.1-0.2 (Robbins and Hynek, 2012) | N/A | Ejecta blanket | $10^1$-$10^3$ (Palucis et al., 2020) |
| Amphitheater-headed valley on Mars hypothesized to have formed by either groundwater sapping or outburst flooding | 1-10 (Laity, 1988) | Not available* | Not available* | Sandstone, not basalt bedrock (Lapotre and Lamb, 2018) | $10^1$-$10^2$ for canyon heads, up to $10^3$ for the main channel (Lapotre et al., 2016) |

Not available*: As of writing this paper, focused studies on the morphometrics of these landforms on the population scale are not widely available for these other landforms.

[n.s.]: "n.s." stands for "not scarp" since landslide morphometrics do not usually include measurements of the morphometrics of just the headscarp and sidewalls of where the landslides initiated.

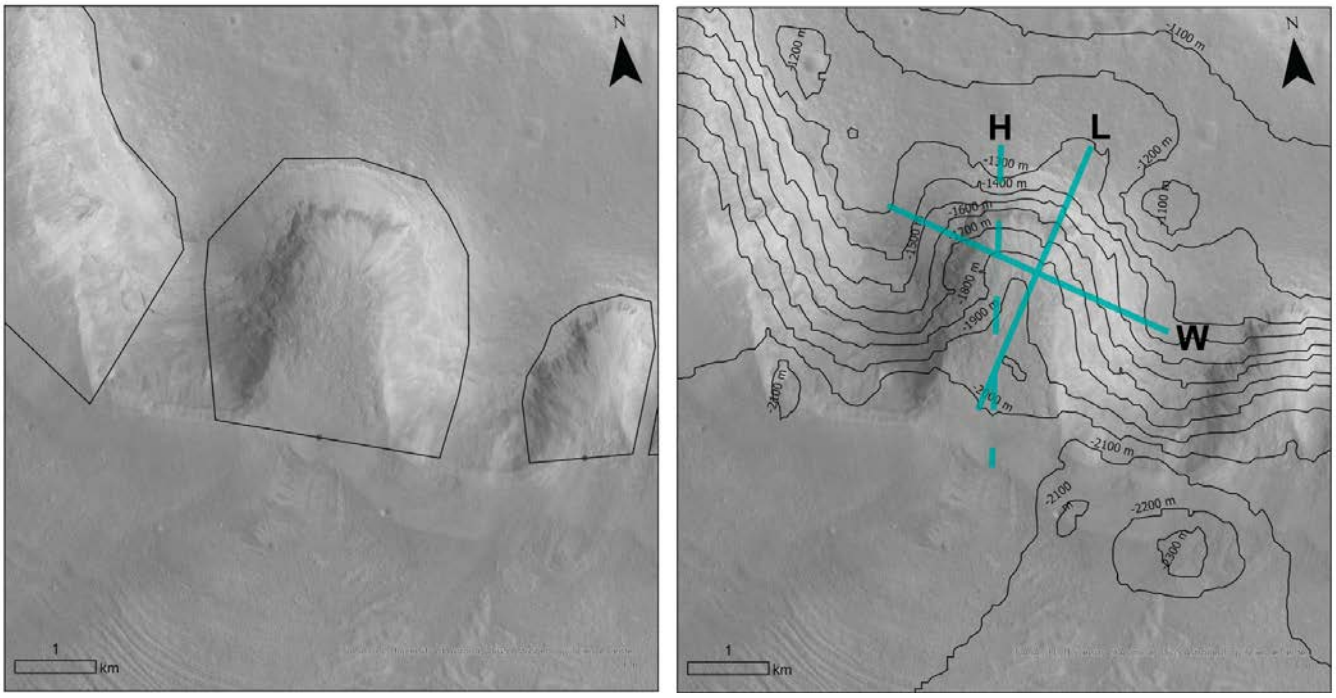


**Figure 4: (a) Inputs for the Automatic Cirque Metric Extraction (ACME2) tool (Spagnolo et al., 2017; Li et al., 2024) include a shapefile for the alcove, a point for the alcove threshold, as pictured here, and a DEM. (b) Outputs from ACME2 include morphometrics such as the length, width, and height of the alcove (see Table 1). CTX data credit: Caltech/NASA/JPL/MSSS.**

### 3.2.3 Uncertainties in elevation and alcove longitudinal profile

We mapped the cirque-like alcove and identified the mid-threshold point using the CTX imagery. As mentioned in Section 3.1, both the CTX imagery and HRSC DEM are aligned to a Sinusoidal projection centered on longitude 25.5 degrees East, and were based on the IAU Mars 2000 Sphere datum. Any misalignment of up to 100 m between the image and the DTM is of little concern when it translates into metrics made by ACME2 since most metrics rely on multiple pixel measurements. This is certainly the case for slope, aspect and average elevation along the cirque length or the entire cirque area. It might affect minimum and maximum elevation, although any effect should be evened out by the large sample size.

Longitudinal profiles of cirques on Earth are typically characterized by a concave bowl-shape with a steep headwall, flatter floor, and a lip or threshold at the end of the profile that separates the cirque from the valley below (e.g., Barr and Spagnolo, 2015). In Deuteronilus Mensae, an alcove threshold may be visible with the HRSC DEM resolution of 50-100 m/pixel (Fig. 5). However, in some cases, we do not see the threshold because of low DEM resolution or because the feature may be covered by other material (Section 4.3). For comparison to the HRSC DEM, we include a CTX DEM generated by the GALE lab at UCLA using the Ames Stereo Pipeline (Beyer et al., 2018; Fig. 5). Not all glacial cirques on Earth have thresholds

either (e.g., Fig. 2), nor is having a threshold a definitional requirement of terrestrial cirques (Barr and Spagnolo, 2015). As a result, we do not use the existence of an observable threshold as a requirement for identification as a cirque-like alcove on Mars.

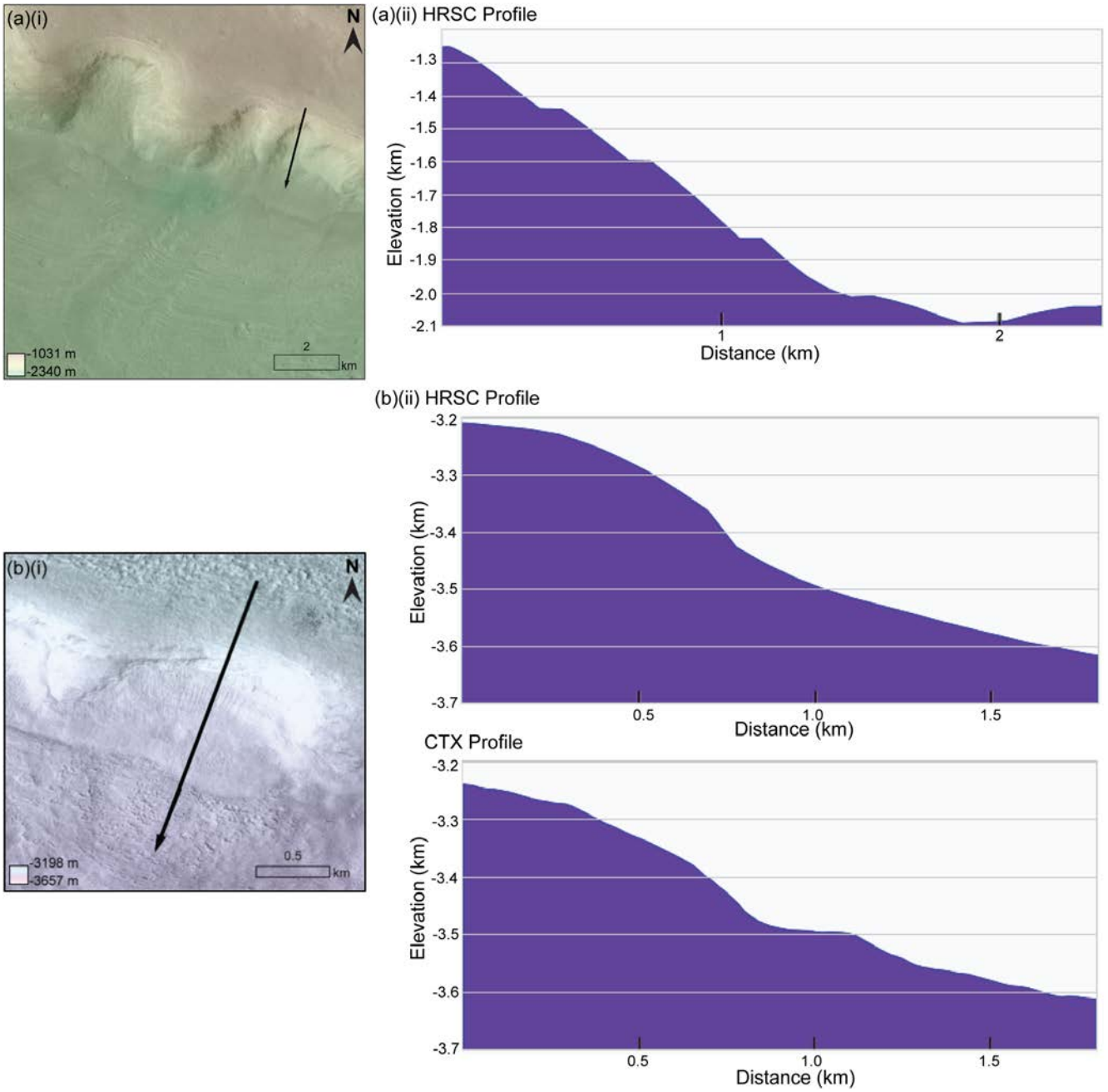


**Figure 5: Examples of HRSC DEM profiles to compare with a CTX DEM profile of an alcove. Arrows represent the path of the profiles from higher to lower elevations for both (a) and (b). (a) Example of the longitudinal profile of a**

**mapped alcove using the HRSC DEM that includes the potential overdeepening (difficult to discern at this resolution) and threshold or lip in the profile. The alcove is centered at 40.22°N, 34.57°E. in the CTX mosaic (Dickson et al., 2023a). (b) Comparison between the HRSC and CTX DEMs. The alcove is centered at 46.55°N, 22.08°E in HiRISE image ESP_019214_2270_RED. The CTX longitudinal profile contains a threshold, but the same feature in the HRSC DEM is not resolvable. CTX data credit: Caltech/NASA/JPL/MSSS. The CTX DEM was constructed by Dr. Mackenzie Day's GALE lab at UCLA. HRSC data credit: ESA/DLR/FU Berlin.**

### 3.3 Criteria for identification of icy geomorphic features

In addition to mapping and calculating the morphometrics of alcoves in Deuteronilus Mensae, we also evaluate the presence of icy geomorphic features in the alcoves where HiRISE imagery is available. While we designed the study so that none of the cirque-like alcoves that we mapped included mapped glacier-like forms, using the available inventory of HiRISE images we observed other features associated with the cirque-like alcoves that appear consistent with the presence of ice or ice loss. The icy geomorphic features that we evaluate for in HiRISE images include flow features, linear terrain, mantle, moraine-like ridges, mound-and-tail terrain, polygonal terrain, moraine-like ridges, rectilinear-ridge terrain, and washboard terrain. We identify these features using the criteria listed in Table 3. Other icy geomorphic features that were observed nearby alcoves but not categorized in this study because they were not directly in or connected to features coming out of alcoves included brain terrain (Levy et al., 2009a) and pitted terrain (Jawin et al., 2018). We note that the icy geomorphic features that we identify may correspond to some of the criteria defined by Souness et al. (2012) for mapping glacier-like forms, which include: 1) surrounded by topography indicative of flow around obstacles, 2) distinct from the surrounding landscape in texture or color, 3) surface foliation indicative of down-slope flow, 4) L/W ratio > 1, 5) discernible head or terminus, 6) appear to contain a volume of ice. However, the icy geomorphic features noted here do not include all of the criteria and were not mapped as glacier-like forms. For example, an icy feature within an alcove might appear to have a terminus, but no convexity from existing ice volume that differentiates it from surrounding topography (Fig. 6).

**Table 3:** Icy geomorphic features with their descriptions, proposed formation, and references.

| Icy Geomorphic Feature | Additional Names | Description | Terrestrial Analog | Proposed Formation Mechanism | Select References |
|---|---|---|---|---|---|
| Flow features | N/A | Longitudinal troughs and ridges | Surface | Formed by downslope ice flow and deformation | Hubbard et al., 2011; Souness et al., 2012<br><br>On Earth: Benn and Evans, 2010 |

| | | | | | |
|---|---|---|---|---|---|
| Linear terrain | If supraglacial: longitudinal foliation | Parallel raised ridges, bumpy in appearance | If supraglacial: flow stripes, longitudinal foliation | If supraglacial: Caused by deformation of ice as it flows; can be due to compressed, accelerating flow | Hubbard et al., 2011; Conway et al., 2018 |
| | If subglacial: pasted-on terrain | | If subglacial: megalineations, striations | If subglacial: Ice flow over water-lubricated sediment | |
| Mantle | Latitude-dependent mantle, thicker version is commonly known as pasted-on terrain | "Raised curvilinear edge for the upslope boundary" (Khuller et al. 2021) | N/A | Airfall of ice on dust; sublimation of ice generates a lag that protects underlying ice deposit | Mustard et al. 2001; Christensen et al., 2003; Conway et al., 2018; Khuller et al. 2021 |
| Moraine-like ridge | Moraine ridge | Ridge of debris at the terminus (end) of the ice mass | Terminal moraine | Dumping, squeezing, and pushing of debris by a glacier; left behind after ice recedes | Arfstrom and Hartmann, 2005 |
| Mound-and-tail terrain | N/A, similar to linear terrain | Steep upglacier-facing core of ice with a shallow elongate tail; typically 30-50 m long, 10-30 m across, and 2-4 m high | Closest to drumlins | Subglacial bedforms formed from subglacial sediment moulding and/or deposition beneath wet-based ice masses | Hubbard et al., 2011 |
| Polygonal terrain | Polygonized terrain and scaly terrain (we group the two together here under the term "polygonal" terrain); mantle polygons | Polygonized terrain: ~10° slope, 5-10 m across, tessellating polygons;<br><br>Scaly terrain: 12-16° slope, 10-20 m across, tessellating polygons | Periglacial patterned ground | Frost heave and thermal contraction cracking | On Mars: Hubbard et al., 2011; Levy et al., 2009b; Soare et al., 2022<br><br>On Earth e.g.,: French, 2018; Marchant and Head, 2007 |

| | | | | | |
|---|---|---|---|---|---|
| | | | | | |
| Rectilinear-ridge terrain | Push moraines | Series of ridges tens of meters across and 2-3 m high, elongated in an arc parallel to former glacier terminus | Thrust-block moraines, push moraines, moraine-mound complex | Basal debris thrust up from the glacier bed, basal crevasse fills, or ice-contact outwash deposits | On Mars: Hubbard et al., 2011<br><br>On Earth e.g.,: Hambrey et al., 1997; Sharp, 1985; Lukas, 2005 |
| Washboard terrain | Crevasse-like features | Transverse scarps, commonly at the base of a steep slope | Crevasses, bergschrunds | Formed from debuttressing and oversteepening of ice on slopes | Hubbard et al., 2011; Jawin et al., 2018; Jawin and Head, 2021 |

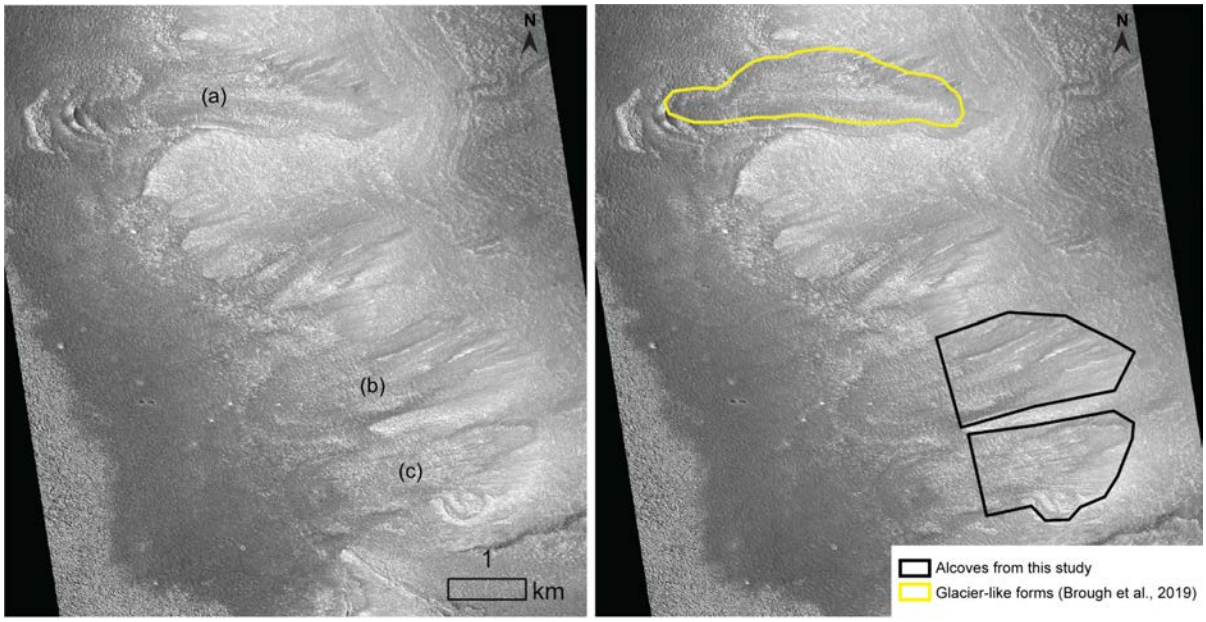


**Figure 6: (a) Previously mapped glacier-like form (Brough et al., 2019). (b) and (c) represent previously unmapped cirque-like alcoves no longer appear to contain a volume of ice and raised moraine-like ridge at the terminus. However, they still do contain surface foliations suggesting down-slope flow near the headwall. Cirque-like alcove mapping only extends to where the sidewalls end. This HiRISE image ESP_025873_2230_RED is centered at 42.63°N, 25.02°E. HiRISE data credit: NASA/JPL/University of Arizona.**

## 4 Results

### 4.1 Trends in aspect, size, area, latitude, slope, and elevation of cirque-like alcoves

By examining the aspect of the population of 435 cirque-like alcoves, we observe a south to southeast bias with an average of 153.09° (Fig. 8). The largest binned median size, defined as $\sqrt[3]{LWH}$, and area for cirque-like alcoves are located at lower latitudes (Fig. 9a). Most of the largest binned median size and area cirque-like alcoves correspond to slopes of 20-25° (Fig. 9b), and cirque-like alcoves have an average slope of ~21.1°. The binned median size and area of the cirque-like alcoves increase with elevation (Fig. 9c). Above 46° in latitude, most cirque-like alcoves cluster between 100-275° in aspect (Fig. 10a). We also notice a lower density of cirque-like alcoves facing 250°-360° at all latitudes (Fig. 10a). Cirque-like alcove elevation decreases as latitude increases (Fig. 10b). Similarly, cirque-like alcove height also decreases as latitude increases (Fig. 10c).

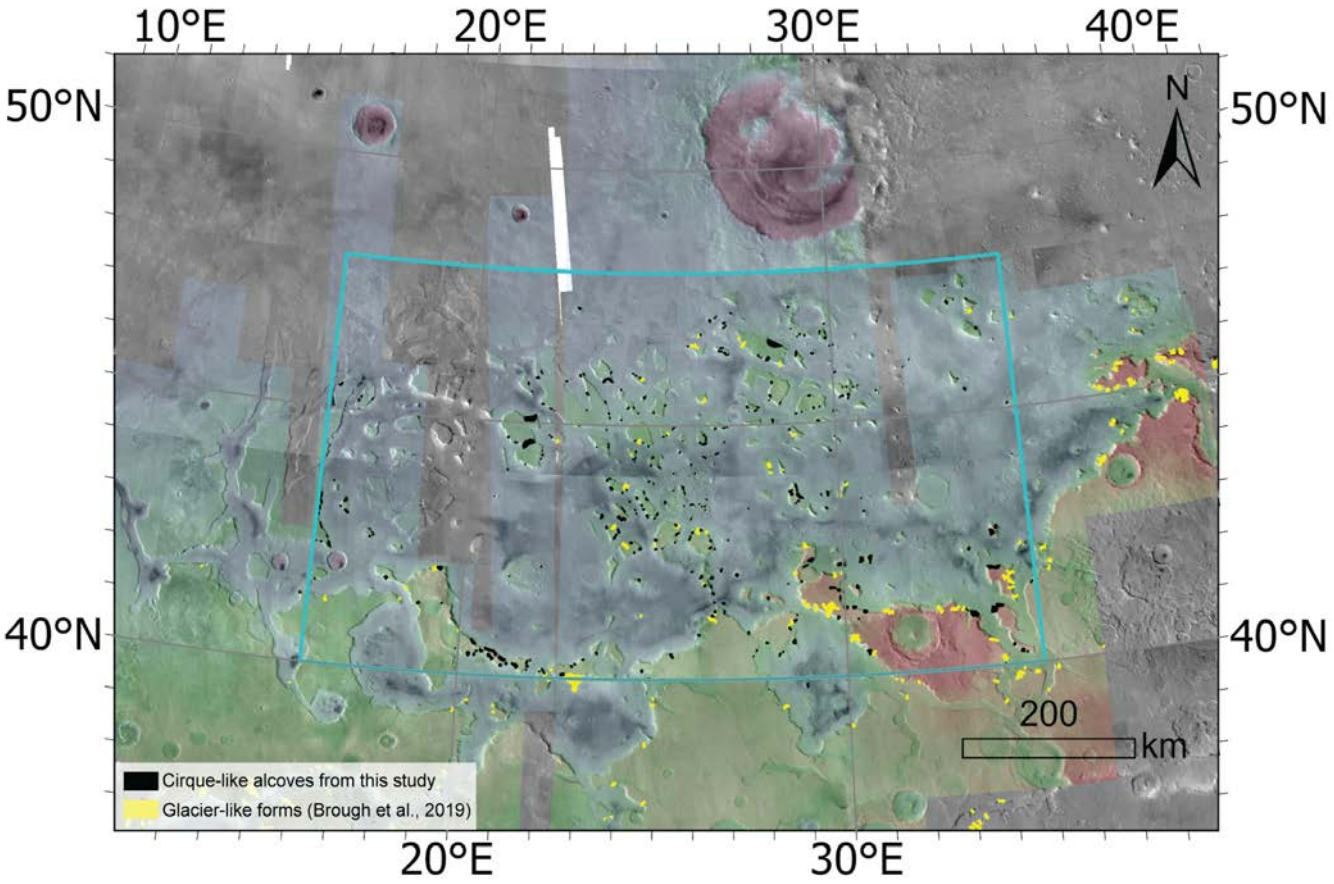


**Figure 7. Distribution of 435 cirque-like alcoves and 74 glacier-like forms in the study region Deuteronilus Mensae. Note that while glacier-like forms (Brough et al., 2019) and cirque-like alcoves exist outside of the teal boundary lines, they are not included in the analyses reported in this study.**

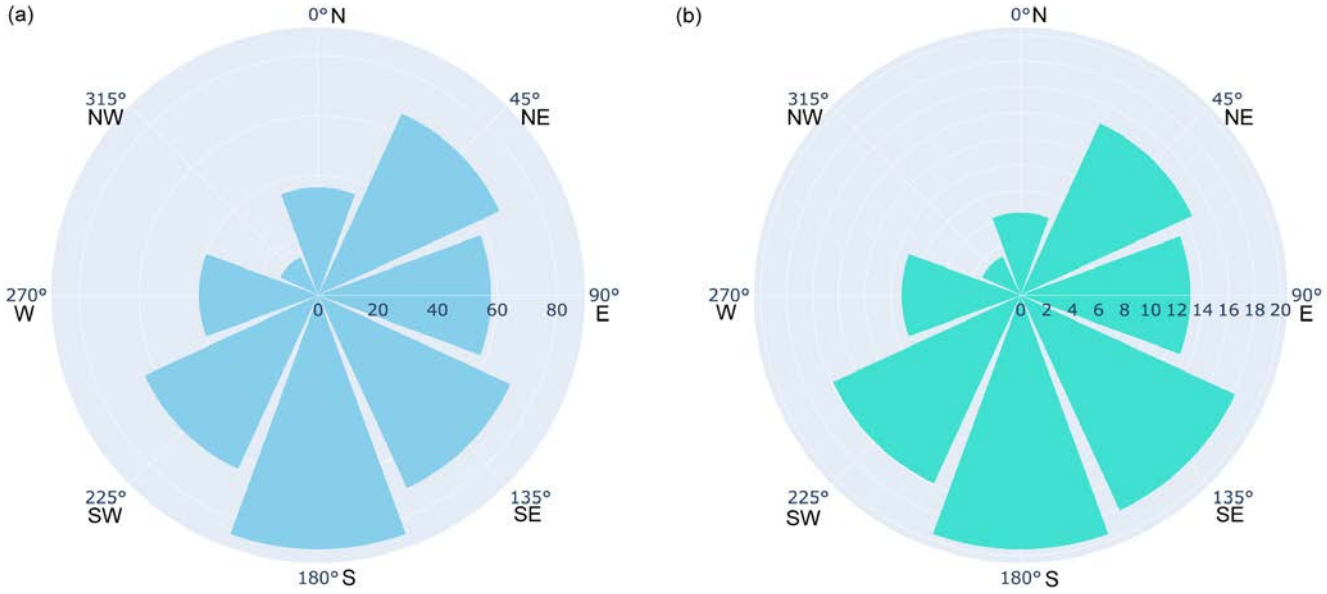


**Figure 8: (a) Rose diagram showing the aspect of cirque-like alcoves. Cirque-like alcove aspect averages 153.09° between the south and southeast directions. (b) Rose diagram showing the relative percentages of cirque-like alcoves in each aspect bin after normalizing by the percent of the total land surface in each aspect bin (we explain the method in Table 1). After normalizing, we found that the same southeastward trend persisted. Aspect bins are as follows: 337.5 ≤ N < 22.5°; 22.5 ≤ NE < 67.5°; 67.5 ≤ E < 112.5°; 112.5 ≤ SE < 157.5°; 157.5 ≤ S < 202.5°; 202.5 ≤ SW < 247.5°; 247.5 ≤ W < 292.5°; 292.5 ≤ NW < 337.5.**

Mean Size

Mean Area

a) Latitude

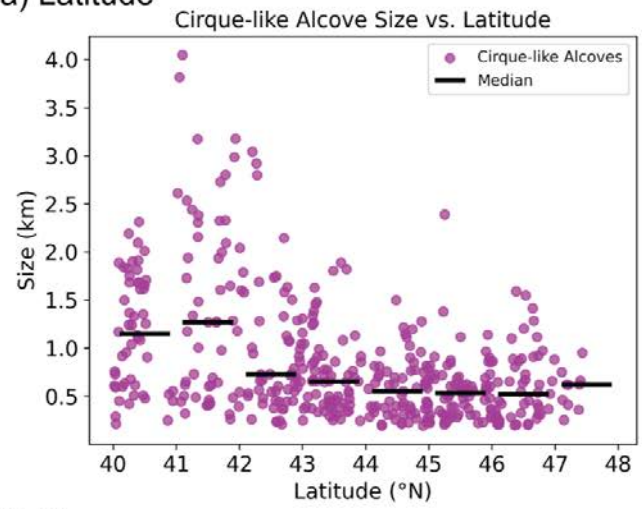


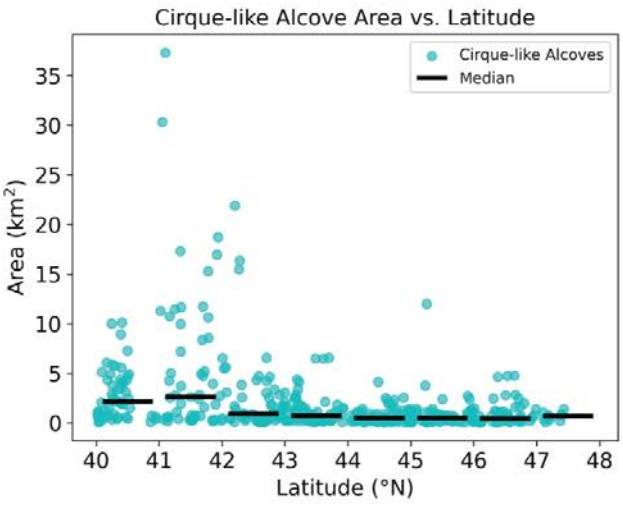


b) Slope

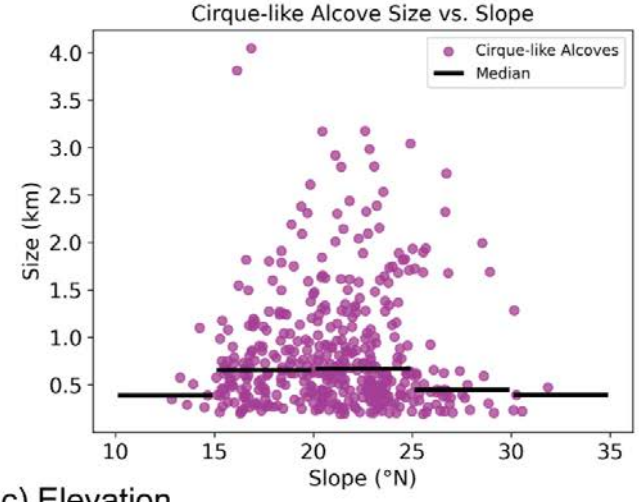


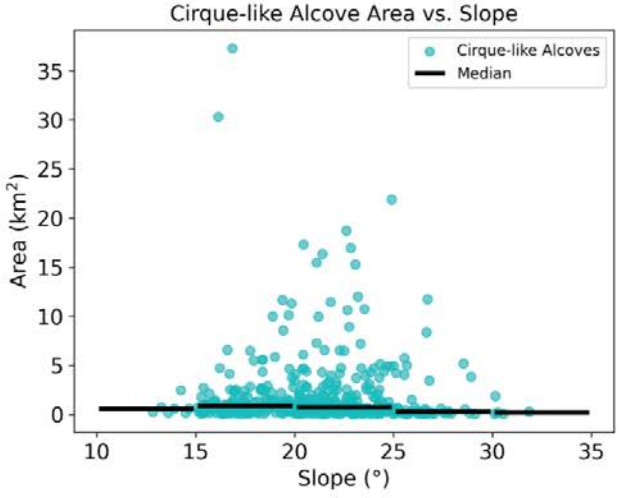


c) Elevation

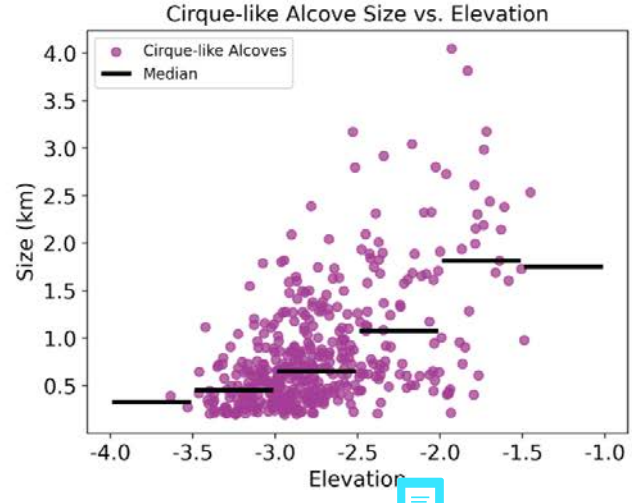


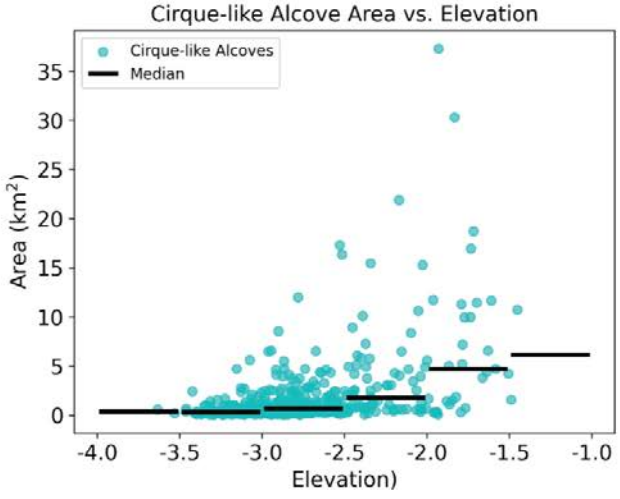

**Figure 9: Mean cirque-like alcove size $\sqrt[3]{LWH}$ and mean area vs. a) latitude, b) slope, and c) elevation for only cirque-like alcoves in Deuteronilus Mensae. Medians are displayed as black bars for each interval.**

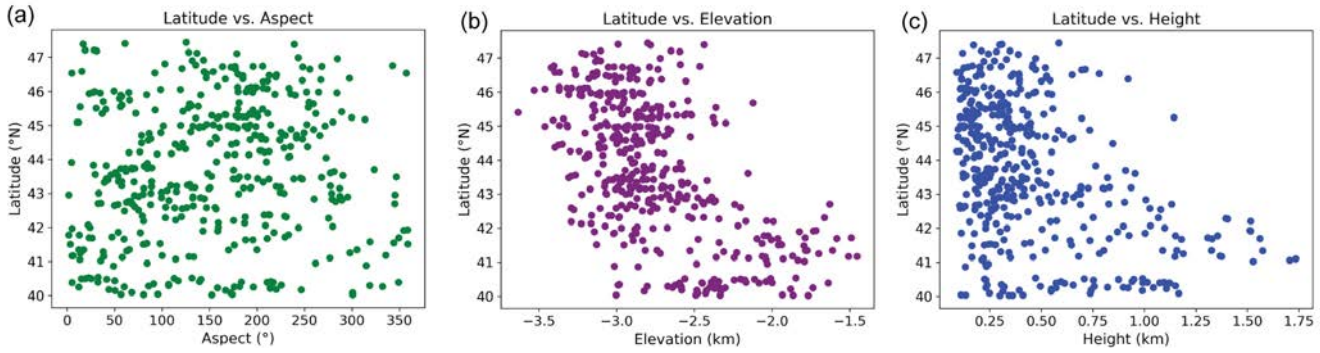


**Figure 10: Cirque-like alcoves in Deuteronilus Mensae plotted by latitude versus a) aspect, b) elevation, and c) height.**

### 4.2 Comparison between cirque-like alcoves and glacier-like forms mapped in Deuteronilus Mensae

Both the largest cirque-like alcoves and glacier-like forms are located in the southeast part of the study region (Fig. 7). By comparing the measurements of glacier-like forms (Brough et al., 2019) with cirque-like alcoves, we find that while the average area of an alcove is smaller than a glacier-like form, the total area of all the cirque-like alcoves is larger than the total area of the glacier-like forms (Table 4). There are 74 mapped glacier-like forms in Deuteronilus Mensae (Brough et al., 2019), which is only about 16% of the total 435 cirque-like alcoves in this study area. As a result, the aggregate total area and aggregate total volume for the cirque-like alcoves are larger than for the glacier-like forms. In addition, the average volume of an alcove is larger than that for a glacier-like form because the cirque-like alcoves have a greater height than the typical estimated thickness of a glacier-like form. ~70% of all cirque-like alcoves are within 10 km of a glacier-like form.

**Table 4:** Area and volume statistics of cirque-like alcoves versus glacier-like forms. Statistics for the cirque-like alcoves come from the topographic expression of the alcove, whereas the statistics for the glacier-like forms are from the present-day ice-rich form. We use total volume as an approximation here, though alcoves are rarely completely full of ice.

| | Average Area (km$^2$) | Total Area (km$^2$) | Average Volume (km$^3$) | Total Volume (km$^3$) |
|---|---|---|---|---|
| **Cirque-like alcoves (435)** | 1.95 | 848.98 | 2.03 | 881.42 |
| **Glacier-like forms (74)** | 7.79 | 576.82 | 1.14 | 84.01 |

While the highest percentage (22%) of glacier-like forms have a northeast orientation (based on data from Brough et al., 2019), the highest percentage (20%) of cirque-like alcoves have a southward orientation (Fig. 11a). For both glacier-like forms and cirque-like alcoves, the west and northwest aspects have relatively low numbers ranging from 2% to 9% of the entire population, though unlike glacier-like forms (15%), cirque-like alcoves also have a low proportion of 7% for the north-

facing aspect. For mean glacier-like form volume grouped by aspect, the largest glacier-like forms face southwards in Deuteronilus Mensae, whereas the largest cirque-like alcoves by volume face the north (Fig. 11b).

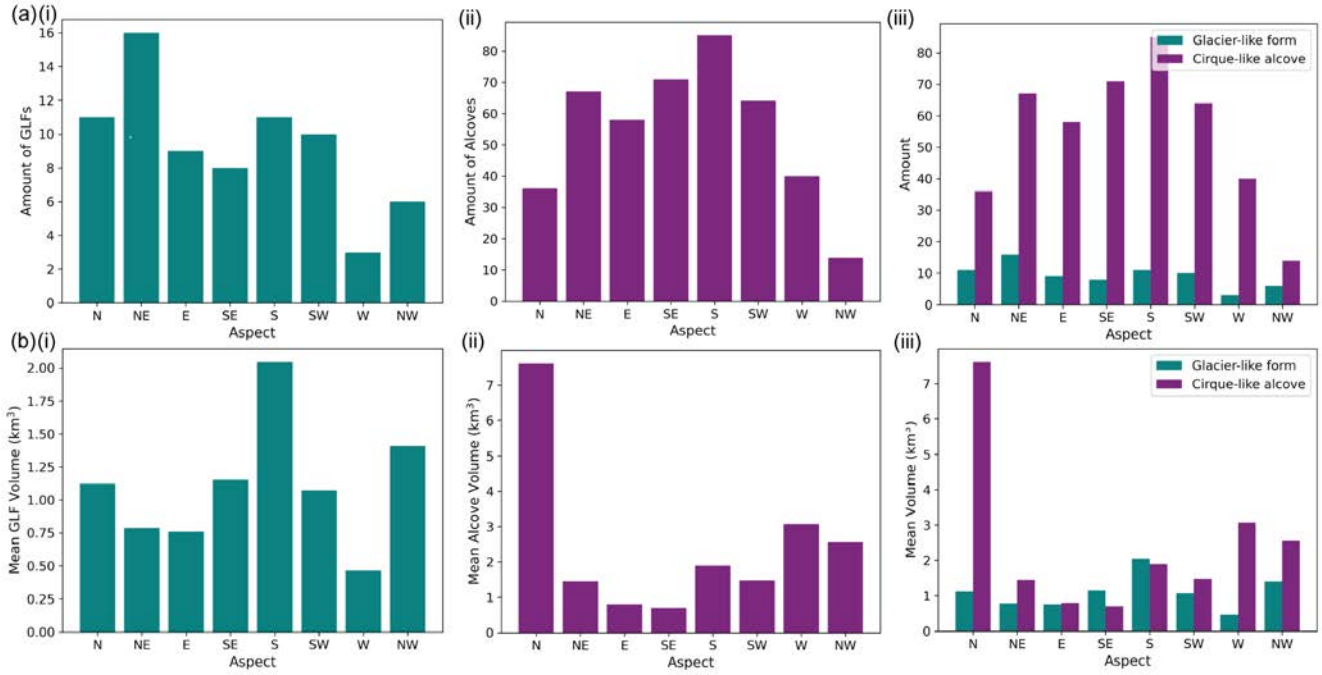


**Figure 11: a) Bar plots of the aspect compared to the quantity of i) cirque-like alcoves, ii) glacier-like forms, and iii) both cirque-like alcoves and glacier-like forms. b) Bar plots of the aspect compared to the average area in each aspect direction for i) cirque-like alcoves, ii) glacier-like forms, and iii) both cirque-like alcoves and glacier-like forms.**

### 4.3 Icy geomorphic features identified

In addition to morphometric observations, we identified geomorphic features in association with the cirque-like alcoves as consistent with either remnant or active ice in order to evaluate aspects of the glacial history in the cirque-like alcoves. Using the criteria stated in Table 3, we identified flow features, linear terrain, mantle, moraine-like ridges, mound-and-tail terrain, polygonal terrain, rectilinear-ridge terrain, and washboard terrain in available HiRISE imagery. Out of 435 cirque-like alcoves, there was complete overlap in available HiRISE frames with 26 cirque-like alcoves (8%) and partial overlap with only 10 cirque-like alcoves (1%). In CTX imagery, we were also able to identify flow features, linear terrain, mantle, moraine-like ridges, and washboard terrain. However, at the CTX resolution, it was more difficult to identify features such as mound-and-tail terrain, polygonal terrain, and rectilinear-ridge terrain. For both HiRISE and CTX imagery, the linear terrain and mantle were the two most common features. We provide the percentages of each feature in both HiRISE and CTX imagery in Table 5.

**Table 5: Percent of HiRISE and CTX imagery with each type of icy geomorphic feature.**

| Icy Geomorphic Feature | Percent of HiRISE imagery (%) | Percent of CTX imagery (%) |
|---|---|---|
| Flow features | 8 | 9 |
| Linear terrain | 81 | 57 |
| Mantle | 58 | 90 |
| Moraine-like ridges | 14 | 5 |
| Mound-and-tail terrain | 6 | N/A |
| Polygonal terrain | 53 | N/A |
| Rectilinear-ridge terrain | 3 | N/A |
| Washboard terrain | 42 | 2 |

Fig. 12 provides examples of washboard terrain, linear terrain, rectilinear ridges, and polygonal terrain, which all correspond to the presence of ice and/or ice loss, as described in Table 3. In Fig. 12, the linear terrain extends out from the washboard terrain at the base of the cirque-like alcoves (Fig. 12). The rectilinear ridges are downslope of both the washboard terrain and linear terrain. The polygonal terrain is between the two sections of linear terrain (Fig. 12f). In addition, the polygonal terrain is observed farther downslope of the rectilinear ridges (Fig. 12f).

Approximately 14% of cirque-like alcoves with HiRISE imagery coverage have moraine-like ridges. Fig. 13 contains examples of moraine-like ridges. Fig. 13b also shows additional examples of moraine-like ridges downslope of alcoves (that are not all cirque-like), with along-flow linear terrain between the alcove headwall and the moraine-like ridge. As in Fig. 12, washboard terrain, linear terrain, and polygonal terrain are all present.

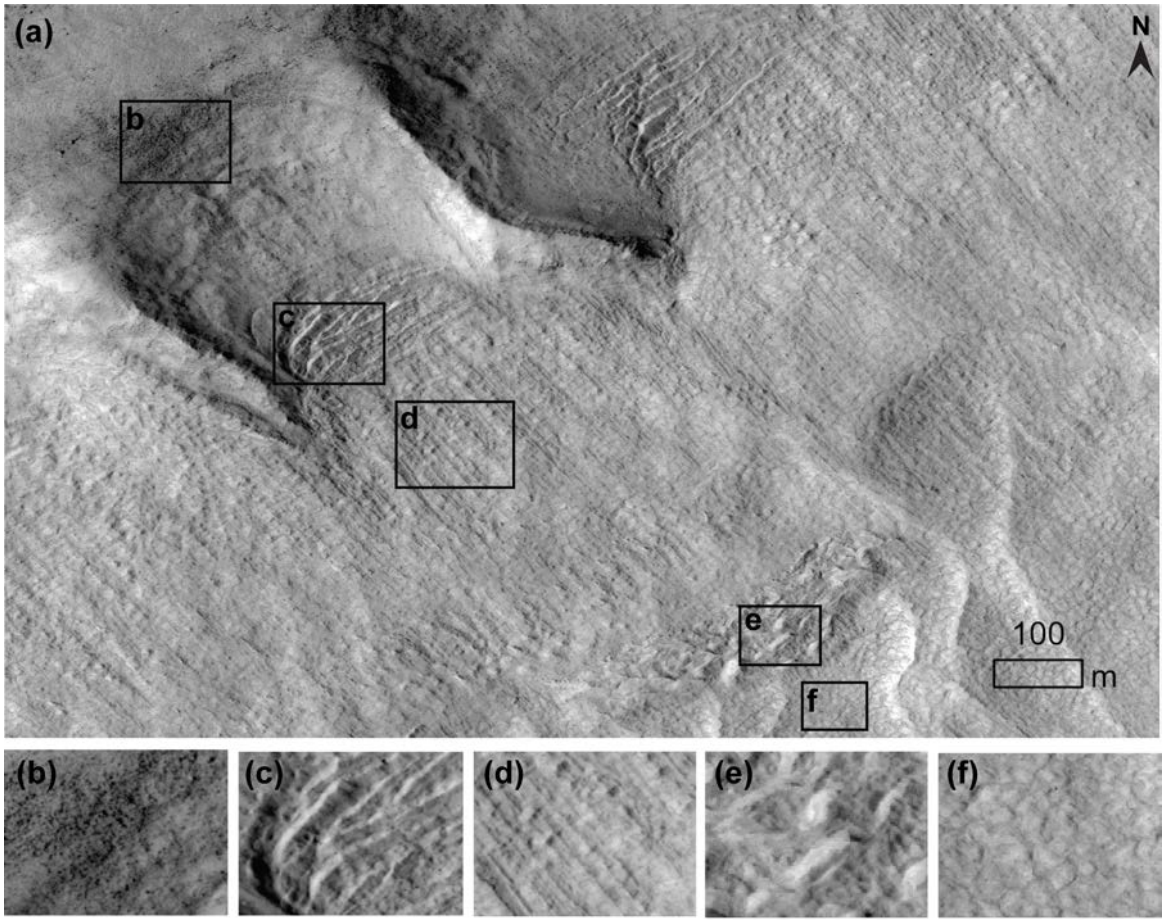


**Figure 12: a) Cirque-like alcove with evidence for remnant ice centered at 46.57°N, 22.12°E, 46.57°N in HiRISE image ESP_019214_2270_RED. b) Boulders near the top of the headwall indicating erosion. Features corresponding to ice-loss include the following: c) washboard terrain (Jawin and Head, 2021), d) linear terrain, e) rectilinear ridges (Hubbard et al., 2011), and f) polygonal terrain. (e.g., Hubbard et al., 2011).**

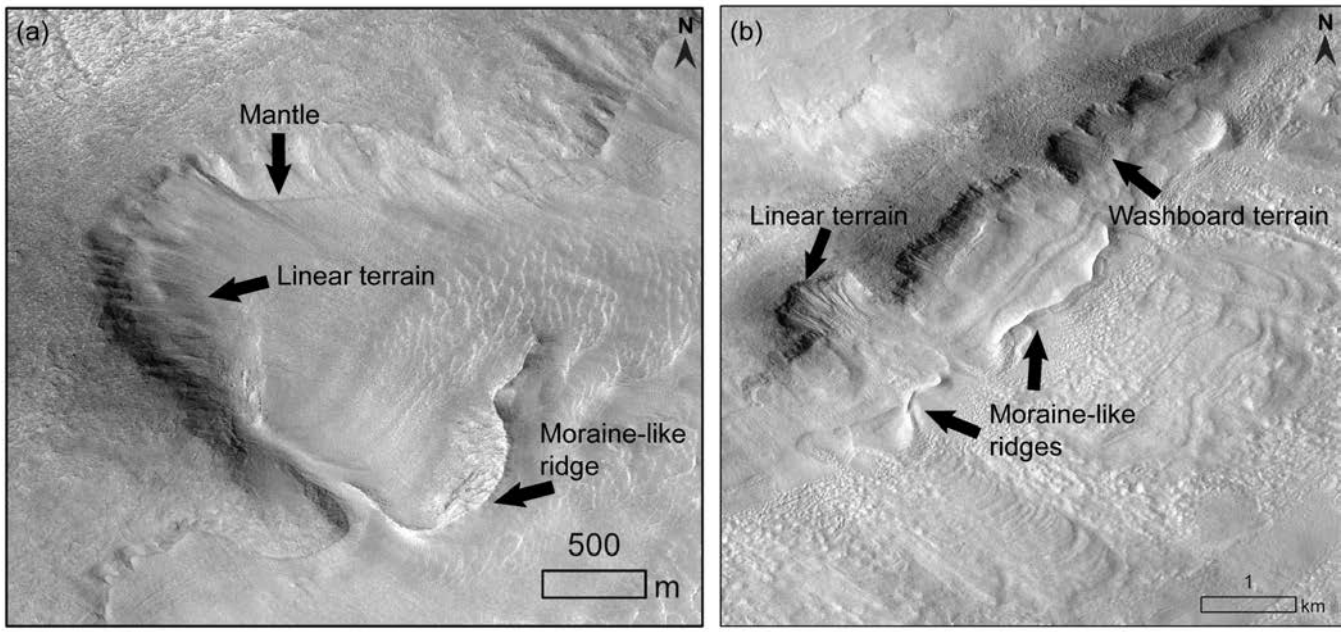


**Figure 13: (a) Potential icy form with a clear moraine-like ridge observed in a cirque-like alcove. HiRISE image ESP_033745_2270_RED is centered at 46.64°N, 29.83°E. (b) Possible unconstrained (known as piedmont) glaciation and moraine-like ridges. Linear terrain, washboard terrain features, and polygonal terrain are all present, though not all alcoves are cirque-like as defined in Section 3. HiRISE image ESP_026941_2275 is centered at 47.09°N, 26.74°E. HiRISE data credit: NASA/JPL/University of Arizona.**

## 5 Discussion

### 5.1 Geologic context of morphometrics

#### 5.1.1 Comparison of length, width, and height of cirque-like alcoves on Mars with cirques on Earth

We further evaluate whether cirque-like alcoves are candidate cirques by comparing them to cirques on Earth. Table 6 compares the length, width, and height for the cirque-like alcoves in Deuteronilus Mensae (as defined by morphometrics and the simple alcove class in Section 3.2.2) to a global population of 10,362 cirques on Earth as compiled in a review by Barr and Spagnolo (2015). Similar to Earth, both length and width are on average over twice the value for height in all cirques (Table 6). On average, cirque-like alcoves have length, width, and height values that are larger than cirques on Earth.

**Table 6**. A comparison of the length (L), width (W), and height (H) for cirque-like alcoves mapped in this study in Deuteronilus Mensae, Mars, and a population of 10,362 cirques on Earth (Barr and Spagnolo, 2015).

| | **Mean L (m)** | **Range in L (m)** | **Mean W (m)** | **Range in W (m)** | **Mean H (m)** | **Range in H (m)** |
|---|---|---|---|---|---|---|
| **Cirque-like alcoves in Deuteronilus** | 1127 *Median:* 831 | 217–5990 | 1207 *Median:* 904 | 249–6387 | 447 *Median:* 334 | 89–1735 |

| | | | | | | |
|---|---|---|---|---|---|---|
| **Mensae (435 cirque-like alcoves)** | | | | | | |
| **Cirques on Earth (10,362 cirques)** | 744 | 53–4584[1]<br>*Typical:*<br>100–1500 | 749 | 99–3240[1]<br>*Typical:*<br>100–1500 | 309 | 20–1328<br>*Typical:*<br>150–600 |

[1]*Both 4584 m for the maximum length and 3240 m for the maximum width are specific to cirques in the Dry Valleys of Antarctica (Aniya and Welch, 1981).*

The median cirque-like alcove size ($\sqrt[3]{LWH}$) in Deuteronilus Mensae is ~11% larger than the average cirque on Earth. This suggests that in comparison with Earth, either more episodes of glaciation occurred on Mars and lasted a longer amount of time to erode the cirque-like alcoves in Deuteronilus Mensae, the erosion rates on Mars were much more rapid, or the initial hollow for snow to accumulate in was larger on Mars. Future modeling may better investigate which is the most likely cause.

### 5.1.2 Trends in aspect

The eastward bias for cirque-like alcove aspect is similar to the trend of cirques in the mid-latitudes on Earth, where cirque aspect commonly faces eastward because glaciers are more likely to grow on the lee side of westerly winds present at these latitudes (Barr and Spagnolo, 2015). On Mars a slight eastward bias has also been identified in the overall glacier-like form population (Souness et al., 2012). Climate modeling shows that both westerly winds and ice deposition are expected in Deuteronilus Mensae during the northern winter (Madeleine et al., 2009). Both cirque-like alcoves and glacier-like forms have an eastward bias that might be consistent with atmospheric control, but further work is needed to understand this. The southern bias is less intuitive. Cirques in the northern hemisphere on Earth are generally biased toward having a northerly (poleward) orientation, where total solar radiation is lowest and lower air temperatures allow for glaciers to persist for longer (Barr and Spagnolo, 2015).

This pattern is seen for glacier-like forms too: for example, Souness et al. (2012) found glacier-like forms to have a poleward bias, although in Deuteronilus Mensae, the largest glacier-like forms face southwards, though the largest cirque-like alcoves by volume face north and southwest. However, this may be due to a localized topographic effect for glacier-like forms in Deuteronilus Mensae because overall for the northern hemisphere, glacier-like forms flowing northward are larger than those flowing southward by about 20% (Brough et al., 2019). For both glacier-like forms and cirque-like alcoves, the aspect with the highest percentage of the population does not correspond to the aspect with the largest mean volume. However, in all cases, the aspect south or southwest does correspond to one of the maxima in each plot for the amount and volume of glacier-like forms and cirque-like alcoves (Fig. 11). To explain the southward bias of cirque-like alcoves, we propose that this is consistent with periods of higher obliquity >45° on Mars, when poleward facing slopes received higher insolation and summer day temperatures (Costard et al., 2002; Kreslavsky et al., 2008), and equator-facing slopes received less insolation. As a result, southward facing cirque-like alcoves in the northern mid-latitudes were more favorable for ice accumulation during periods of

high obliquity. Similarly, for regions poleward of 40° like Deuteronilus Mensae, gullies are primarily observed on on equator-facing slopes (Harrison et al., 2015; Conway et al., 2018), possibly due to the melting of ground ice during periods of high obliquity (Costard et al., 2022), though the exact formation mechanism of gullies remains unclear (e.g., Conway et al., 2019; Dundas et al.. 2022). Regardless of how gullies are initiated, they may act as a local depression in a location where water-ice precipitation could later accumulate for cirque-like alcove formation, such as if the gullies acted as a cold trap for snow (e.g., Dickson et al., 2023b). For example, gullies could provide the initial concavity for a later cirque-like alcove to develop when glaciation occurs (Section 5.2.2), which is consistent with gully heads that have been proposed as initiation points for cirques on Earth (Derbyshire and Evans; 1976). However, in the case of meltwater, we note that cirque-like alcoves may prefer to reside on equator-facing slopes because this would allow for increased insolation (e.g., Pilorget and Forget; 2016; Dundas et al., 2022) and the chance for meltwater as temperatures increase (Dickson et al., 2023b). We explored this potential association between gullies and cirque-like alcoves in Section 5.1.2. On the other hand, glacier-like forms are mostly pole-facing in Deuteronilus Mensae, which corresponds to present-day conditions that are favorable for ice preservation. This may indicate that cirque-like alcoves were generated during an earlier phase of glaciation before the glacier-like forms or this may be due to preservation bias as poleward facing glacier-like forms may have outlasted other directions. If cirque-like alcoves do in fact correspond to an earlier phase of glaciation, it is unclear if this glaciation was on the scale of glacier-like forms versus larger scales like the lobate debris apron. It is also possible that valley glaciers in the cirque-like alcoves eventually connected with larger ice bodies like the lobate debris apron and lineated valley fill.

### 5.1.3 Trends between size, area, latitude, slope, and elevation

Relationships between size, area, latitude, mean elevation, and height of the cirque-like alcoves (Fig. 10) are likely due to the nature of the topography in this region. The mean elevation in Deuteronilus Mensae decreases toward the north (Fig. 14) and at lower latitudes, the mesas are at a higher elevation relative to the basin than at lower latitudes (Fig. 3, Fig. 14). These two factors combined mean that at lower latitudes, the cirque-like alcoves have a higher mean value for elevation and height due to the topography. Since size is calculated as $\sqrt[3]{LWH}$, the larger height at the lower latitudes corresponds to a larger cirque-like alcove size. Height also scales with length and width for cirque-like alcoves (Section 4.1), which is why both larger sizes and areas of cirque-like alcoves correspond to lower latitudes (Fig. 10b). Thus, the local elevation and local mesa height limit the local cirque-like alcove height at different latitudes in Deuteronilus Mensae.

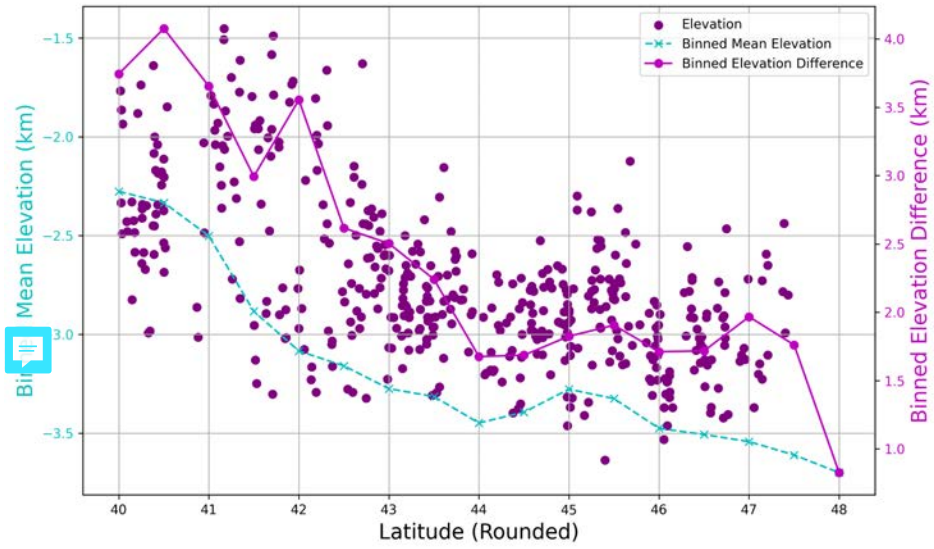


**Figure 14: Using the raster to point tool in ArcGIS Pro led to 41,618,659 points from the HRSC DEM. The binned mean elevation represents the mean elevation value of all the points at each half latitude in the study region. The binned elevation difference was calculated based on the difference between the mean of the highest 10,000 points and the mean of the lowest 10,000 points at each half latitude.**

### 5.1.4 Comparison between cirque-like alcoves and glacier-like forms mapped in Deuteronilus Mensae

Since both the largest cirque-like alcoves and glacier-like forms are located in southeast Deuteronilus Mensae, this may indicate that there is a local factor impacting both glacier-like form size and cirque-like alcove size or that the two are linked in how they form. For the first option, this may be because of local topography that enhances the conditions for precipitation and snow accumulation. If we assume that the cirque-like alcoves were eroded by the same phase of glaciation as the glacier-like forms, then the cirque-like alcoves may now be empty of glacier-like forms because their preservation became unfavorable in current obliquity conditions. In that case, conditions in the southeast of this region resulted in both the largest glacier-like forms and cirque-like alcoves. If we instead assume that all cirque-like alcoves had reached most of their current size before the glaciation cycle that brought the glacier-like forms, then the size of glacier-like forms may be limited to the initial size of the cirque-like alcove that it occupies. While we do not distinguish between these hypotheses in this study, we recommend future work to investigate the direct cause of the larger glacier-like forms and cirque-like alcoves in the southeast part of Deuteronilus Mensae.

Overall, the average glacier-like form has a larger area than the average cirque-like alcove because glacier-like forms typically extend beyond the cirque-like alcoves that they emerge from. Although the average area of a cirque-like alcove is smaller than a glacier-like form, the total area of all the cirque-like alcoves is larger than the total area of the mapped glacier-

like forms in our study area (Table 4). If the simple cirque-like alcoves that we identify here are in fact representative of glacial erosion, then we extend our previous knowledge of the areal extent of past glaciation in Deuteronilus Mensae by at least 48%.

While the largest glacier-like forms face southwards in Deuteronilus Mensae and the largest cirque-like alcoves face the north, this may be due to a localized topographic effect for glacier-like forms in Deuteronilus Mensae because overall for the northern hemisphere, glacier-like forms flowing northward are larger than those flowing southward by about 20% (Brough et al., 2019).

## 5.2 Geomorphic interpretations of cirque-like alcoves and associated features

### 5.2.1 Icy geomorphic features

We find that 42% of available HiRISE images contained washboard terrain, while only 2% of CTX images did, though this is likely due to a resolution issue since finer textures cannot be resolved at CTX scale. Except for two exceptions, cirque-like alcoves that contained washboard terrain did not also have an identifiable mantling unit. Similar to its presence at the bottom of crater walls (Jawin et al., 2018; Jawin and Head, 2021), the presence of washboard terrain here at the bottoms of the mesa sidewalls indicates deglaciation.

In both HiRISE (81%) and CTX imagery (57%), a high percentage of images of cirque-like alcoves contained observable linear terrain. In Fig. 12, since the linear terrain extended out from the washboard terrain, which is due to surficial crevasses, this suggests that the linear terrain there may be most similar to supraglacial longitudinal foliation. However, linear terrain could still result from subglacial erosion despite superposing a mantle unit since a mantle unit consists of layers of dust and snow that build up in the mantle over multiple obliquity cycles (e.g., Khuller et al., 2021). Applied here, this would imply that the ridges could have been subglacially eroded, but from another layer of ice of the mantle unit (compacted from dust and snow) that formerly existed on top of the rest of what is left of the mantle unit today.

At a potentially earlier stage of evolution of the glacier-like forms, moraine-like ridges [illegible]lack elongation outside of the alcove (Fig. 13a), potentially similar to a terrestrial cirque glacier sitting within the cirque basin instead of extending into the valley below. In Fig. 13b, the alcoves are not well-developed and do not have morphometrics corresponding to the criteria we set for cirque-like alcoves. Nevertheless, since the moraine-like ridges correspond to upslope alcoves, similar to Arfstrom and Hartmann (2005), we suggest that the moraine-like ridges in Fig. 13b reflect the initiation of cirque-style glaciation before the alcove headwalls and sidewalls develop more as they are increasingly eroded and steepened. This is also referred to as unconstrained piedmont glaciation by Conway et al. (2018).

### 5.2.2 Evidence for different stages of cirque-like alcove generation linked with gully evolution

Different stages of cirque-like alcove evolution, likely linked to different histories of glacial occupation and erosion, can be seen in and near mapped cirque-like alcoves. For example, in Fig. 15a and 15b, [illegible]hes (feature #1 in Fig. 15b) may indicate initial ice-associated erosion of the mesa sidewall. Stratigraphically, these notches predate the slab of detached mesa sidewall since the notches on the slab can be traced, but are now offset, from the notches above the slab (Fig. 15a). The notches resemble gullies elsewhere on Mars, which is relevant in this work because previous work has shown that gully formation may

occur during glacier retreat on Mars during paraglacial stages (Jawin and Head, 2021), where degrading ice no longer provides structural support for slopes of sediment. Gully incision may initiate through sediment flow assisted by either liquid water or $CO_2$, or dry mass wasting (e.g., Conway et al., 2019; Dundas et al., 2022; Dickson et al., 2023b). Since the slabs formed after the notches, this is consistent with increased mass wasting of the mesa sidewall during deglaciation.

Here, we assume that the side of the mesa evolves from a straight edge to an increasing number and depth of depressions. An alternative interpretation might be that the deeper depressions were subsequently filled up to create a straight edge, however, we do not see evidence for this amount of infilling. In the middle panel of Fig. 15a, for feature #2, there is evidence that the notches undergo further erosion and begin to connect, eventually forming feature #3 where the outlet between the larger notch head is overridden and enlarged. We suggest that an icy mantling deposit is responsible for this erosion since we see linear terrain that are consistent with pasted-on terrain. Fig. 15a feature #4 in the middle panel demonstrates continued erosion and enlargement of these alcoves as they grow and connect with neighboring alcoves until they lose internal ridges as glacial erosion smoothes the interior of the alcove.

In Fig. 15b, the alcoves are smoother, appear to be more U-shaped (though CTX DEMs did not have high enough resolution for profiles), have more arcuate headwalls, and have narrower ridges between alcoves. We suggest that this represents a later, more advanced stage of cirque-like alcove evolution, perhaps after multiple cycles of glaciation, where ice could erode repeatedly over time into the mesa sidewalls so that the cirque-like alcove basin becomes smoother and the sidewalls develop into narrow ridges as in Fig. 12. In Fig. 15b, as in Fig. 15a, we see downslope debris and deposits indicating mesa sidewall erosion. In the middle panel, we see examples of deposits of mesa material that are pushed outwards from the cirque-like alcoves (Fig. 15b). While it is likely that multiple processes contributed to the incipient form of a cirque-like alcove like those mentioned in Table 2, we suggest that the morphometrics and conditions observed eventually require substantial glacial erosion. For example, for impact cratering, while glacial geomorphic features may override any signature of impact ejecta, it is very unlikely that similarly sized impacts all happened to occur along mesa edges. Ultimately, we acknowledge that these other processes likely contributed to at least some erosion of cirque-like alcoves, but the prevalent glacial geomorphic features and consistently sized features correspond most to glacial erosion.

We suggest that the observed notches are gullies and would be able to act as necessary initiation points for ice accumulation that would later support glaciation and erosion that could form cirque-like alcoves. This is consistent with the mechanism proposed by Jawin et al. (2018). However, the formation of cirque-like alcoves is not dependent on how the gullies are formed. Gully formation hypotheses currently include $CO_2$ ice sublimation, dry mass wasting, meltwater generation, and a combination of these factors. For example, meltwater generation is more commonly invoked for older, inactive gullies during periods of higher obliquity (e.g., Dickson et al., 2023; Noblet et al., 2024), while gullies that have been observed to be recently active invoke $CO_2$ frost, as well as dry mass wasting during frost-free seasons (e.g., Dundas et al. 2022).

While determining how these gullies formed is outside the scope of this work, we include a discussion of the current hypotheses. Dry mass wasting alone for gully formation has recently been challenged since the mean gradient of gullies is lower than the angle of repose of dry material on Mars (e.g., Noblet et al., 2024). Gullies that are either in 1) the northern

hemisphere at latitudes lower than ~50° or 2) non-polar regions and are equator-facing are modeled to be inactive gullies (Roelofs et al., 2024). These inactive gullies are inconsistent with where $CO_2$ frost deposition is expected to occur on pole-facing slopes (e.g., Lange et al. 2023). For example, in the southern hemisphere, $CO_2$ frost is only observed on pole facing slopes between 30-50°S and is not expected on equator-facing gullied slopes between 40°S and 50°S during current obliquity conditions (Noblet et al., 2024). Nevertheless, we note that $CO_2$ sublimation cannot be completely ruled out for equator-facing slopes since seasonal deposition of $CO_2$ frost at these latitudes could have been more prevalent in the past (Noblet et al., 2024). For present-day gully activity, rather than inactive gullies, sublimation of $CO_2$ is typically invoked (e.g., Dundas et al., 2022), though $H_2O$ ice melt has been suggested to occur within dusty ice (e.g., Khuller et al., 2021).

Gullies are preferentially found on terrains that have subsurface water ice (Noblet et al., 2024). It is suggested that these inactive gullies are formed from the meltwater of ground ice during past high obliquities (e.g., Noblet et al., 2024; Dickson et al., 2023). This may be possible because modeling found temperatures above freezing for meltwater and gully formation during high obliquity excursions in the mid-latitudes (Costard et al., 2002; Williams et al., 2008; Williams et al., 2009; Dickson et al., 2023b). According to Dickson et al. (2023), at high obliquities of 35° in the past, meltwater was possible during the Amazonian because pressures exceed the triple point of water, and transient melting may be possible in the present as well (Hecht et al., 2002). Future work is necessary to elucidate the potential relationship between gullying as initiation points for cirque-like alcove formation and how that is tied to cyclicity in ice accumulation and melt.

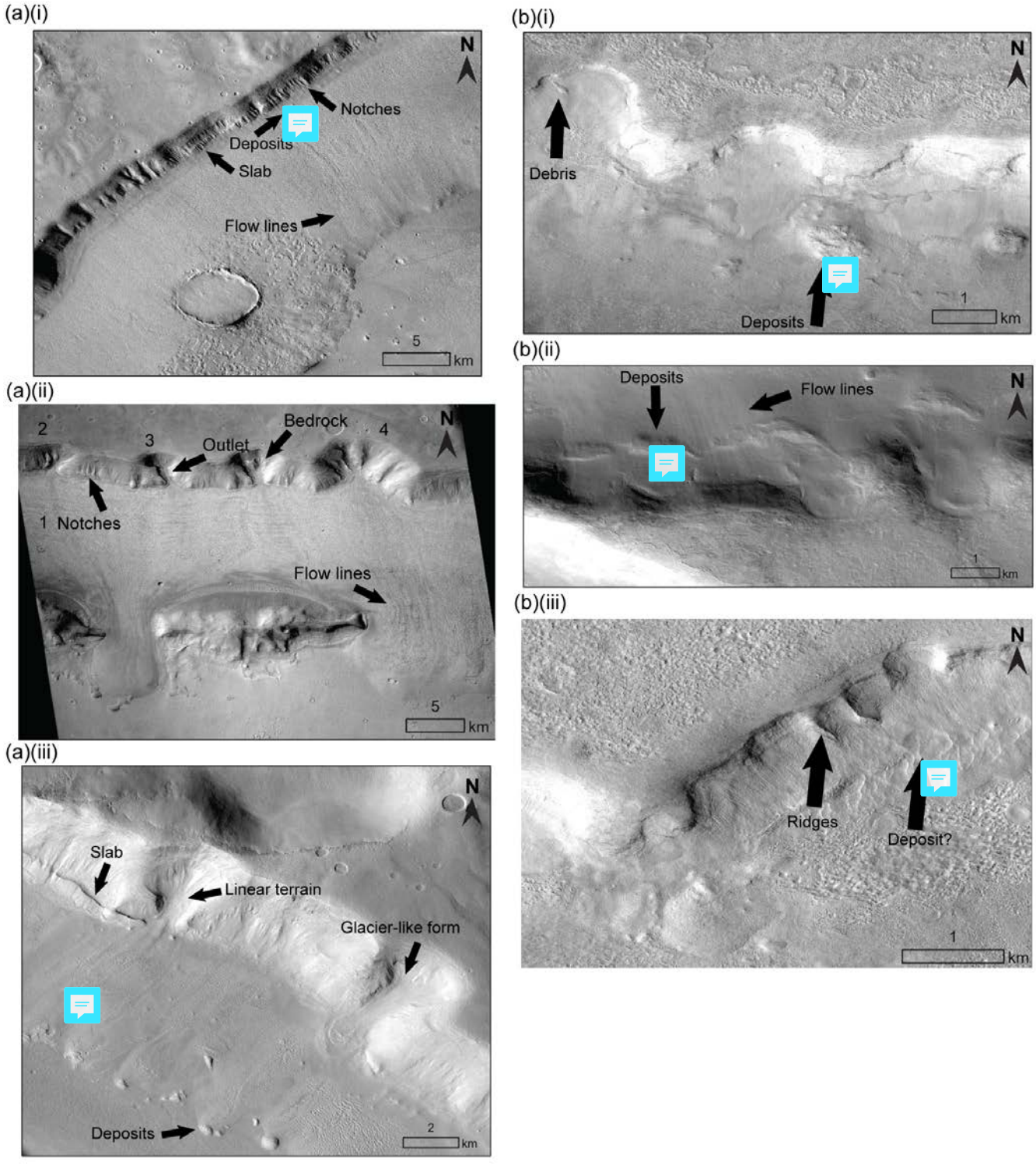
(a)(i)
N
Notches
Deposits
Slab
Flow lines
5
km
(a)(ii)
2
3
Outlet
Bedrock
4
N
1 Notches
Flow lines
5
km
(a)(iii)
N
Slab
Linear terrain
Glacier-like form
Deposits
2
km
(b)(i)
N
Debris
Deposits
1
km
(b)(ii)
Deposits
Flow lines
N
1
km
(b)(iii)
N
Ridges
Deposit?
1
km

20

**Figure 15: (a) Top panel is centered at 41.06°N, 17.88°E in CTX image D04_0288880_2193_XI_39N342W. Notches may indicate ice-associated erosion of the mesa sidewall. Slabs and deposits suggesting active mass wasting from the slopes. Flow lines indicate the downslope direction of flow. Middle panel is centered at 40.02°N, 23.20°E in CTX image D21_035499_2203_XN_40N336W. Feature #1 represents initial notches, #2 represents the initial notches undergoing further erosion and beginning to connect, #3 demonstrates an outlet being overridden and enlarged, as indicated by flow lines, and #4 demonstrates the continual enlargement of these alcoves. Bottom panel is centered at 41.60°N, 18.46°E in CTX image N01_062743_2222_XI_42N341W. The slab indicates the unstable slopes. We see an alcove with linear terrain and leading to deposits, adjacent to a nearby glacier-like form on the same mesa sidewall. (b) Top panel is centered at 46.67°N, 26.13°E in HiRISE image ESP_016247_2270. Debris label in the top panel points to a possible detached block that is ~160x80m. Middle panel is centered at 46.57°N, 26.02°E in CTX image P13_006160_2252_XN_45N334W. Flow lines indicate a flow toward the top of the image (north direction), consistent with the deposits detaching from the mesa in the south and being transported northwards. Bottom panel is centered at 46.56°N, 22.13°E in HiRISE image ESP_019214_2270. These alcoves represent the most mature cirque-like forms due to their defined ridges. A deposit has an outline similar to the mesa sidewall, suggesting downslope flow. HiRISE data credit: NASA/JPL/University of Arizona. CTX data credit: Caltech/NASA/JPL/MSSS.**

### 5.3 Estimating the timescales for cirque-like alcove erosion on Mars

From terrestrial studies we know that cirques are formed by glacial erosion, which generally requires liquid water at the base of a wet-based glacier (Glasser and Bennett, 2004). On the other hand, cold-based glaciers on Earth are minimally erosive (Table 7) and are therefore not typically associated with large-scale glacial erosion features such as glacial valleys, troughs or cirques, though it cannot be excluded that minimally erosive cold-based glaciers operating over orders of magnitude larger timescales than a few glaciation cycles might still contribute to the erosion of large features. For example, measurements at cold-based Meserve Glacier in Antarctica find an erosion rate of $9 \times 10^{-7}$ to $3 \times 10^{-6}$ $myr^{-1}$ (Cuffey et al. 2000), meaning that it would take 100-330 millions of years of continuous glacial erosion to produce a 300 m deep cirque on Earth. In locations such as the Dry Valleys of Antarctica where cold-based glaciers currently reside within cirques, it is likely that much of the erosion of the cirque occurred during an earlier more temperate phase of glaciation during the Miocene (e.g., Selby and Wilson, 1971; Sugden and Denton, 2004; Clinger et al., 2020). If these martian cirque-like alcoves are analogous to terrestrial glacial cirques, then they may have formed either during an earlier wet-based phase at the scale of an active glacier-like form, or formed during a prior cold-based glacial cycle separate from the glacier-like forms, such as when lobate debris aprons formed.

**Table 7: Comparison of published erosion rates for cold-based glaciers, wet-based glaciers, and glacial cirques (wet-based) on Earth.**

| Type of glacier | Erosion rate (m/Myr) | Reference |
|---|---|---|
| Cold-based and debris-covered on Mars | 0.1–10 | Levy et al., (2016) |
| Cold-based on Earth | 0.2–3 | Balco and Shuster, (2009); Cuffey, (1999a) |
| Wet-based on Mars | $10^2$ | Conway et al. (2018) |
| Wet-based on Earth | 10–10,000 | Hallet et al., (1996) |

| | | |
|---|---|---|
| Cirque (wet-based) on Earth | 8–5,900 | Reviewed by Barr and Spagnolo, (2015) |

Using terrestrial understanding of glacier erosion we can calculate approximately how long the glacial erosion of a median cirque-like alcove would take based on different assumptions. First, we take into account that the surface gravity of Mars is about one third of Earth's at 3.71 m/s$^2$. Second, in order to calculate erosion rates in the past we estimate the former ice-surface velocity to derive the basal sliding velocity, keeping in mind that sliding velocities are notably higher for wet-based glaciers than for cold-based glaciers. Third, we estimate the total occupation time of active (flowing) glaciers in the cirque-like alcoves, which on Mars is likely a function of orbital forcing (e.g., Laskar et al., 2002). We estimated erosion rates for both wet- and cold-based ice. From the calculations below, our estimated erosion rates indicate that a cold-based glacier would take an order of magnitude longer than a wet-based glacier to erode the cirque-like alcoves, and that depending on whether cold-based or wet-based erosion occurred, our estimates can be consistent with previous estimates of erosion rates (Levy et al., 2016; Conway et al., 2018) and timescales of past episodes of glaciation on Mars (Berman et al., 2015; Hepburn et al., 2020).

Our erosion rate estimates are derived from basal sliding velocities ($U_S$) which are in turn derived from glacier surface velocities, using an empirical relationship from a terrestrial global dataset of 38 glaciers (Cook et al., 2020):

$$U_s = U_{surf} - \frac{2A}{n+2}(\rho g sin\alpha)^n \, h^{n+1}, \quad (1)$$

where $A$ is a temperature-dependent ice softness parameter (for warm ice at 0 °C, $A = 24 \times 10^{-25} s^{-1} Pa^{-3}$; for cold ice at -20 °C, $A = 1.2 \times 10^{-25} s^{-1} Pa^{-3}$; Cuffey and Paterson, 2010), $n$ is a flow-law exponent that is typically 3, $\rho$ is ice density, $g$ is gravitational acceleration, $\alpha$ is ice surface slope, $h$ is ice thickness, and $U_{surf}$ is glacier surface velocity. For the A parameter, since it is unknown how much the temperature of ice on Mars has fluctuated throughout the Amazonian, we use both a warm and cold ice scenario. While we do not know the ice temperature on Mars, when keeping the other values the same, our calculated erosion rates are approximately the same for a value of A associated with -50 °C and with -20 °C (values from Cuffey and Paterson, 2010). Here, we use the A parameter corresponding to -20 °C to match the temperature near the surface of the rock glacier in Beacon Valley (Rignot et al., 2002), which is the glacier that the surface velocity we use is based on. We also do not know how the Mars temperatures have fluctuated throughout the Amazonian epoch. For glacier-like forms on Mars, average $h$ is 130 m and, since $\alpha$ ranges from 2 to 8° (Brough et al., 2019), we use 5° here to represent an order-of-magnitude estimate. Since surface velocities of glacier-like forms on Mars are unknown (Brough et al., 2019; Hubbard et al., 2014), for the wet-based case, we use a surface velocity of 2 m/yr (Cook et al., 2020) and for the cold-based case we use a surface velocity of $1 \times 10^{-3}$ m/yr, which was measured for a rock glacier in the Beacon Valley sector of the McMurdo Dry Valleys of Antarctica, which represents a low glacier flow speed on Earth. Erosion rate $E$ was calculated as:

$$E = K_G U_s^l, \quad (2)$$

where $K_G$ is a bedrock erodibility constant and $l$ is an erosion exponent. While $K_G$ and $l$ can vary depending on the bedrock type, $K_G$ is commonly $10^{-4}$ (Cook et al., 2020). Cook et al. (2020) empirically estimated $l$ to be 0.69 based on the relationship between the erosion rate and glacier sliding velocity of 38 glaciers, including Meserve Glacier, and we use that value in our estimates.

While this study does not provide exact age constraints for cirque-like alcoves, our erosion rate estimates help constrain the minimum length of time required for their development. For the wet-based glaciation scenario, we estimate an erosion rate of ~160 m/Myr, which is close to the upper end of the 0.08 to 181 m/Myr range estimated by Conway et al. (2018) for glaciated crater walls on Mars. To estimate the amount of time necessary to erode a cirque-like alcove, we divide the erosion rate by the median height of a cirque-like alcove of 335 m, rounded down to 300 m. For continuous glacial occupation and ignoring that glaciers may have only been active (and eroding their bed) during certain obliquity periods, this would suggest that a total of ~1.9 Myr would be required for the cirque-like alcoves to form. However, accounting for obliquity changes when conditions may not have always been optimal for active glaciation would extend this time. As an estimate, over the last 10 Myr, there were 100 kyr orbital cycles, with periods of high obliquity lasting 20-40 kyr (Head et al., 2003). On Earth, cirques are presumed to be mostly eroded at the beginning and the end of glaciations (e.g., Barr et al., 2019), so assuming that the cirque-like alcoves only have 20 kyr of erosion time during every 100 kyr period, or 20% of the total time passing by, it would take ~9.4 Myr total time to erode a median height cirque-like alcove. This timescale is consistent with previous estimates of the age of certain populations of glacier-like forms (Hepburn et al., 2020), which means that at least some of the glacier-like forms could have eroded the cirque-like alcoves which they currently occupy and that at least some of the empty cirque-like alcoves could have hosted glaciers in the past tens of millions of years.

On the other hand, if we assume cold-based conditions for glaciers that occupied the cirque-like alcoves, then the erosion rate estimated from the median values for cirque-like alcoves is ~0.85 m/Myr, which is consistent with the wide-ranging estimate of 0.1-10 m/Myr for cold-based viscous flow features on Mars (Levy et al., 2016) but is lower than the Conway et al. (2018) estimates for glaciated crater walls. Thus, for a cold-based glacier, a total glacier occupation time of ~350 Myr would be required for the cirque-like alcoves to form, which is consistent with the ~500 Myr timescale of LDA- and CCF-forming glaciation based on crater counts (Fassett et al., 2014). However, accounting for obliquity variations, a median height cirque-like alcove would require ~1.8 Gyr to erode from only cold-based glaciation during periods of high obliquity with erosion rates of ~0.85 m/Myr. If the glaciers were cold-based during their entire evolution, the erosion timescale is longer and therefore the alcoves must be much older than if they evolved with periods of wet-based glaciation. A timescale of hundreds of millions to a billion years is in the range of when lobate debris aprons were thought to have formed, such as in Deuteronilus Mensae, the lobate debris aprons are estimated to be as old as 1.1 Gyr (Berman et al., 2015).

Using the slowest estimated erosion rate corresponding to cold-based glaciers in Antarctica, the initiation of the cirque-like alcoves likely predated the lobate debris aprons and involved erosion rates faster than cold-based glaciation. Then they could continue to develop in size during and/or after when the lobate debris aprons formed. However, since debris from

the cirque-like alcoves often superposes the lobate debris aprons (e.g., Baker and Carter, 2019), this means that the process eroding the cirque-like alcoves have been actively eroding after when the lobate debris aprons formed. . The supraglacial debris covering the lobate debris aprons averages ~25 meters in thickness and a major fraction of the debris was sourced as rockfall from the mesas (Baker et al., 2019). Thus, it is reasonable to expect that the present state of the mesa sidewalls, including the cirque-like alcoves, formed either concurrently with or after the lobate debris aprons evolved and became covered with debris. Otherwise, the erosional process sourcing the supraglacial debris would likely have erased the cirque-like alcoves. Here we use the maximum age estimate of lobate debris aprons of 1.1 Gyr as the earliest time that glaciers could have begun the erosion process that led to the formation of the cirque-like alcoves. By also including the consideration of obliquity that only around 20% of the 1.1 Gyr would have been conducive for ice accumulation, the maximum erosion depth achievable by cold-based glacier erosion would be ~790 m. Since ~20% of the cirque-like alcoves are larger than 790 m, we conclude that at least some of the cirque-like alcoves could have required a faster erosion rate than the ~0.85 m/Myr suggested for cold-based glaciers. Some have suggested cold-based glaciers erosion rate on Mars up to 10 m/Myr (Table 7; Levy et al., 2016). If this upper-end rate of 10 m/Myr is applied, then all heights of the cirque-like alcoves could have formed via cold-based glacier erosion within ~930 Myr. Given these timescales, it is more likely that the cirque-like alcoves had erosion rates higher than 0.85 m/Myr, corresponding to glaciers with surface velocities faster than 1 mm/yr. This surface velocity is also faster than what recent modeling found for a viscous flow feature with a maximum surface velocity of $20 \times 10^{-6}$ m/yr (Butcher et al., 2024), which would yield an unrealistic age for the cirque-like alcoves that is older than the age of Mars.

On Earth, the chronology of cirque formation is difficult to constrain (e.g., Turbull and Davies, 2006), and estimates for total glacial cirque erosion time range from 125 Kyr (Larsen and Mangerud, 1981) to a few million years (Andrews and Dugdale, 1971; Anderson, 1978; Sanders et al., 2013). Our estimates here find that a median height cirque-like alcove in Deuteronilus Mensae would take in the range of ~9.4 Myr to form if occupied by a wet-based glacier with an erosion rate of 160 m/Myr, and ~1.8 Gyr if occupied by a cold-based glacier with an erosion rate of 0.85 m/Myr. However, since cold-based erosion rates may vary by up to two orders of magnitude, maximum cold-based erosion rates closer to 10 m/Myr would allow for timescales of hundreds of millions of years. Whether the cold-based erosion rates on Mars were more similar to what has been observed at Meserve Glacier in Antarctica at ≤3 m/Myr (Cuffey et al., 2000) or at much higher values closer to 10 m/Myr (Levy et al., 2014) remains unknown.

## 6 Conclusions

This is the first in-depth, regional population scale study of the morphometrics and geomorphic evidence of previous ice occupation associated with cirque-like alcoves on Mars, that uses terrestrial knowledge to make a case that a sub-population of the mapped alcoves were likely eroded by past glaciation. By mapping ~2000 alcoves in Deuteronilus Mensae that did not contain previously mapped glacier-like forms, grouping them into six classes, and then downselecting to only simple alcoves with length/width (L/W) between 0.5 to 4.25, length/height (L/H) of 1.5 to 4.0, and width/height (W/H) of 1.5 to 4.0, which are consistent with terrestrial cirques, we are able to identify a population of 435 “cirque-like alcoves.” We constrained our

dataset to a total of 435 cirque-like alcoves in the study area, where only 74 glacier-like forms had been previously mapped (Brough et al., 2019). Thus, if cirque-like alcoves are indeed glacially eroded, we greatly extend what we know about the extent of kilometer-scale glaciation in the region. Using HiRISE imagery that was available for ~9% of these cirque-like alcoves, we find evidence of associated icy geomorphic features, including flow features, linear terrain, mantle, moraine-like ridges, mound-and-tail terrain, polygonal terrain, moraine-like ridges, rectilinear-ridge terrain, and washboard terrain (Figs. 12-13). All of these features have been found in association with glacier-like forms in previous work (e.g., Arfstrom and Hartmann, 2005; Morgan et al., 2009; Hubbard et al., 2011; Hubbard et al., 2014). This data analysis leads us to draw the following conclusions:

- The cirque-like alcoves in Deuteronilus Mensae have a median size ~11% larger than the average size of cirques on Earth (Section 5.1), which may suggest that cirques in Deuteronilus Mensae underwent more or longer episodes of erosive glaciation than cirques on Earth. The largest cirques are in the lower latitudes of the study region at 40-42.9°N (Fig. 9a). This likely suggests cirque-like alcove formation during a period of high obliquity when conditions were more favorable for glacier growth at these latitudes.
- Cirque-like alcoves contain icy deposits, as signified by the presence of flow features, linear terrain, mantling unit, washboard terrain, rectilinear-ridge terrain, moraine-like ridges, and polygonal terrain. While these icy deposits do not have all of the criteria to correspond to glacier-like forms, the features in many cirque-like alcoves represent a continuum of ice evolution, potentially as ice in viscous flow features such as glacier-like forms degrade and contain less ice volume.
- There is a dominant southward bias in the aspect of the cirque-like alcoves (Fig. 8), which becomes more pronounced above 46.5°N. We proposed this may be due to either poleward facing slopes receiving higher insolation and warmer summer daytime temperatures during high obliquity (>45°) and/or an association with gully formation, since gullies also preferentially face the equator for slopes poleward of 40° (Harrison et al., 2015; Conway et al., 2018). Overall, both cirque-like alcoves and glacier-like forms tend to have greater volumes when facing south, which may suggest a relationship between glacier-like form size and cirque-like alcove size.
- In addition to a southward bias, a slight eastward bias in aspect aligns with previous studies of both glacier-like forms on Mars (e.g., Souness et al., 2012; Brough et al., 2019) and climate models of westerly winds in Deuteronilus Mensae (Madeleine et al., 2009). Terrestrial cirques also show a similar pattern due to westerly winds. Future work could help to better understand the atmospheric controls on cirque-like alcove formation in Deuteronilus Mensae, as well as other locations on Mars.
- Headwall notches (similar to gullies) are observed adjacent to increasing sizes of larger alcoves (Fig. 15). Notches and subsequent stages of their development may act as an initiation point for ice accumulation, similar to what happens on Earth for local-slope glaciation. Larger alcoves may have undergone multiple cycles of glaciation and erosion. This process is consistent with previous work by Jawin et al. (2018).

- We estimate the time required for cirque-like alcove formation in Deuteronilus Mensae using Mars' surface gravity, obliquity models, and glacial conditions. Assuming wet-based glacial erosion (~160 m/Myr), formation would take ~9.4 Myr, consistent with age constraints for glacier-like forms and lobate debris aprons. Assuming cold-based glacial erosion (~0.85 m/Myr), formation would take ~1.8 Gyr—older than all known viscous flow features. However, cold-based erosion rates on Mars may have been higher in the past, with some estimates reaching ~10 m/Myr, which could reduce formation time to ~930 Myr. Further research is needed to evaluate the potential for cold-based glaciers to erode cirques on Mars, even though this process is minimal on Earth.

Here we show that cirque-like alcoves are consistent with the morphometrics of terrestrial cirques and retain geomorphic features indicative of ice. In addition, cirque-like alcoves have trends in aspect similar to other features such as gullies on Mars. Future work may evaluate additional regions on Mars and further explore the main factors influencing cirque-like alcove development throughout multiple cycles of glaciation and deglaciation. While we bring forward new evidence and associations using our understanding of geomorphology for Earth and Mars, further work, especially using additional high-resolution imagery and topography that may be available in the future, will be necessary to determine the style and timing of glacial activity on Mars.

## Data availability

The shapefiles and spreadsheet of the cirque-like alcoves mapped in this study may be obtained by emailing the first author. The HRSC DEM was mosaicked using the following 29 Level 4 HRSC data frames: h5436, h5418, h5400, h5364, h5339, h5328, h5321, h5310, h5303, h5285, h5267, h5249, h5231, h5213, h3304, h3293, h3249, h3183, h2191, h1644, h1622, h1571, h1289, h1395, h1461, h1450, h1428, h1483, and h1201. The Level 4 HRSC data frames can be accessed at the ESA Planetary Science Archive: http://www.rssd.esa.int/index.php?project=PSA, HRSCview by FU Berlin/DLR: http://hrscview.fu-berlin.de/, or the NASA Planetary Data Science (PDS) http://pds-geosciences.wustl.edu/missions/mars_express/. The CTX mosaic is available through ArcGIS Pro by selecting "Portal" and selecting "Mars CTX V01" or for download at the Murray Lab website: https://murray-lab.caltech.edu/CTX/. HiRISE frames were accessed from the University of Arizona's HiRISE website: https://www.uahirise.org/hiwish/browse and are also available through the PDS. The HiRISE frames that we examined for geomorphic features included the following: ESP_041934_2265, ESP_040853_2275, ESP_036844_2225, ESP_036580_2260, ESP_036514_2210, ESP_026941_2275, ESP_025873_2230, ESP_025781_2220, ESP_025477_2280, ESP_025253_2245, ESP_023618_2270, ESP_023605_2205, ESP_019768_2220, ESP_019214_2270, ESP_016748_2255, ESP_016471_2260, ESP_016247_2270, ESP_016194_2260, ESP_067108_2240, ESP_060013_2250, ESP_057877_2245, ESP_056004_2255, ESP_055872_2270, ESP_055661_2230, ESP_054527_2225, ESP_053762_2280, ESP_052826_2240, ESP_052681_2240, ESP_052417_2220, ESP_050558_2245, ESP_048949_2230, ESP_046853_2200, ESP_046220_2235, ESP_046075_2200, ESP_046022_2265, ESP_043688_2245, ESP_025319_2240, ESP_016959_2240, ESP_027574_2245, ESP_035011_2240, PSP_006147_2250, ESP_068441_2230, ESP_033745_2270, ESP_035156_2220, and

ESP_028418_2240. The CTX DEM used in Figure 5 was made by Mackenzie Day's GALE lab at UCLA by request and is publicly accessible here: https://github.com/GALE-Lab/Mars_DEMs.

## Author contribution

Project conceptualization by MRK and AYL with funding obtained by MRK. Methodology development by AYL, MRK, and SB. Mapping, classification, initial analyses, and figures were created by AYL. All authors contributed to discussions of the interpretations. All authors also revised and approved the submitted manuscript.


## Acknowledgments

AYL and MRK acknowledge funding from NASA SSW 80NSSC20KO747. We thank Anjali Manoj for her work on alcove classifications. We are very grateful to Mackenzie Day and the GALE lab at UCLA for making CTX DEMs. We also appreciate Yingkui Li for helping us to apply ACME 2 to datasets for Mars. The reviewers Joseph Levy, Susan Conway, and Rishitosh Sinha, as well as the editor Frances Butcher, have contributed comments that immensely improved this manuscript.


## Supplementary Material

**Table S1:** Icy geomorphic features identified in cirque-like alcoves using available HiRISE frames.

| Alcove ID | HiRISE ID | Coverage | Latitude, Longitude | Icy geomorphic features identified |
|---|---|---|---|---|
| 50 | PSP_007439_2205 | Partial | 40.18°N, 24.72°E | Linear terrain, mantle, mound-and-tail terrain |
| 56 | ESP_072529_2265 | Partial | 40.29°N, 23.00°E | Mantle |
| 57 | ESP_072529_2265 | Full | 40.26°N, 22.98°E | Mantle |
| 145 | PSP_008810_2225 | Full | 41.85°N, 26.36°E | polygonal terrain, mantle |
| 572 | ESP_067108_2240 | Partial | 43.70°N, 27.92°E | Mantle |
| 631 | ESP_068441_2230 | Full | 42.63°N, 25.30°E | Linear terrain, mantle, washboard terrain |
| 637 | ESP_025873_2230 | Partial | 42.76°N, 25.06°E | Linear terrain |
| 650 | ESP_054527_2225 | Partial | 41.97°N, 24.63°E | Linear terrain, mantle |
| 704 | ESP_046220_2235 | Full | 42.94°N, 24.06°E | Linear terrain, polygonal terrain, washboard terrain |

| | | | | |
|---|---|---|---|---|
| 705 | ESP_046220_2235 | Full | 42.97°N, 24.05°E | Linear terrain, polygonal terrain, washboard terrain |
| 769 | ESP_052681_2240 | Full | 43.64°N, 24.52°E | Flow features, linear terrain, moraine-like ridges, polygonal terrain |
| 783 | ESP_052826_2240 | Partial | 43.43°N, 26.02°E | Linear terrain, mantle |
| 878 | ESP_025253_2245 | Partial | 44.48°N, 29.82°E | Linear terrain, mound-and-tail terrain, polygonal terrain, washboard terrain |
| 911 | PSP_007162_2250 | Full | 44.60°N, 27.66°E | Linear terrain, mantle |
| 1061 | ESP_046022_2265 | Partial | 46.38°N, 29.00°E | Mantle, polygonal terrain, washboard terrain |
| 1088 | ESP_033745_2270 | Full | 46.66°N, 29.85°E | Linear terrain, mantle, moraine-like ridges, polygonal terrain, washboard terrain |
| 1125 | ESP_043688_2245 | Full | 44.16°N, 25.19°E | Linear terrain, polygonal terrain, washboard terrain |
| 1161 | ESP_053762_2280 | Full | 47.40°N, 27.37°E | Polygonal terrain, linear terrain, broad pit |
| 1170 | EPS_026941_2275 | Full | 47.12°N, 26.71°E | Linear terrain, polygonal terrain, moraine-like ridges, washboard terrain |
| 1171 | ESP_026941_2275 | Full | 47.14°N, 26.75°E | Linear terrain, polygonal terrain, washboard terrain |
| 1218 | ESP_055872_2270 | Full | 46.39°N, 27.09°E | Mantle, linear terrain, washboard terrain |
| 1227 | ESP_056004_2255 | Full | 45.25°N, 24.53°E | Linear terrain, polygonal terrain, mantle |
| 1230 | ESP_056004_2255 | Full | 45.25°N, 24.58°E | Mantle, polygonal, linear terrain |
| 1302 | ESP_057877_2245 | Full | 44.13°N, 23.86°E | Linear terrain, mantle, polygonal terrain |
| 1425 | PSP_002890_2205 | Full | 40.09°N, 22.72°E | Linear terrain, polygonal terrain, washboard terrain |
| 1438 | ESP_046853_2200 | Full | 40.25°N, 22.92°E | Mantle |
| 1487 | ESP_016471_2260 | Full | 45.63°N, 33.47°E | Linear terrain, washboard terrain |
| 1594 | ESP_019768_2220 | Full | 41.67°N, 18.43°E | Flow features, linear terrain, rectilinear ridge terrain, washboard terrain |
| 1616 | PSP_005857_2225 | Partial | 42.07°N, 19.52°E | Mantle |

| | | | | |
|---|---|---|---|---|
| 1802 | ESP_035156_2220 | Full | 41.90°N, 23.90°E | Linear terrain, mantle, moraine-like ridges |
| 1808 | ESP_046075_2200 | Full | 40.29°N, 24.23°E | Linear terrain, mantle, moraine-like ridges, polygonal terrain |
| 1840 | ESP_025781_2220 | Full | 41.63°N, 16.28°E | Flow features, linear terrain, mantle |
| 1842 | ESP_025781_2220 | Partial | 41.64°N, 16.19°E | Linear terrain, mantle |
| 1965 | ESP_019214_2270 | Full | 46.57°N, 22.14°E | Linear terrain, polygonal terrain, washboard terrain |
| 1967 | ESP_019214_2270 | Full | 46.58°N, 22.14°E | Linear terrain, polygonal terrain, washboard terrain |
| 2026 | PSP_006147_2250 | Full | 44.63°N, 21.05°E | Linear terrain, polygonal terrain |

**S2 Classifications of all alcoves**

We identified six broad classes of alcoves a) simple, b) joined, c) interiorly ridged, d) staircase, e) channel-related, and f) branching were not included in our database (Fig. S1). However, for the purposes of this paper to assess possible glacial erosion, we only focus on simple alcoves. Descriptions and interpretations of each class are in Table S1. Note that the joined and staircase alcoves were mapped as one alcove, but due to their larger scale, branching alcoves offshooting from the same valley were mapped as individual alcoves. As such, smaller simple alcoves that reside within the larger branching alcoves would fall into both classes. ~4% of the alcoves were classified as two or more types. Channel-related alcoves suggest that a different erosional mechanism other than glaciation may have dominated their formation.

The ACME2 tool is designed for classic cirques on Earth and while the tool works with complex shapes, it should not be relied on for curving, elongated features (Spagnolo et al., 2017). As a result, we do not apply ACME2 for all alcove classifications. For the classes including compound, joined, staircase, and branching, the way that each class of alcoves was mapped would affect the subsequent morphometric values. For example, while we mapped branching alcoves as separate alcoves, it is possible that they should instead be considered as one large alcove if the development of individual alcoves are all dependent on the main trunk. This has a significant impact on how morphometrics would be reported because not only will the length greatly vary, but other morphometrics like the aspect will also differ across different alcoves branching off of the same trunk. As a result, there is subjectivity introduced from the mapping decisions that subsequently affect evaluations of each alcove class relative to each other. Thus we do not report on the morphometrics of all classes.

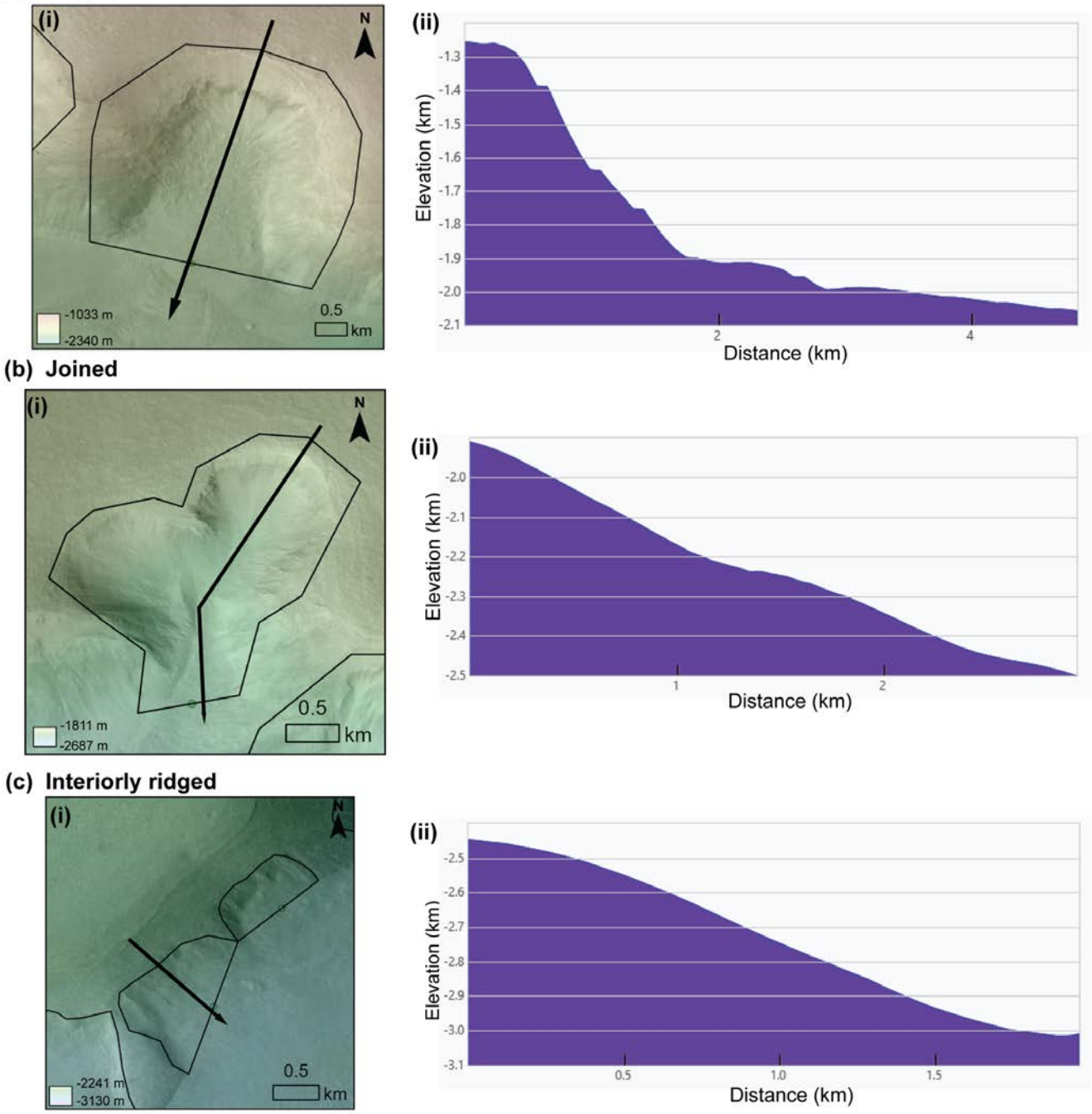
(a) Simple
(i)
N
-1033 m
-2340 m
0.5
km
(ii)
Elevation (km)
-1.3
-1.4
-1.5
-1.6
-1.7
-1.8
-1.9
-2.0
-2.1
2
4
Distance (km)
(b) Joined
(i)
N
-1811 m
-2687 m
0.5
km
(ii)
Elevation (km)
-2.0
-2.1
-2.2
-2.3
-2.4
-2.5
1
2
Distance (km)
(c) Interiorly ridged
(i)
N
-2241 m
-3130 m
0.5
km
(ii)
Elevation (km)
-2.5
-2.6
-2.7
-2.8
-2.9
-3.0
-3.1
0.5
1.0
1.5
Distance (km)

46

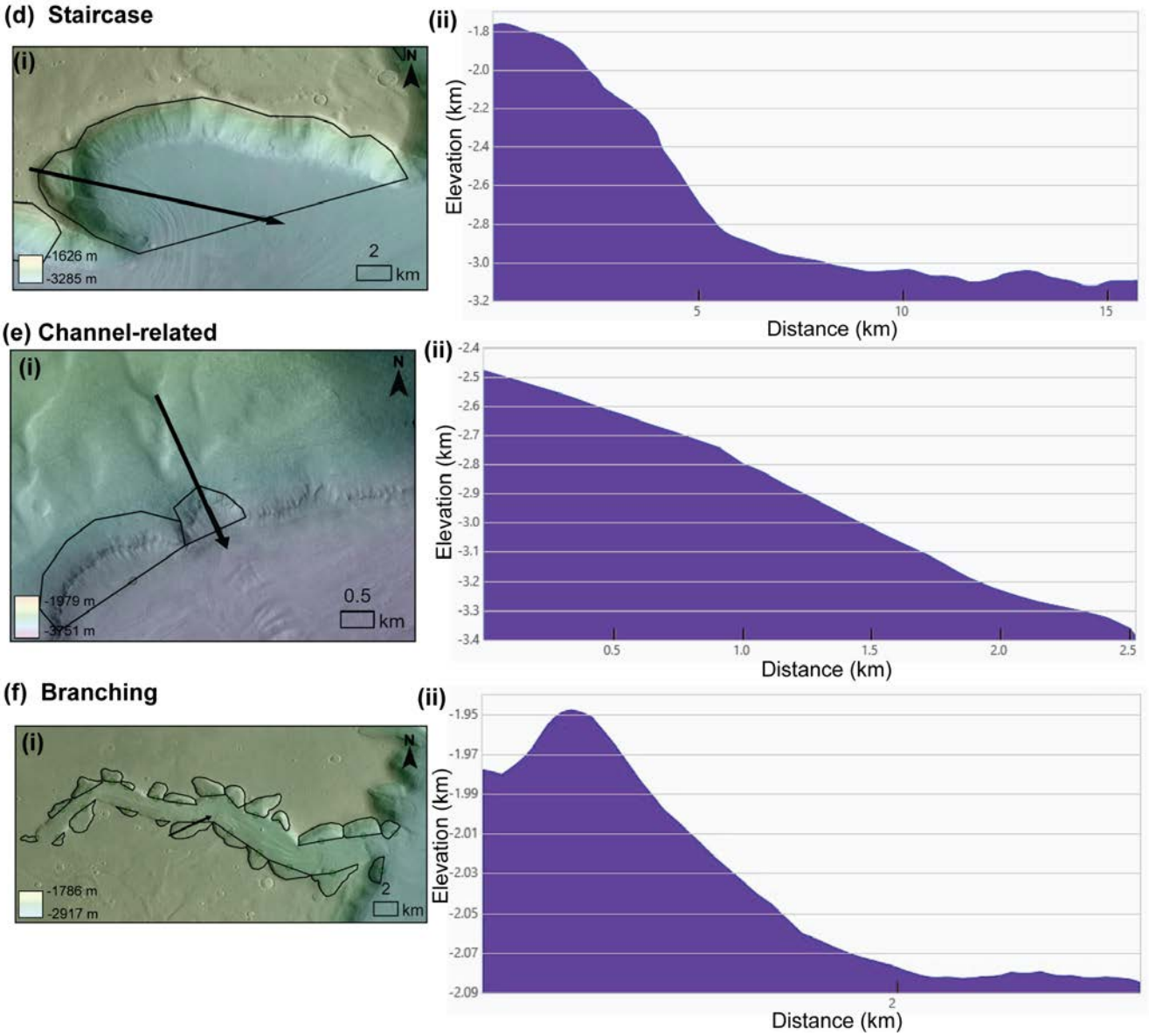


**Figure S1: Our preliminary classification of these alcoves assigns six classes. For each alcove class, panels (i) on the left correspond to an image example, and panels (ii) on the right correspond to an example of the profile. (a) Simple: characterized by its armchair shape, a defined headwall, two sidewalls, and an opening downslope (40.24°N, 34.48°E). (b) Joined: two simple alcoves adjacent to one another that join together downslope (37.72°N, 20.35°E). (c) Interiorly ridged: An alcove that has ridges within it rather than a clean headwall (44.62°N, 24.95°E). (d) Staircase: A simple alcove**

**that has a step up to another simple alcove (37.62°N, 19.59°E). (e) Channel-related: a channel is adjacent to if not feeding into this class of alcove (42.34°N, 18.30°E). (f) Branching: a large alcove that is much longer than it is wide with multiple offshoots of smaller simple alcoves (37.97°N, 19.58°E). All images are using the CTX mosaic (Dickson et al., 2023a) overlaid on HRSC (Neukum et al., 2004) colorized elevation data. HRSC elevation values are included in the elevation profiles. Arrows all point downslope. CTX data credit: Caltech/NASA/JPL/MSSS. HRSC data credit: ESA/DLR/FU Berlin.**

**Table S2: Six broad classes of alcoves on Mars identified in this study.**

| Feature classification | Description of feature on Mars | Number of alcoves with this classification (and subsampled number that fit in multiple classes) | Percent of alcoves with only this classification | Evaluation |
|---|---|---|---|---|
| Simple alcove | Simple alcoves are characterized by an armchair shape with a defined headwall, two sidewalls, and are open downslope. | 1266 (81) | 64% | Morphologies of simple alcoves on Mars are most similar to simple cirques on Earth (e.g., Barr and Spagnolo, 2015). |
| Joined alcove | Joined alcoves consist of two adjacent simple alcoves that join together downslope. | 282 (8) | 14% | Joined alcoves are most similar to compound cirques on Earth since compound cirques have two simple cirques in the headwall (e.g., Barr and Spagnolo, 2015). |
| Interiorly ridged alcove | Interiorly ridged alcoves do not have a well-defined single headwall with an armchair shape, but instead contain down-slope oriented ridges within the headwall. | 279 (25) | 14% | These alcoves may represent a prior stage of simple alcove formation and are discussed further in Section 5.2. |

| | | | | |
|---|---|---|---|---|
| Staircase alcove | Staircase alcoves include a simple alcove that has a step up to another simple alcove. | 30 (8) | 1.5% | Morphologies of staircase alcoves are most similar to staircase cirques on Earth (e.g., Barr and Spagnolo, 2015). |
| Channel-related alcove | Channel-related alcoves have channels near, or feeding into, the headwall of the alcove. | 7 (17) | 0.35% | Some of these channels are near impact craters and may have arisen from melting induced by the impact (e.g., Morgan et al., 2009). Since the channels connect or nearly connect with the headwall of this class of alcoves, it is possible that the erosion of some of these alcoves was initiated by–if not heavily influenced by–channels. |
| Branching alcove | Branching alcoves consist of an alcove that is much longer than wide, with multiple tributaries to smaller simple alcoves. We chose to map the individual alcoves in the system that defines a branching alcove. Smaller simple alcoves that reside within the larger branching alcoves would fall into both classifications. | 21 (28) | 1% | These branching alcoves appear qualitatively most similar to theater-headed valleys that have been hypothesized to have originated from groundwater sapping or outburst flooding in previous work (e.g., Lapotre and Lamb; 2018). We discuss these further in Section 6.4. |

## References


Anderson, L.W. Cirque glacier erosion rates and characteristics of Neoglacial tills, Pangnirtung Fiord area, Baffin Island, NWT, Canada. Arct. Alp. Res., 10(4), 749–760, 1978.

Anderson, R. S., Anderson, L. S., Armstrong, W. H., Rossi, M. W., and Crump, S. E. Glaciation of alpine valleys: The glacier–debris-covered glacier–rock glacier continuum. Geomorphology, 311, 127-142, 2018.

Andrews, J.T., Dugdale, R.E. Late Quaternary glacial and climatic history of northern Cumberland Peninsula, Baffin Island,

NWT, Canada. Part V: factors affecting corrie glacierization in Okoa Bay. Quat. Res., 1, 532–551, 1971.
Aniya, M., Welch, R. Morphometric analyses of Antarctic cirques from photogrammetric measurements. Geogr. Ann. Ser. A Phys. Geogr., 63(1/2), 41–53, 1981.
Arfstrom, J., and Hartmann, W. K. Martian flow features, moraine-like ridges, and gullies: Terrestrial analogs and interrelationships. Icarus, 174(2), 321-335, 2005.
Baker, D. M. H., and Carter, L. M. Radar reflectors associated with an ice-rich mantle unit in Deuteronilus Mensae, Mars. In 48th Annual Lunar and Planetary Science Conference, The Woodlands, Texas, March 2017, No. 1964, p. 1575, 2017.
Baker, D. M., and Carter, L. M. Probing supraglacial debris on Mars 1: Sources, thickness, and stratigraphy. Icarus, 319, 745-769, 2019.
Baker, D. M., & Head, J. W. Extensive Middle Amazonian mantling of debris aprons and plains in Deuteronilus Mensae, Mars: Implications for the record of mid-latitude glaciation. 260, 269-288, 2015.
Baker, V. R., and Milton, D. J. Erosion by catastrophic floods on Mars and Earth. Icarus, 23(1), 27-41, 1974.
Baker, V. R. Water and the Martian landscape. Nature, 412(6843), 228-236, 2001.
Balco, G., and Shuster, D. L. Production rate of cosmogenic 21Ne in quartz estimated from 10Be, 26Al, and 21Ne concentrations in slowly eroding Antarctic bedrock surfaces. Earth and Planetary Science Letters, 281(1-2), 48-58, 2009.
Ballantyne, C. K. Periglacial geomorphology. John Wiley and Sons, 2018.
Barr, I. D., and Spagnolo, M. Palaeoglacial and palaeoclimatic conditions in the NW Pacific, as revealed by a morphometric analysis of cirques upon the Kamchatka Peninsula. Geomorphology, 192, 15-29, 2013.
Barr, I. D., and Spagnolo, M. Glacial cirques as palaeoenvironmental indicators: Their potential and limitations. Earth-Science Reviews, 151, 48-78, 2015.
Barr, I. D., Ely, J. C., Spagnolo, M., Evans, I. S., and Tomkins, M. D. The dynamics of mountain erosion: cirque growth slows as landscapes age. Earth Surface Processes and Landforms, 44(13), 2628-2637, 2019.
Barr, I. D., Spagnolo, M., & Tomkins, M. D. Cirques in the Transantarctic Mountains reveal controls on glacier formation and landscape evolution. Geomorphology, 445, 108970, 2024.
Berger, J., Krainer, K., and Mostler, W. Dynamics of an active rock glacier (Ötztal Alps, Austria). Quaternary Research, 62(3), 233-242, 2004.
Berman, D. C., Crown, D. A., and Joseph, E. C. Formation and mantling ages of lobate debris aprons on Mars: Insights from categorized crater counts. Planetary and Space Science, 111, 83-99, 2015.
Berthling I. Slow periglacial mass wasting — processes and geomorphological impact. Dissertation submitted to the Faculty of Mathematics and Natural Sciences, University of Oslo, No. 113, Unipub forlag: Oslo, 2001.
Beyer, R. A., Alexandrov, O., & McMichael, S. The Ames Stereo Pipeline: NASA's open source software for deriving and processing terrain data. Earth and Space Science, 5(9), 537-548, 2018.

Bingham, R. G., Nienow, P. W., Sharp, M. J., and Copland, L. Hydrology and dynamics of a polythermal (mostly cold) High Arctic glacier. Earth Surface Processes and Landforms: The Journal of the British Geomorphological Research Group, 31(12), 1463-1479, 2006.

Brough, S., Hubbard, B., and Hubbard, A. Area and volume of mid-latitude glacier-like forms on Mars. Earth and Planetary Science Letters, 507, 10-20, 2019.

Buffo, J. J., Ojha, L., Meyer, C. R., Ferrier, K. L., and Palucis, M. C. Revisiting subglacial hydrology as an origin for Mars' valley networks. Earth and Planetary Science Letters, 594, 117699, 2022.

Butcher, F. E. G., Arnold, N. S., Conway, S. J., Berman, D. C., Davis, J. M., & Balme, M. R. The internal structure of a debris-covered glacier on Mars revealed by gully incision. Icarus, 419, 115717, 2024.

Butcher, F. E., Balme, M. R., Gallagher, C., Arnold, N. S., Conway, S. J., Hagermann, A., and Lewis, S. R. Recent basal melting of a mid-latitude glacier on Mars. Journal of Geophysical Research: Planets, 122(12), 2445-2468, 2017.

Christensen, P. Formation of recent martian gullies through melting of extensive water-rich snow deposits. Nature, 422(6927), 45–48, 2003.

Clinger, A. E., Fox, M., Balco, G., Cuffey, K., & Shuster, D. L. Detrital thermochronometry reveals that the topography along the Antarctic Peninsula is not a Pleistocene landscape. Journal of Geophysical Research: Earth Surface, 125(6), e2019JF005447, 2020.

Conway, S. J., Butcher, F. E., de Haas, T., Deijns, A. A., Grindrod, P. M., & Davis, J. M. Glacial and gully erosion on Mars: A terrestrial perspective. Geomorphology, 318, 26-57, 2018.

Conway, S. J., & Balme, M. R. Decameter thick remnant glacial ice deposits on Mars. Geophysical Research Letters, 41(15), 5402-5409, 2014.

Coquin, J., Mercier, D., Bourgeois, O., & Decaulne, A. A paraglacial rock-slope failure origin for cirques: a case study from Northern Iceland. Géomorphologie: relief, processus, environnement, 25(2), 117-136, 2019.

Cuffey, K. M., Conway, H., Hallet, B., Gades, A. M., & Raymond, C. F. Interfacial water in polar glaciers and glacier sliding at −17 C. Geophysical Research Letters, 26(6), 751-754, 1999.

Derbyshire, E., and Evans, I.S. The climatic factor in cirque variation. In Geomorphology and Climate, 447, 494, 1976.

Dickson, J. L., Ehlmann, B. L., Kerber, L. H., & Fassett, C. I. Release of the global CTX mosaic of Mars: An Experiment in information-preserving image data processing. LPI contributions, 2806, 2353, 2023a.

Dickson, J. L., Palumbo, A. M., Head, J. W., Kerber, L., Fassett, C. I., & Kreslavsky, M. A. Gullies on Mars could have formed by melting of water ice during periods of high obliquity. Science, 380(6652), 1363-1367, 2023b.

Dundas, C. M., Conway, S. J., & Cushing, G. E. Martian gully activity and the gully sediment transport system. Icarus, 386, 115133, 2022.

Evans, I. S. Local aspect asymmetry of mountain glaciation: a global survey of consistency of favoured directions for glacier

numbers and altitudes. Geomorphology, 73(1-2), 166-184, 2006.
Evans, I. S. Glaciers, rock avalanches and the 'buzzsaw' in cirque development: Why mountain cirques are of mainly glacial origin. Earth Surface Processes and Landforms, 46(1), 24-46, 2020.
Evatt, G. W., Fowler, A. C., Clark, C. D., and Hulton, N. R. J. Subglacial floods beneath ice sheets. Philosophical Transactions of the Royal Society A: Mathematical, Physical and Engineering Sciences, 364(1844), 1769-1794, 2006.
Fassett, C. I., Levy, J. S., Dickson, J. L., & Head, J. W. An extended period of episodic northern mid-latitude glaciation on Mars during the Middle to Late Amazonian: Implications for long-term obliquity history. Geology, 42(9), 763-766, 2014.
Fastook, J. L., Head, J. W., Forget, F., Madeleine, J. B., and Marchant, D. R. Evidence for Amazonian northern mid-latitude regional glacial landsystems on Mars: Glacial flow models using GCM-driven climate results and comparisons to geological observations. Icarus, 216(1), 23-39, 2011.
Fran, J. S., and Martin, Y. High spatial resolution satellite imagery, DEM derivatives, and image segmentation for the detection of mass wasting processes. Photogrammetric Engineering, 72(6), 687-692, 2006.
French, H. M. The periglacial environment. John Wiley and Sons, 2018.
Gallagher, C., and Balme, M. Eskers in a complete, wet-based glacial system in the Phlegra Montes region, Mars. Earth and Planetary Science Letters, 431, 96-109, 2015.
Gallagher, C., Butcher, F. E., Balme, M., Smith, I., and Arnold, N. Landforms indicative of regional warm-based glaciation, Phlegra Montes, Mars. Icarus, 355, 114173, 2021.
Glasser, N. F., and Bennett, M. R. Glacial erosional landforms: origins and significance for palaeoglaciology. Progress in Physical Geography, 28(1), 43-75, 2004.
Graf, W.L., Cirques as glacier locations. Arct. Alp. Res. 8, 79–90, 1976.
Hallet, B., Hunter, L., and Bogen, J. Rates of erosion and sediment evacuation by glaciers: A review of field data and their implications. Global and Planetary Change, 12(1-4), 213-235, 1996.
Hambrey, M.J., Huddart, D., Bennett, M.R., Glasser, N.F., Genesis of 'hummocky moraines' by thrusting in glacier ice: Evidence from Svalbard and Britain. J. Geol. Soc. Lond. 154, 623–632, 1997.
Harrison, K. P., and Grimm, R. E. Groundwater-controlled valley networks and the decline of surface runoff on early Mars. Journal of Geophysical Research: Planets, 110(E12), 2005.
Harrison, T. N., Osinski, G. R., Tornabene, L. L., and Jones, E. Global documentation of gullies with the Mars Reconnaissance Orbiter Context Camera and implications for their formation. Icarus, 252, 236-254, 2015.
Head, J. W., and Marchant, D. R. Cold-based mountain glaciers on Mars: western Arsia Mons. Geology, 31(7), 641-644, 2003.
Head, J. W., Marchant, D. R., Agnew, M. C., Fassett, C. I., and Kreslavsky, M. A. Extensive valley glacier deposits in the northern mid-latitudes of Mars: Evidence for Late Amazonian obliquity-driven climate change. Earth and Planetary Science Letters, 241(3-4), 663-671, 2006.

Hecht, M. H. Metastability of liquid water on Mars. Icarus, 156(2), 373-386, 2002.
Hepburn, A. J., Ng, F. S. L., Livingstone, S. J., Holt, T. O., and Hubbard, B. Polyphase mid-latitude glaciation on Mars: Chronology of the formation of superposed glacier-like forms from crater-count dating. Journal of Geophysical Research: Planets, 125(2), e2019JE006102, 2020.
Herman, F., Beyssac, O., Brughelli, M., Lane, S.N., Leprince, S., Adatte, T., Lin, J.Y., Avouac, J.P. and Cox, S.C. Erosion by an Alpine glacier. Science, 350, 193, 2015.
Herman, F., De Doncker, F., Delaney, I., Prasicek, G., & Koppes, M. (2021). The impact of glaciers on mountain erosion. Nature Reviews Earth & Environment, 2(6), 422-435.
Howat, Ian, et al., "The Reference Elevation Model of Antarctica – Strips, Version 4.1", https://doi.org/10.7910/DVN/X7NDNY, Harvard Dataverse, V1. Accessed: 2024-05-31. 2022.
Hubbard, B., Milliken, R. E., Kargel, J. S., Limaye, A., and Souness, C. Geomorphological characterisation and interpretation of a mid-latitude glacier-like form: Hellas Planitia, Mars. Icarus, 211(1), 330-346, 2011.
Hubbard, B., Souness, C., and Brough, S. Glacier-like forms on Mars. The Cryosphere, 8(6), 2047-2061, 2014.
Janke, J. R., Regmi, N. R., Giardino, J. R., and Vitek, J. D. Rock Glaciers. Treatise on Geomorphology (Vol. 8), 2013.
Jawin, E. R., Head, J. W., and Marchant, D. R. Transient post-glacial processes on Mars: geomorphologic evidence for a paraglacial period. Icarus, 309, 187-206, 2018.
Jawin, E. R., and Head, J. W. Patterns of late Amazonian deglaciation from the distribution of martian paraglacial features. Icarus, 355, 114117, 2021.
Khuller, A. R., Christensen, P. R., Harrison, T. N., and Diniega, S. The distribution of frosts on Mars: Links to present-day gully activity. Journal of Geophysical Research: Planets, 126(3), 2021.
Kite, E. S. Geologic constraints on early Mars climate. Space Science Reviews, 215, 1-47, 2019.
Kleman, J., and Stroeven, A.P., Preglacial surface remnants and Quaternary glacial regimes in northwestern Sweden. Geomorphology 19 (1), 35–54, 1997.
Knight, J., Harrison, S., and Jones, D. B. Rock glaciers and the geomorphological evolution of deglacierizing mountains. Geomorphology, 324, 14-24, 2019.
Koutnik, M., Butcher, F. E., Soare, R. J., Hepburn, A. J., Hubbard, B., Brough, S., C. Gallagher, L. McKeown, and Pathare, A. (2024). Glacial deposits, remnants, and landscapes on Amazonian Mars: Using setting, structure, and stratigraphy to understand ice evolution and climate history. In Ices in the Solar-System (pp. 101-142). Elsevier.
Kreslavsky, M. A., Head, J. W., & Marchant, D. R. Periods of active permafrost layer formation during the geological history of Mars: Implications for circum-polar and mid-latitude surface processes. Planetary and Space Science, 56(2), 289-302, 2008.
Laity, J. The Role of Groundwater Sapping in Valley Evolution. Sapping Features of the Colorado Plateau: A Comparative Planetary Geology Field Guide, 491, 63, 1988.
Lamb, M. P., Howard, A. D., Johnson, J., Whipple, K. X., Dietrich, W. E., and Perron, J. T. Can springs cut canyons into

rock?. Journal of Geophysical Research: Planets, 111(E7), 2006.

Lapotre, M. G., Lamb, M. P., and Williams, R. M. Canyon formation constraints on the discharge of catastrophic outburst floods of Earth and Mars. Journal of Geophysical Research: Planets, 121(7), 1232-1263, 2016.

Lapotre, M. G., and Lamb, M. P. Substrate controls on valley formation by groundwater on Earth and Mars. Geology, 46(6), 531-534, 2018.

Larsen, E., Mangerud, J., Erosion rate of a Younger Dryas cirque glacier at Krakenes, western Norway. Ann. Glaciol. 2 (1), 153–158, 1981.

Laskar, J., Levrard, B., & Mustard, J. F. Orbital forcing of the Martian polar layered deposits. Nature, 419(6905), 375-377, 2002.

Lehmann, B., Anderson, R. S., Bodin, X., Cusicanqui, D., Valla, P. G., and Carcaillet, J. Alpine rock glacier activity over Holocene to modern timescales (western French Alps). Earth Surface Dynamics, 10(3), 605-633, 2022.

Levy, J. S., Head, J. W., and Marchant, D. R. Concentric crater fill in Utopia Planitia: History and interaction between glacial "brain terrain" and periglacial mantle processes. Icarus, 202(2), 462-476, 2009a.

Levy, J. S., Head, J., and Marchant, D. Thermal contraction crack polygons on Mars: Classification, distribution, and climate implications from HiRISE observations. Journal of Geophysical Research: Planets, 114(E1), 2009b.

Levy, J. S., Fassett, C.I., Head, J.W., Schwartz, C., Watters, J.L., Sequestered glacial ice contribution to the global Martian water budget: Geometric constraints on the volume of remnant, midlatitude debris-covered glaciers. J. Geophys. Res. Planets 119, doi: 10.1002/2014JE004685, 2014.

Levy, J. S., Fassett, C. I., & Head, J. W. Enhanced erosion rates on Mars during Amazonian glaciation. Icarus, 264, 213-219, 2016.

Levy, J.S., Fassett, C.I., Holt, J.W., Parsons, R., Cipolli, W., Goudge, T.A., Tebolt, M., Kuentz, L., Johnson, J., Ishraque, F. and Cvijanovich, B. Surface boulder banding indicates Martian debris-covered glaciers formed over multiple glaciations. Proceedings of the National Academy of Sciences, 118(4), p.e2015971118, 2021.

Lewkowicz, A. G. Morphology, frequency and magnitude of active-layer detachment slides, Fosheim Peninsula, Ellesmere Island, NWT. In Proceedings of the 5th Canadian Permafrost Conference (Vol. 54, pp. 111-118). Université Laval, Québec: Centre d'études nordiques, 1990.

Lewkowicz, A. G. Dynamics of active-layer detachment failures, Fosheim peninsula, Ellesmere Island, Nunavut, Canada. Permafrost and Periglacial Processes, 18(1), 89-103, 2007.

Li, Y., Evans, I. S., Spagnolo, M., Pellitero, R., Barr, I. D., & Ely, J. C. ACME2: An extended toolbox for automated cirque metrics extraction. Geomorphology, 445, 108982, 2024.

Lillquist, K., and Weidenaar, M. Rock glaciers in the Eastern Cascades, Washington State, USA: Impacts of selected variables on spatial distribution and landform dimensions. Geomorphology, 389, 107839, 2021.

Lukas, S., A test of the englacial thrusting hypothesis of 'hummocky' moraine formation: Case studies from the northwest Highlands, Scotland. Boreas 34, 287–307, 2005.

Mackay, S.L., Marchant, D.R., Lamp, J.L., Head, J.W. Cold-based debris-covered glaciers: Evaluating their potential as climate archives through studies of ground-penetrating radar and surface morphology. J. Geophys. Res. Earth Surf. 119, 2505–2540. https://doi.org/10.1002/2014JF003178, 2014.

Madeleine, J. B., Forget, F., Head, J. W., Levrard, B., Montmessin, F., and Millour, E. Amazonian northern mid-latitude glaciation on Mars: A proposed climate scenario. Icarus, 203(2), 390-405, 2009.

Malin, M.C., Bell, J.F., Cantor, B.A., Caplinger, M.A., Calvin, W.M., Clancy, R.T., Edgett, K.S., Edwards, L., Haberle, R.M., James, P.B., Lee, S.W., Ravine, M.A., Thomas, P.C., Wolff, M.J., Context camera investigation on board the Mars Reconnaissance Orbiter. J. Geophys. Res. 112, E05S04, doi: 10.1029, 2007.

Mangold, N., and Allemand, P. Topographic analysis of features related to ice on Mars. Geophysical Research Letters, 28(3), 407-410, 2001.

Marchant, D. R., and Head III, J. W. Antarctic dry valleys: Microclimate zonation, variable geomorphic processes, and implications for assessing climate change on Mars. Icarus, 192(1), 187-222, 2007.

McEwen, A.S., Eliason, E.M., Bergstrom, J.W., Bridges, N.T., Hansen, C.J., Delamere, W. A., Grant, J.A., Gulick, V.C., Herkenhoff, K.E., Keszthelyi, L., Kirk, R.L., Mellon, M.T., Squyres, S.W., Thomas, N., Weitz, C.M., Mars Reconnaissance Orbiter's High Resolution Imaging Science Experiment (HiRISE). J. Geophys. Res. 112, E05S02, doi: 10.1029/2005JE002605, 2007.

Michael, G. G. Planetary surface dating from crater size-frequency distribution measurements: Multiple resurfacing episodes and differential isochron fitting, Icarus, 226, 885–890, 2013.

Milliken, R. E., Mustard, J. F., and Goldsby, D. L. Viscous flow features on the surface of Mars: Observations from high-resolution Mars Orbiter Camera (MOC) images. Journal of Geophysical Research: Planets, 108(E6), 2003.

Mîndrescu, M., Evans, I. S., and Cox, N. J. Climatic implications of cirque distribution in the Romanian Carpathians: palaeowind directions during glacial periods. Journal of Quaternary Science, 25(6), 875-888, 2010.

Morgan, G. A., Head III, J. W., and Marchant, D. R. Lineated valley fill (LVF) and lobate debris aprons (LDA) in the Deuteronilus Mensae northern dichotomy boundary region, Mars: Constraints on the extent, age and episodicity of Amazonian glacial events. Icarus, 202(1), 22-38, 2009.

Morgan, G. A., Putzig, N. E., Perry, M. R., Sizemore, H. G., Bramson, A. M., Petersen, E. I., ... and Campbell, B. A. Availability of subsurface water-ice resources in the northern mid-latitudes of Mars. Nature Astronomy, 5(3), 230-236, 2021.

Mustard, J. F., Christopher, D. C., and Moses, K. R. Evidence for recent climate change on Mars from the identification of youthful near-surface ground ice. Nature, 412(6845), 411, 2001.

NASA Shuttle Radar Topography Mission (SRTM). Shuttle Radar Topography Mission (SRTM) Global. Distributed by OpenTopography. https://doi.org/10.5069/G9445JDF. Accessed: 2024-08-02. 2013.

Neukum, G., Jaumann, R., The HRSC Co-Investigator and Experiment Team, HRSC: the high resolution stereo camera of Mars Express. In: Wilson, A. (Ed.), Mars Express: The Scientific Payload, 1240. European Space Agency Special

Publication, pp. 17–35, 2004.
Oliva, M., Andrés, N., Fernández-Fernández, J. M., and Palacios, D. The evolution of glacial landforms in the Iberian Mountains during the deglaciation. In European Glacial Landscapes (pp. 201-208), 2023.
Palucis, M. C., Jasper, J., Garczynski, B., and Dietrich, W. E. Quantitative assessment of uncertainties in modeled crater retention ages on Mars. Icarus, 341, 113623, 2020.
Pilorget, C., and Forget, F. Formation of gullies on Mars by debris flows triggered by CO2 sublimation. Nature Geoscience, 9(1), 65-69, 2016.
Plaut, J. J., Safaeinili, A., Holt, J. W., Phillips, R. J., Head III, J. W., Seu, R., Radar evidence for ice in lobate debris aprons in the mid-northern latitudes of Mars. Geophysical Research Letters, 36(2), 2009.
Rignot, E., Hallet, B., & Fountain, A. Rock glacier surface motion in Beacon Valley, Antarctica, from synthetic-aperture radar interferometry. Geophysical Research Letters, 29(12), 48-1, 2002.
Robbins, S. J., & Hynek, B. M. (2012). A new global database of Mars impact craters≥ 1 km: 2. Global crater properties and regional variations of the simple-to-complex transition diameter. Journal of Geophysical Research: Planets, 117(E6).
Rudberg, S. Multiple glaciation in Scandinavia: seen in gross morphology or not? Geogr. Ann. Ser. A Phys. Geogr. 74, 231–243, 1992.
Sanders, J. W., Cuffey, K. M., Moore, J. R., MacGregor, K. R., & Kavanaugh, J. L. Periglacial weathering and headwall erosion in cirque glacier bergschrunds. Geology, 40(9), 779-782, 2012.
Sanders, J. W., Cuffey, K. M., MacGregor, K. R., and Collins, B. D. The sediment budget of an alpine cirque. GSA Bulletin, 125(1-2), 229-248, 2013.
Schon, S. C., Head, J. W., & Fassett, C. I. Unique chronostratigraphic marker in depositional fan stratigraphy on Mars: Evidence for ca. 1.25 Ma gully activity and surficial meltwater origin. Geology, 37(3), 207-210, 2009.
Schon, S. C., Head, J. W., & Fassett, C. I. Recent high-latitude resurfacing by a climate-related latitude-dependent mantle: Constraining age of emplacement from counts of small craters. Planetary and Space Science, 69(1), 49-61, 2012.
Selby, M. J., and Wilson, A. T. Possible Tertiary age for some Antarctic cirques. Nature, 229(5287), 623-624, 1971.
Sharp, R.P., 1973. Mars: Fretted and chaotic terrains. J. Geophys. Res. 78, 4073–4083.
Sharp, M., ‘‘Crevasse-fill’’ ridges – a landform type characteristic of surging glaciers? Geografiska Annaler 67A, 213–220, 1985.
Shean, D. E., Head, J. W., and Marchant, D. R. Origin and evolution of a cold-based tropical mountain glacier on Mars: The Pavonis Mons fan-shaped deposit. Journal of Geophysical Research: Planets, 110(E5), 2005.
Sholes, S. F., and Rivera-Hernández, F. Constraints on the uncertainty, timing, and magnitude of potential Mars oceans from topographic deformation models. Icarus, 378, 114934, 2022.
Squyres, S.W. Martian fretted terrain: Flow of erosional debris. Icarus, 34, 600– 613, 1978.
Squyres, S. W. The distribution of lobate debris aprons and similar flows on Mars. Journal of Geophysical Research:

Solid Earth, 84(B14), 8087-8096, 1979.
Soare, R. J., Williams, J. P., Hepburn, A. J., & Butcher, F. E. A billion or more years of possible periglacial/glacial cycling in Protonilus Mensae, Mars. Icarus, 385, 115115, 2022.
Souness, C., Hubbard, B., Milliken, R. E., and Quincey, D. An inventory and population-scale analysis of martian glacier-like forms. Icarus, 217(1), 243-255, 2012.
Souness, C. J., and Hubbard, B. An alternative interpretation of late Amazonian ice flow: Protonilus Mensae, Mars. Icarus, 225(1), 495-505, 2013.
Spagnolo, M., Pellitero, R., Barr, I. D., Ely, J. C., Pellicer, X. M., and Rea, B. R. ACME, a GIS tool for automated cirque metric extraction. Geomorphology, 278, 280-286, 2017.
Thomson, L. I., & Copland, L. Multi-decadal reduction in glacier velocities and mechanisms driving deceleration at polythermal White Glacier, Arctic Canada. Journal of Glaciology, 63(239), 450-463, 2017.
Turnbull J. M., Davies T. R. H. A mass movement origin for cirques. Earth Surface Processes and Landforms 31: 1129–1148, 2006.
White, W. A. Erosion of cirques. The Journal of Geology, 78(1), 123-126, 1970.
Williams, K. E., Toon, O. B., Heldmann, J. L., McKay, C., and Mellon, M. T. Stability of mid-latitude snowpacks on Mars. Icarus, 196(2), 565-577, 2008.
Williams, K. E., Toon, O. B., Heldmann, J. L., and Mellon, M. T. Ancient melting of mid-latitude snowpacks on Mars as a water source for gullies. Icarus, 200(2), 418-425, 2009.
Williams, J. M., Scuderi, L. A., McClanahan, T. P., Banks, M. E., and Baker, D. M. Comparative planetology–Comparing cirques on Mars and Earth using a CNN. Geomorphology, 440, 108881, 2023.
Willmes, M., Reiss, D., Hiesinger, H., & Zanetti, M. Surface age of the ice–dust mantle deposit in Malea Planum, Mars. Planetary and Space Science, 60(1), 199-206, 2012.
Woodley, S. Z., Butcher, F. E., Fawdon, P., Clark, C. D., Ng, F. S., Davis, J. M., and Gallagher, C. Multiple sites of recent wet-based glaciation identified from eskers in western Tempe Terra, Mars. Icarus, 386, 115147, 2022.